2 361

1072
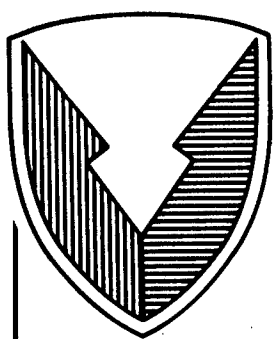
A181273

RD&E

CENTER

Technical Report

No. __13197__

EXPLORATORY DEVELOPMENT OF A TWIN-SPOOL

TURBOCHARGER FOR A HIGH OUTPUT DIESEL ENGINE

FINAL REPORT

CONTRACT NUMBER DAAE07-83-C-R129

AUGUST 1986

By
R. Hess, J. F. King & J. L. Harp, Jr.
Thermo Mechanical Systems Company
7957 Alabama Avenue
Canoga Park, California 91304
TMS Report No. SR-41

20030617001

**U.S. ARMY TANK-AUTOMOTIVE COMMAND
RESEARCH, DEVELOPMENT & ENGINEERING CENTER
Warren, Michigan 48397-5000**

20020726064

NOTICES

This report is not to be construed as an official Department of the Army position.

Mention of any trade names or manufacturers in this report shall not be construed as an official indorsement or approval of such products or companies by the U.S. Government.

Destroy this report when it is no longer needed. Do not return it to the originator.

REPORT DOCUMENTATION PAGE

1a. REPORT SECURITY CLASSIFICATION	1b. RESTRICTIVE MARKINGS
Unclassified	

2a. SECURITY CLASSIFICATION AUTHORITY	3. DISTRIBUTION/AVAILABILITY OF REPORT
2b. DECLASSIFICATION/DOWNGRADING SCHEDULE	Approved for public release: distribution is unlimited

4. PERFORMING ORGANIZATION REPORT NUMBER(S)	5. MONITORING ORGANIZATION REPORT NUMBER(S)
SR-41	13197

6a. NAME OF PERFORMING ORGANIZATION	6b. OFFICE SYMBOL (If applicable)	7a. NAME OF MONITORING ORGANIZATION
Thermo Mechanical Systems Co.		U.S. Army Tank-Automotive Command

6c. ADDRESS (City, State, and ZIP Code)	7b. ADDRESS (City, State, and ZIP Code)
7957 Alabama Avenue Canoga Park, CA 91304	Attn: AMSTA-RGRT Warren, MI 48397-5000

8a. NAME OF FUNDING/SPONSORING ORGANIZATION	8b. OFFICE SYMBOL (If applicable)	9. PROCUREMENT INSTRUMENT IDENTIFICATION NUMBER
		DAAE07-83-C-R129

8c. ADDRESS (City, State, and ZIP Code)	10. SOURCE OF FUNDING NUMBERS			
	PROGRAM ELEMENT NO.	PROJECT NO.	TASK NO.	WORK UNIT ACCESSION NO.

11. TITLE (Include Security Classification)

Exploratory Development of a Twin-Spool Turbocharger for a High-Output Diesel Engine

12. PERSONAL AUTHOR(S)
Richard Hess, Joseph F. King and James L. Harp, Jr.

13a. TYPE OF REPORT	13b. TIME COVERED	14. DATE OF REPORT (Year, Month, Day)	15. PAGE COUNT
Final	FROM 09/83 TO 06/86	August 1986	118

16. SUPPLEMENTARY NOTATION

17. COSATI CODES			18. SUBJECT TERMS (Continue on reverse if necessary and identify by block number)
FIELD	GROUP	SUB-GROUP	a. Turbochargers
			b. Twin-Spool Turbochargers

19. ABSTRACT (Continue on reverse if necessary and identify by block number)

This report covers the analysis, design, fabrication and experimental testing of a twin-spool turbocharger for the Cummins NTC-475 diesel engine.

20. DISTRIBUTION/AVAILABILITY OF ABSTRACT	21. ABSTRACT SECURITY CLASSIFICATION
☒ UNCLASSIFIED/UNLIMITED ☐ SAME AS RPT. ☐ DTIC USERS	Unclassified

22a. NAME OF RESPONSIBLE INDIVIDUAL	22b. TELEPHONE (Include Area Code)	22c. OFFICE SYMBOL
Harry Koontz	313-574-5834	AMSTA-RGRT

DD FORM 1473, 84 MAR

83 APR edition may be used until exhausted. All other editions are obsolete.

TABLE OF CONTENTS

Preceding Page Blank

1.0 SUMMARY

The analysis, design, fabrication and experimental testing of a twin-spool turbocharger was conducted for the Cummins NTC-475 diesel engine. Two major designs of the twin-spool turbocharger were fabricated and tested:

1) Compact design, concentric shaft-to-shaft bearing coupled turbocharger incorporating a) split 40° backswept impeller, b) split AiResearch T18A85 turbine rotor, c) adjustable vaned compressor diffuser and d) nozzleless AiResearch turbine (volute) housing.

2) Independently supported (shafts dynamically de-coupled) concentric shaft design incorporating a) separate structures for bearing support of the inner shaft, b) split 25° backswept compressor impeller, c) split T18A40/T18A85 turbine rotor/exducer combination and d) divided volute, adjustable nozzle turbine housing.

While bench tests were performed on both designs, actual engine testing was successfully carried out using the latter design. The engine tests indicated that the second twin-spool configuration gave performance comparable to the originally equipped two-stage turbocharger system of the NTC-475 diesel engine (rated BHP of 425 hp at 2100 RPM, best BSFC of 0.35 at engine lug) with the added benefit of extending engine lugging range to 1200 RPM (from 1300 RPM, as originally equipped). This configuration gave peak compressor efficiency of about 75 percent and peak turbine efficiency of about 80 percent, both attributed to the reduction inducer angle of attack and exducer exit swirl angle made possible by the twin-spool concept.

The above results indicate that the twin-spool turbocharger concept is a viable approach for providing wide range in engine torque capability without the size and weight of multiple stage turbocharger systems.

2.0 INTRODUCTION

2.1 Background

Figure 1 presents the turbocharger compressor map for the Army 525 CID VHO diesel engine. This map illustrates the engine limitations imposed by the compressor in conventional turbochargers. At engine speeds of 1200 and 1600 RPM the maximum pressure ratio developed by the compressor is roughly 1.3 and 1.6:1, respectively, due to the intersection of the engine operation line with the compressor low-flow instability limit or surge line. In addition, at low engine speeds, and the corresponding low airflows, the compressor efficiency drops well below the design value. Thus, the engine torque developed at low engine speeds is severely limited by conventional turbochargers.

The variable diffuser vane mechanism of the Variable Area Turbocharger (Ref. 1), as shown in Figure 2, is one technique to partially remedy this situation. With the variable diffuser vanes, the ability to adjust diffuser throat area allows the surge line to be shifted to lower flow rates and avoids surge at most engine operating conditions. A second technique to improve the limited low speed engine performance is the compressor diffuser bleed system (Ref. 2), as shown in Figure 3. This technique accomplishes the same surge control objectives as the variable diffuser system but does so with a simpler fixed geometry system.

Even with these advanced turbocharger concepts, maximum diesel engine torque output at low engine speeds is still limited by turbocharger performance. It appears that the cause of this still-limited turbocharger performance, at lug operating conditions, is primarily due to declining compressor inducer and turbine exducer efficiency. The causes of these poor compressor inducer and turbine exducer efficiencies are as follows:

At rated engine power conditions, it is conventional practice to design the compressor inducer for near zero angle of attack. Also, the inducer is designed just large enough to pass the required airflow. If too small, it will choke--that is, attain sonic velocity in the inducer channel passages, and the engine will not obtain the desired airflow. If the inducer area is too large, the compressor performance at the lower power conditions will decrease substantially.

Also at rated conditions it is conventional practice to design the turbine exducer for near zero swirl just downstream of the exducer. If too small, it will increase leaving losses (due to high velocities) and put substantial back pressure on the engine causing a loss in engine power output. If the exducer is too large, it will not only increase swirl losses at rated power, but will further increase swirl losses at the lower power conditions.

Unfortunately, substantial losses in aerodynamic performance are encountered in going from rated power to lug power. First, the inducer angle of attack increases substantially, as shown in the vector diagram of Figure 4, (e.g., to as much as 20 degrees) causing severe inducer stalling and separation, which in turn causes reverse flow and regurgitation along the compressor shroud. A loss in compressor efficiency of as high as 15 points is frequently encountered in going from full power to lug power operating conditions. Secondly, the turbine exducer swirl losses increase substantially. The primary reason is that, in order to maintain compressor pressure ratio, the turbo speed must remain essentially constant. However, the mass flow at lug may be only about half that at rated; and, therefore, the gas velocity in the exducer channel at lug is about half that at rated. Consequently a very large swirl, as high as 60 degrees, occurs in the direction of wheel rotation, as

shown in the vector diagram of Figure 5. This can result in a turbine efficiency loss of as high as 15 points in going from rated to lug. Even with variable area turbine nozzles, it is difficult for the turbine to overcome this possible combined 30 point loss in turbocharger efficiency and still supply sufficient power to drive the compressor.

2.2 Twin-Spool Concept

Addressing the above problem, a turbocharger design for reducing the at-lug inducer and exducer losses was conceived. This design involves splitting the compressor inducer and the turbine exducer from the radial portions of the wheels, and connecting the inducer and exducer with a separate shaft. With this turbocharger design, the inducer and exducer would operate at reduced speeds at lug as compared to the radial wheels, thereby reducing the inducer angle of attack and exducer leaving angle for improved efficiencies. The radial wheels would continue to operate at whatever speed is necessary to maintain the required pressure ratio.

2.3 Program Objectives

The general objective of this program was to develop a high performance radial flow turbocharger incorporating a unique split inducer/exducer concept. The specific objectives of this program were to develop (i.e. to design, fabricate, and test) a single stage, twin-spool turbocharger, to replace the existing two-stage turbocharger system of the 475 hp, Cummins 855 diesel engine.

COMPRESSOR PRESSURE RATIO

3.0

2.8

2.6

2.4

2.2

2.0

1.8

1.6

1.4

1.2

1.0

0   10   20   30   40   50   60   70   80

CORRECTED AIRFLOW, $\dfrac{\dot{W}\sqrt{T_1/545}}{P_1/28.4}$ (LB/MIN)

63600

$56500 = N/\sqrt{T_1/545}$

2800 RPM

2400 RPM

2000 RPM

$\eta_c = 73\%$

70

65

47100

1600 RPM

38000

28700

1200 RPM
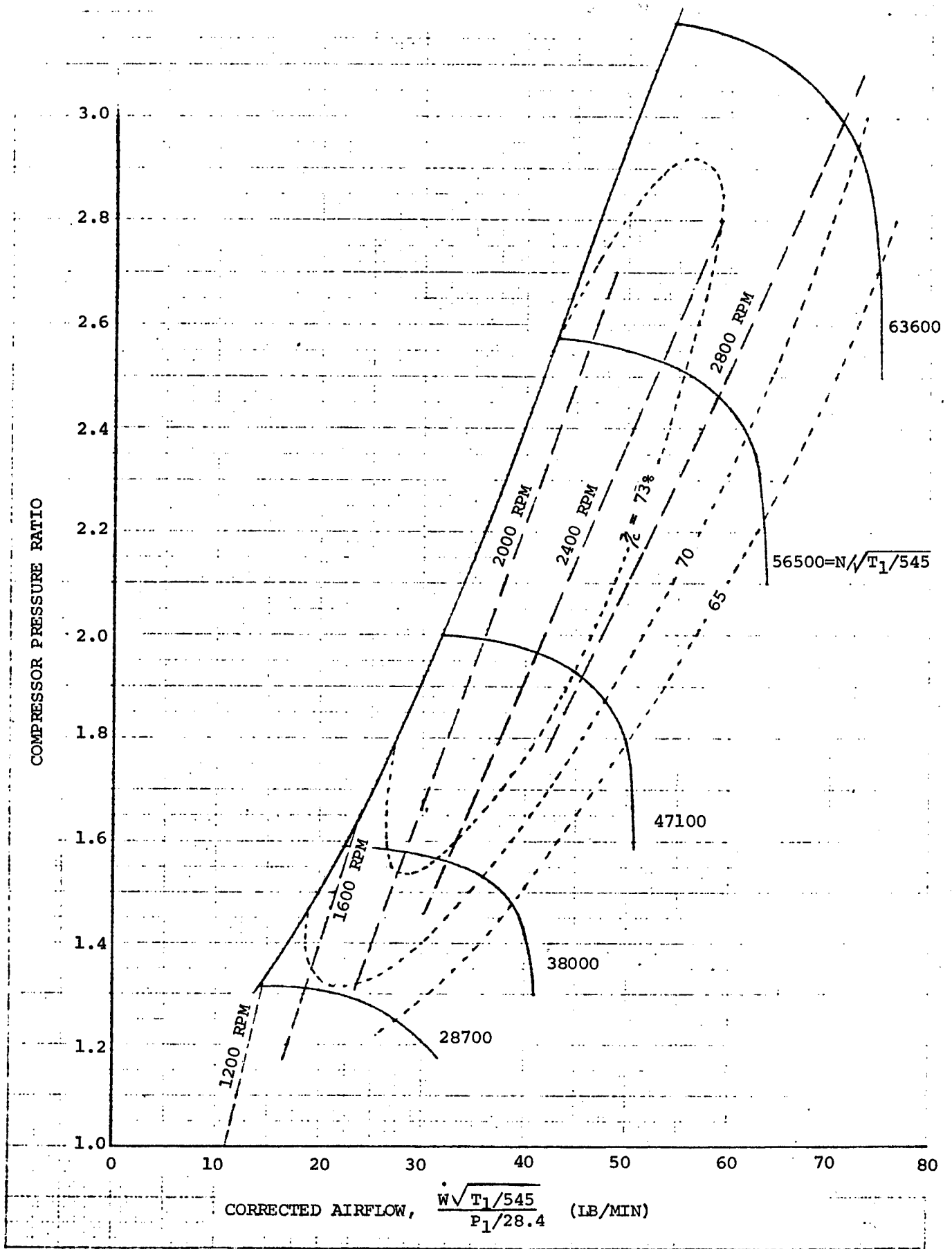
Figure 1. Compressor map for standard T1882 turbocharger for VHO diesel with
engine operating lines superimposed
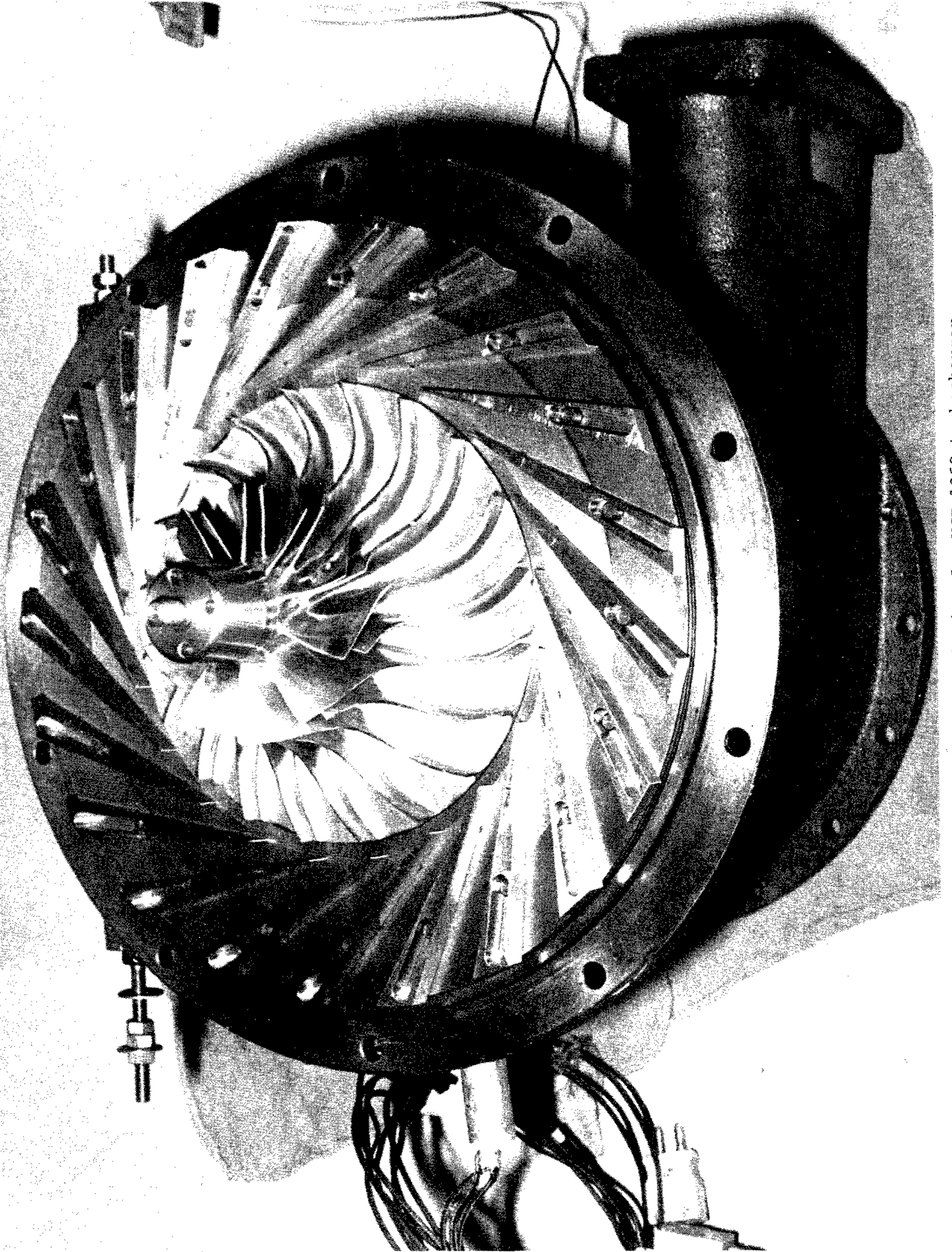
Figure 2. Photograph of variable diffuser mechanism for VCR-1360 turbocharger
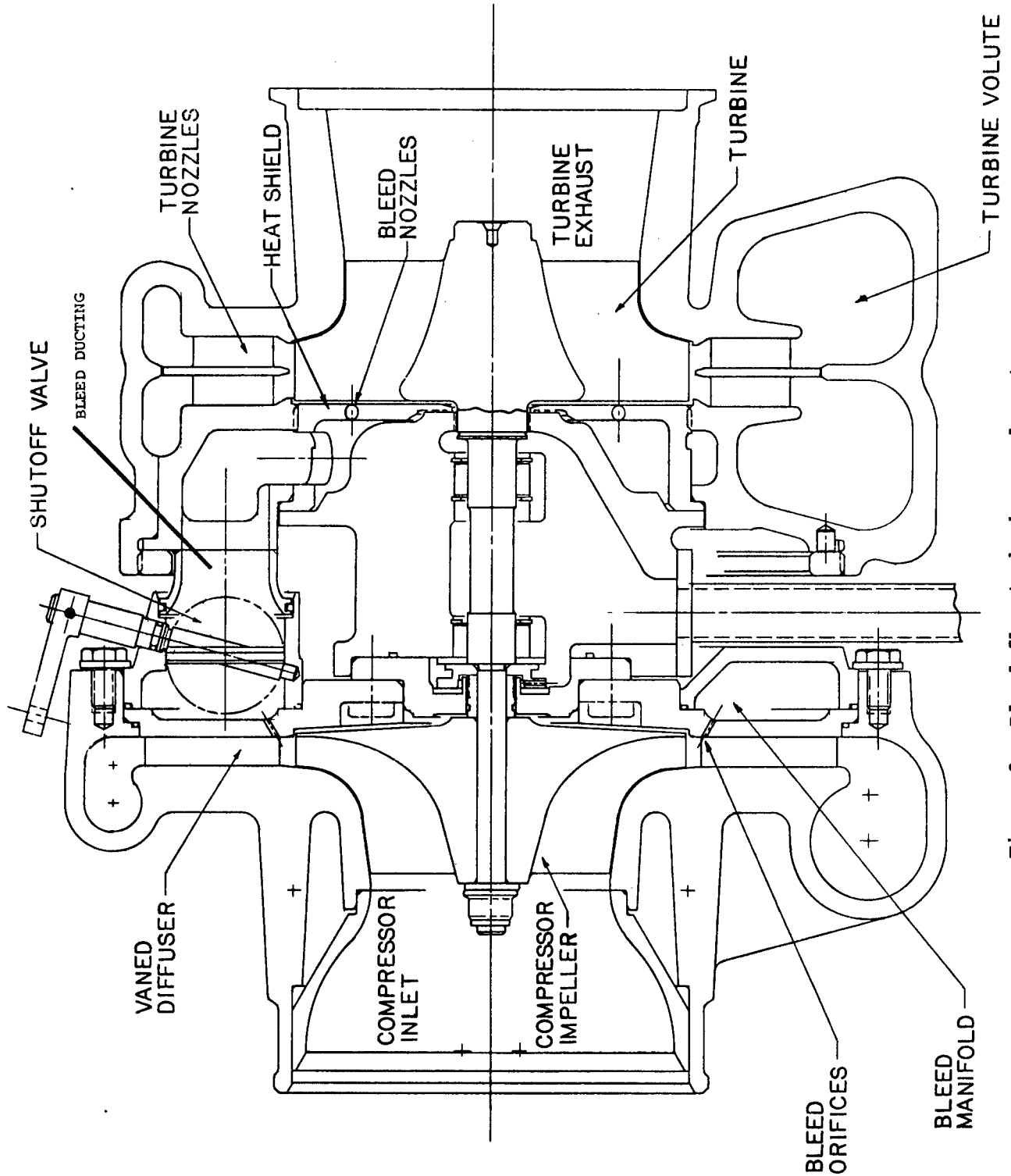
Figure 3. Bleed flow turbocharger layout

V_{inlet}
airflow

RATED CONDITION
Angle of attack =
Angle of blade leading edge -
Relative angle of incident airflow.
Conventional design yields near
zero angle of attack at rated
condition.

W_{inlet}
relative
to blade

θ_{inlet}
relative
to blade

θ_{blade}

$U_{tangential}$
blade RMS

V_{inlet}
airflow

LUG CONDITION
Decreasing inlet airflow =
Decreasing relative angle of
incidence =
Increasing angle of attack to the
point where flow separation and
inducer stall occurs.

$U_{tangential}$
blade RMS

Figure 4.   Vector diagram demonstrating effect of reduced impeller flow on
inducer angle of attack with conventionally designed compressors

-12-

RATED CONDITION
Conventional exducer design yields near axial (zero swirl angle) absolute exit flow velocity.

$U_{tangential}$
blade RMS

$V_{channel}$
gas exit

W_{exit}
absolute
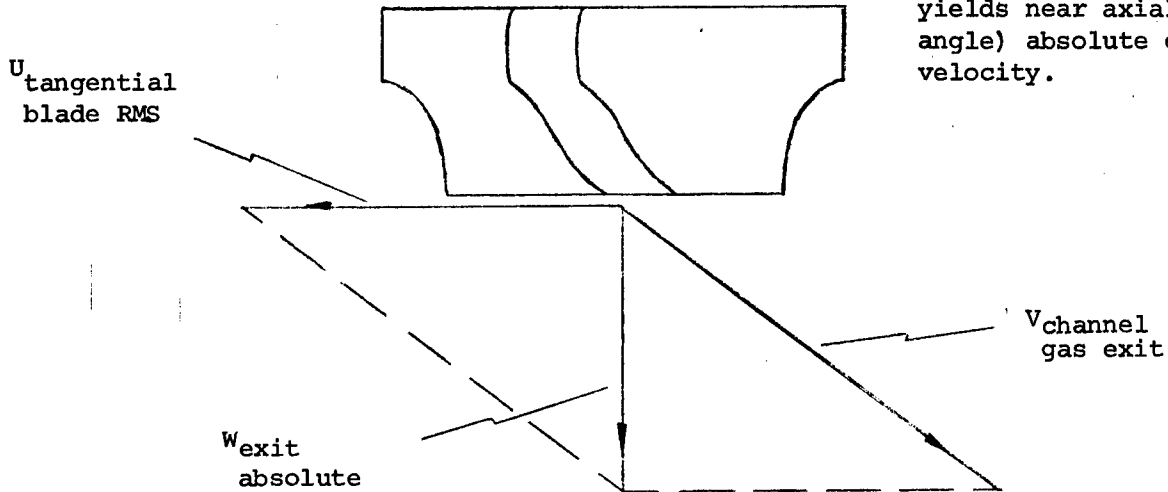
LUG CONDITION
Decreasing exit channel gas flow = increasing angle (positive swirl) of absolute gas exit resultant velocity, which impairs turbine efficiency.

$U_{tangential}$
blade RMS

$V_{channel}$
gas exit

θ_{swirl}
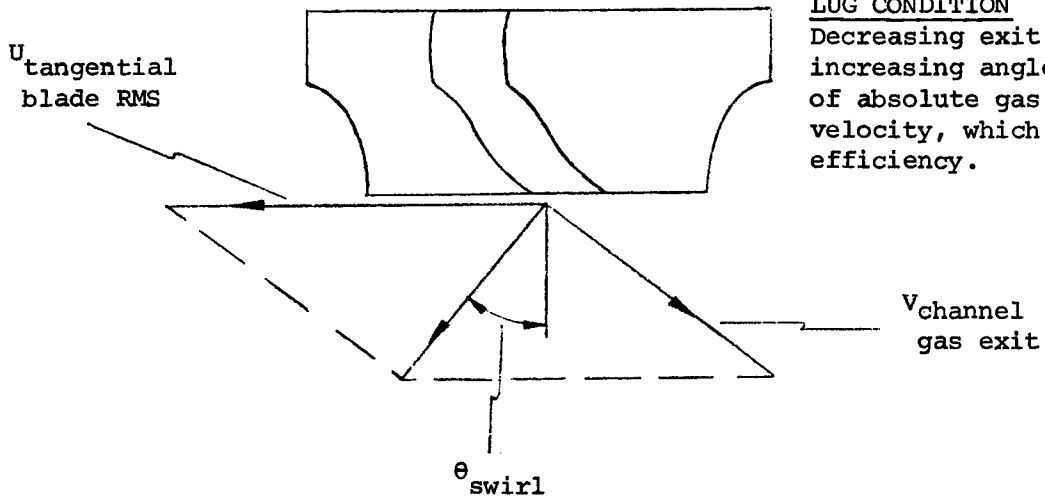
Figure 5. Vector diagrams demonstrating effect of reduced exhaust flow on turbine exducer exit flow angle with conventionally designed turbines

3.0 THEORETICAL CONSIDERATIONS

3.1 Basic Twin-Spool Concept

A schematic layout of the twin-spool turbocharger is presented in Figure 6. As shown there, the basic twin-spool components include:

1. Radial turbine rotor and outer shaft assembly, and

2. Radial compressor wheel coupled to the above.

3. Turbine exducer section, and

4. Compressor inducer section coupled to the above with a separate independent shaft.

The general operation of the twin-spool turbocharger concept is as follows: The radial compressor wheel and turbine rotor operate as would a conventional turbocharger rotating assembly; however, surplus available exhaust gas energy at the radial turbine exit is converted into shaft work via the separate turbine exducer section. This extra work is delivered to the compressor inducer section which, in conjunction with the turbine exducer, turns at a reduced rotational speed with respect to the radial section assembly.

Figure 7 presents a vector diagram which illustrates the aerodynamic boundary conditions affecting each of the axial/radial components in the twin-spool turbocharger. As shown there, near zero inducer angle of attack and near zero exducer gas exit swirl angle are achievable due to the variable speed (a function of turbocharger airflow) of that common assembly. In addition, the transition of flow from one stage to a successive stage can be achieved efficiently (near zero angles of attack) as well, through proper design of channel flow areas and blade angles. The resultant speed of the inducer/exducer assembly (with respect to the radial section assembly) is a function of the aerodynamic design of the twin-spool components and is discussed in detail in Section 4.2.
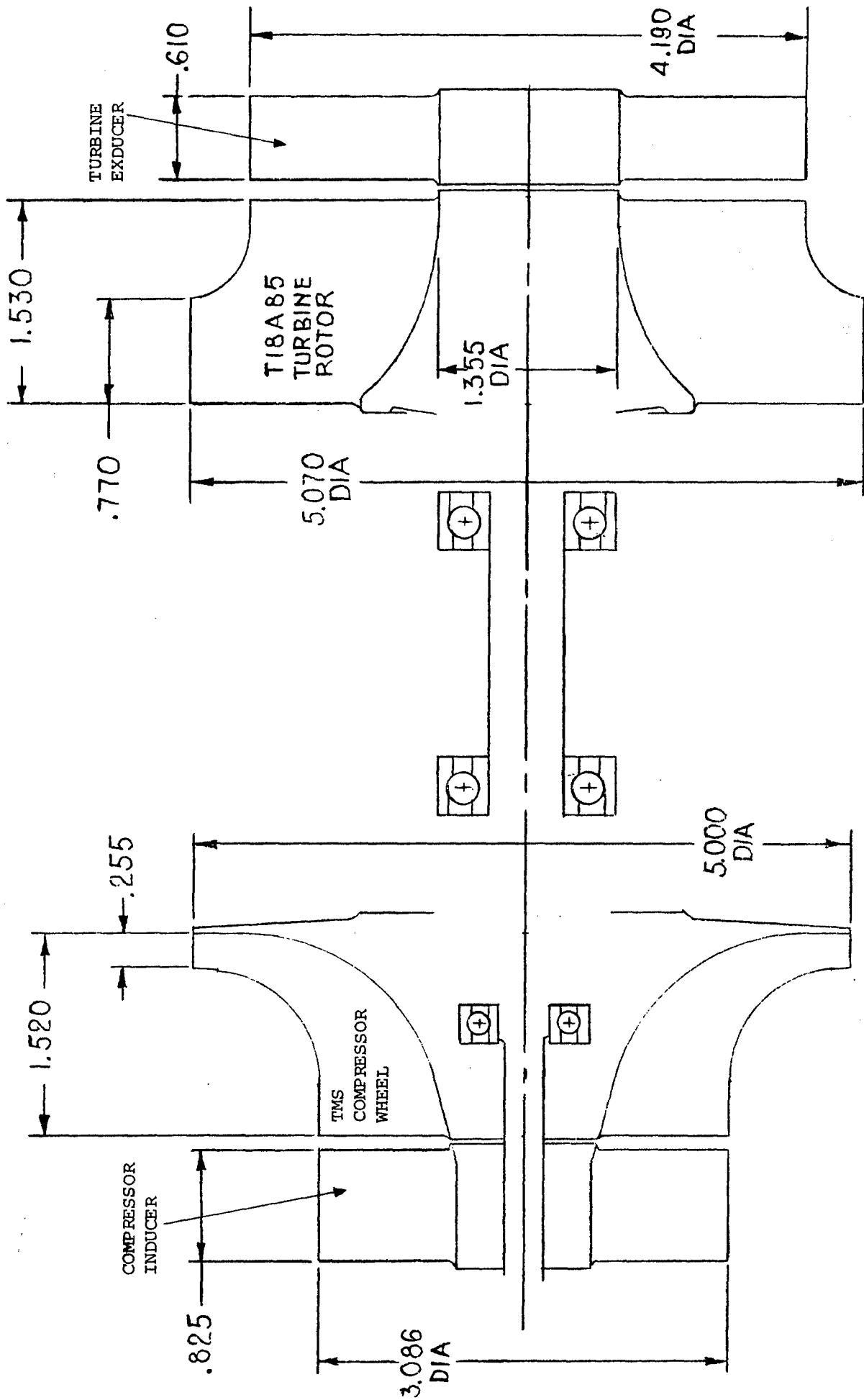
Figure 6. Conceptual layout of twin-spool turbocharger compressor and turbine stages

FULL SIZE

W_{inlet} relative

V_{inlet} axial $= \dfrac{\dot{m}}{A_{inlet} \, A_{inlet}}$

$U_{tang} = \Omega_{axial} R_{RMS}$

INDUCER
SECTION

$V_{channel}$ exit $= \dfrac{\dot{m}}{\rho_{exit} A_{channel}}$ exit

W_{exit} absolute

W_{inlet} relative

RADIAL
COMPRESSOR
SECTION

$U_{tang} = \Omega_{radial} R_{RMS}$

$\dot{m}_{comp}$

$\dot{m}_{turb}$

$U_{tang} = \Omega_{radial} R_{RMS}$

$V_{channel}$ exit $= \dfrac{\dot{m}}{\rho_{exit} A_{channel}}$ exit

RADIAL
TURBINE
SECTION

W_{exit} absolute

W_{inlet} relative

EXDUCER
SECTION

$U_{tang} = \Omega_{axial} R_{RMS}$

$V_{channel}$ exit $= \dfrac{\dot{m}}{\rho_{exit} A_{channel \ exit}}$

W_{exit} absolute

Figure 7. Vector diagram showing aerodynamic relationships affecting twin-spool rotating elements

-16-

4.0 HARDWARE DESIGN AND FABRICATION - FIRST DESIGN TWIN-SPOOL TURBOCHARGER

Figure 8 presents a layout drawing of the complete (first design) twin-spool turbocharger. As shown there, the turbocharger contains separate shafts which allow independent operation of the inducer/exducer assembly from the radial compressor/turbine assembly. The primary design philosophy of the twin-spool turbocharger shown here is to produce a cost-effective unit which is competitive with commercial, existing turbochargers. This is accomplished through the use of many off-the-shelf components (i.e., bearing housing, rotor shaft, floating sleeve bearings, thrust bearing, heat shield, turbine housing, etc.) which could be used as-is or without major modification and through simplicity of design which calls for a minimum of added components.

4.1 Bearing System

Figure 9 presents a detailed layout of the (first design) twin-spool turbocharger rotating assemblies. This design utilizes a modified AiResearch T18A85 turbine rotor (bored through to accept inner shaft) supported on floating sleeve bearings within an AiResearch T18 bearing capsule. The outer shaft "stack-up" is completed with the installation of the thrust spacer, seal ring spacer, radial compressor impeller and spanner nut/belleville washer combination.

The inner shaft is supported by i) a deep groove radial ball bearing at the inducer end, which is retained in a bore within the radial compressor wheel and ii) a coated journal/air bearing sleeve at the exducer end, which is located in a bore within the radial turbine rotor. The ball bearing, which locates the inner shaft axially as well as radially, is grease-packed and sealed. It was rated for long life in the twin-spool turbocharger as it needed only to endure the differential speed between the respective shafts (up to 25,000 RPM). The inner shaft journal surface, at the exducer end, is coated with Everlube 811 compound to provide surface lubricity during start-up and shut-down modes of turbocharger operation. During normal running operation, bleed air from the radial impeller backface region is ducted between the shafts to the exducer journal area to i) cool the journal bearing area and ii) form an air film bearing between the inner shaft journal and corresponding bearing shell. In addition, an Everlube 811 coated snubbing journal is located at the center of the inner shaft which, under static conditions, has a small diametral clearance with respect

-18-

to the outer shaft bore but is provided to restrain inner shaft excursion during dynamic first-order flexural mode.

Two designs for the exducer end air bearing shell were considered: i) a fully machined stainless steel insert with Everlube 811 coating for start-up lubricity (as shown in Figure 9) and ii) a bearing insert made from Graphitar (a formed carbon/graphite composite material) as shown in Figure 10. The study of both approaches showed that either design was capable of withstanding temperatures up to $1200^{\circ}F$ (high temperature limitation of both Everlube 811 and Graphitar materials); but in practice, the Graphitar bearing, when impregnated with synthetic turbine oil prior to operation, demonstrated greater longevity and reliability.
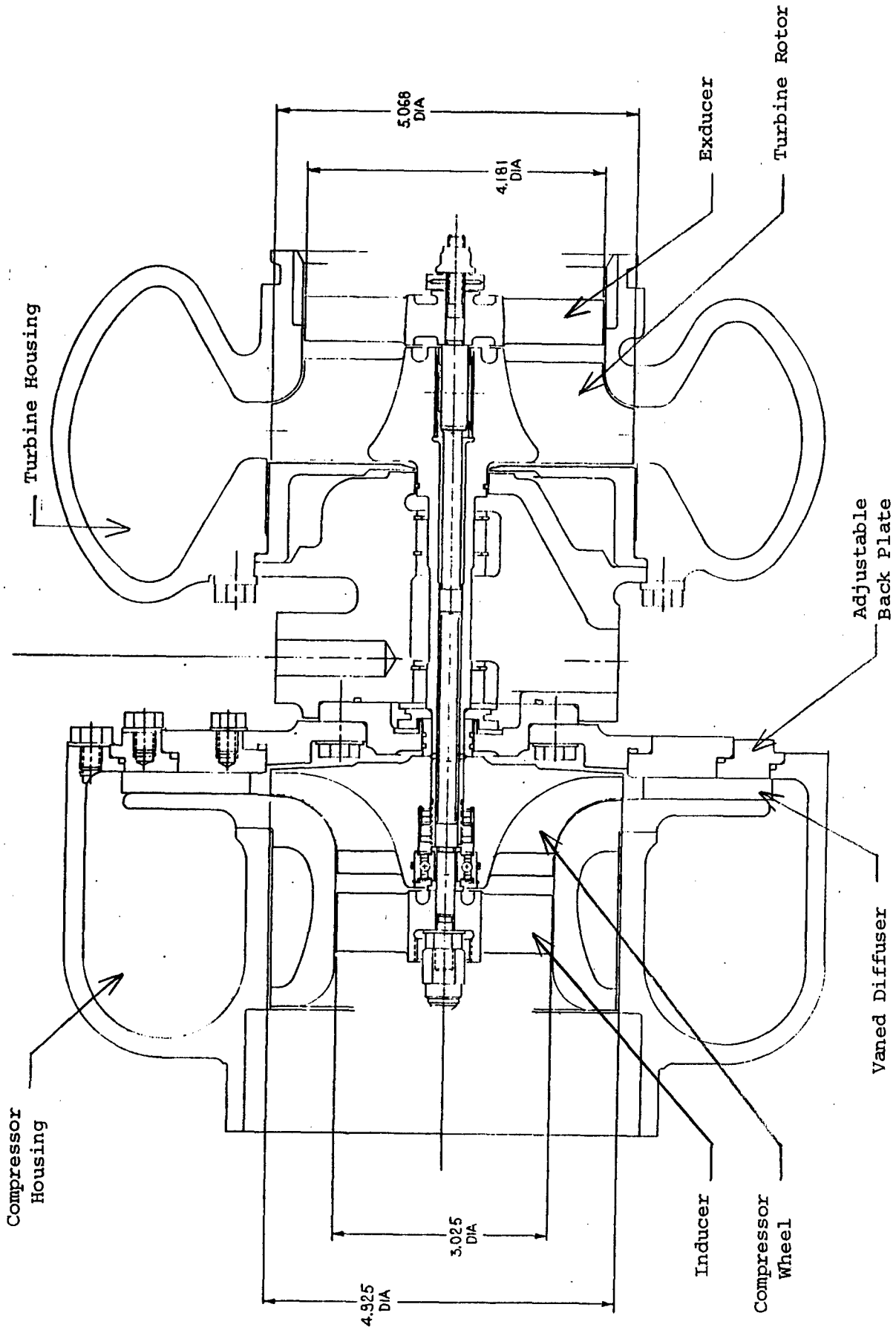
Figure 8. Complete Twin-Spool Turbocharger Layout

Dimensions shown on drawing: .511, .286, 4.32 RE., .040, .251, .560, .044, .561, 1.000, 3.086 DIA, .250, 5.000 DIA

Callouts: 8, 13, 7, 4, 3, 9, 6, 10
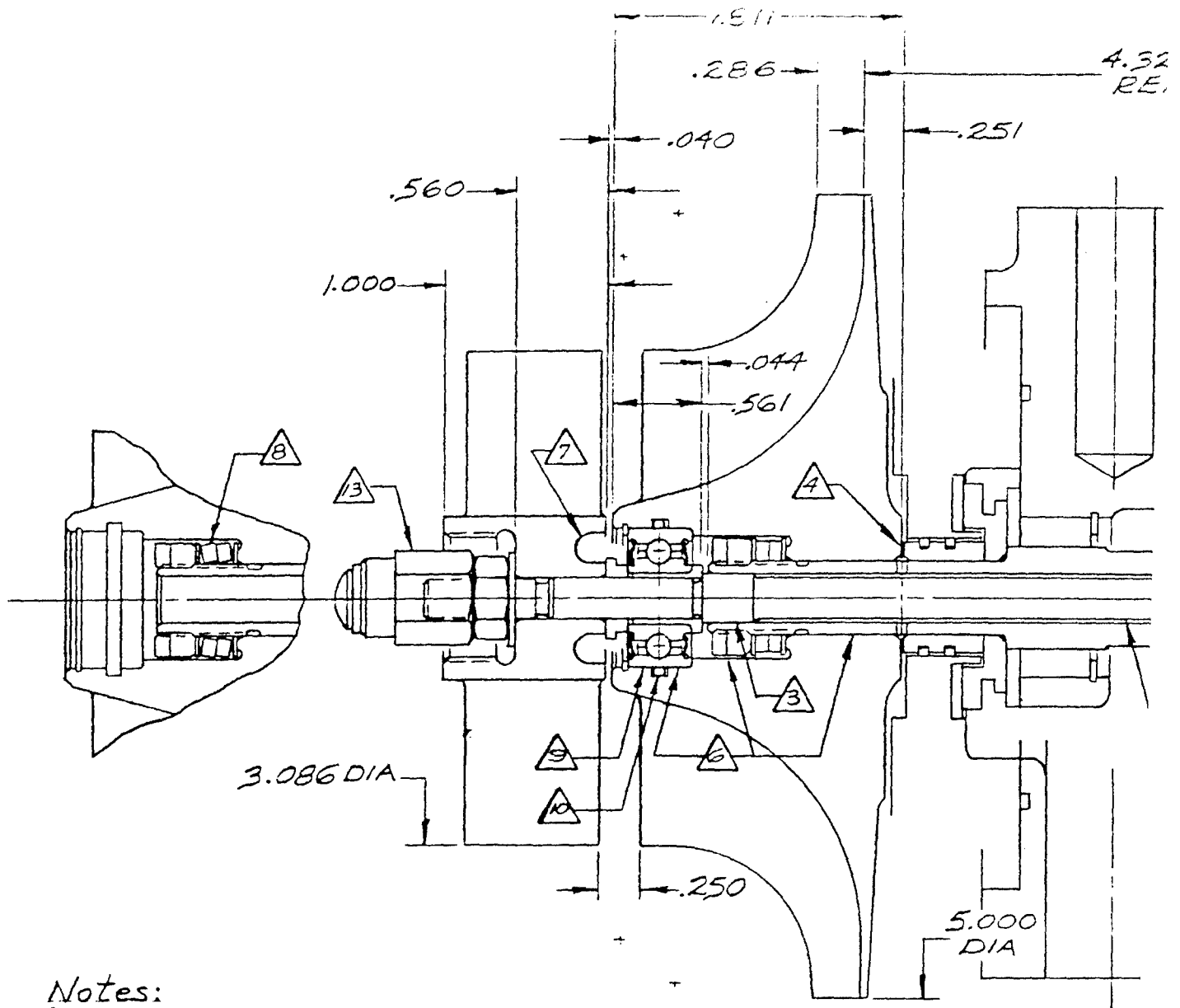
Notes:

1. Air bearing with journal dry lube coated to allow low differential speed operation.

2. Dry lubricant coated bumper land to allow passing thru first & second critical.

3. Dry lubricant coated seal land to minimize air flow thru axial compressor bearing.

4. Clean air for air bearing due to centrifuge.

5. Air inlet to gas bearing.

6. Bores final machined after overspeed spin to hold size & avoid low cycle fatigue.

7. Hubs relieved to decrease overhung weight and enhance pilots.

8. Spring washers to improve short bolt compliance and nut locking.

9. Barden 3BSSTX2 ABEC 7 bearing

10. "O" ring

11. Radial

12. .25 di shear rotor rotati

13. Axial

①

T-18 FRAME

.911
.286
.040
.251
4.320 REF
1.570
.040
.770

.044
.561

⑤
④

③

⑥

①

②

⑪

⑥

⑫

.250

.250

5.000 DIA

5.068 DIA
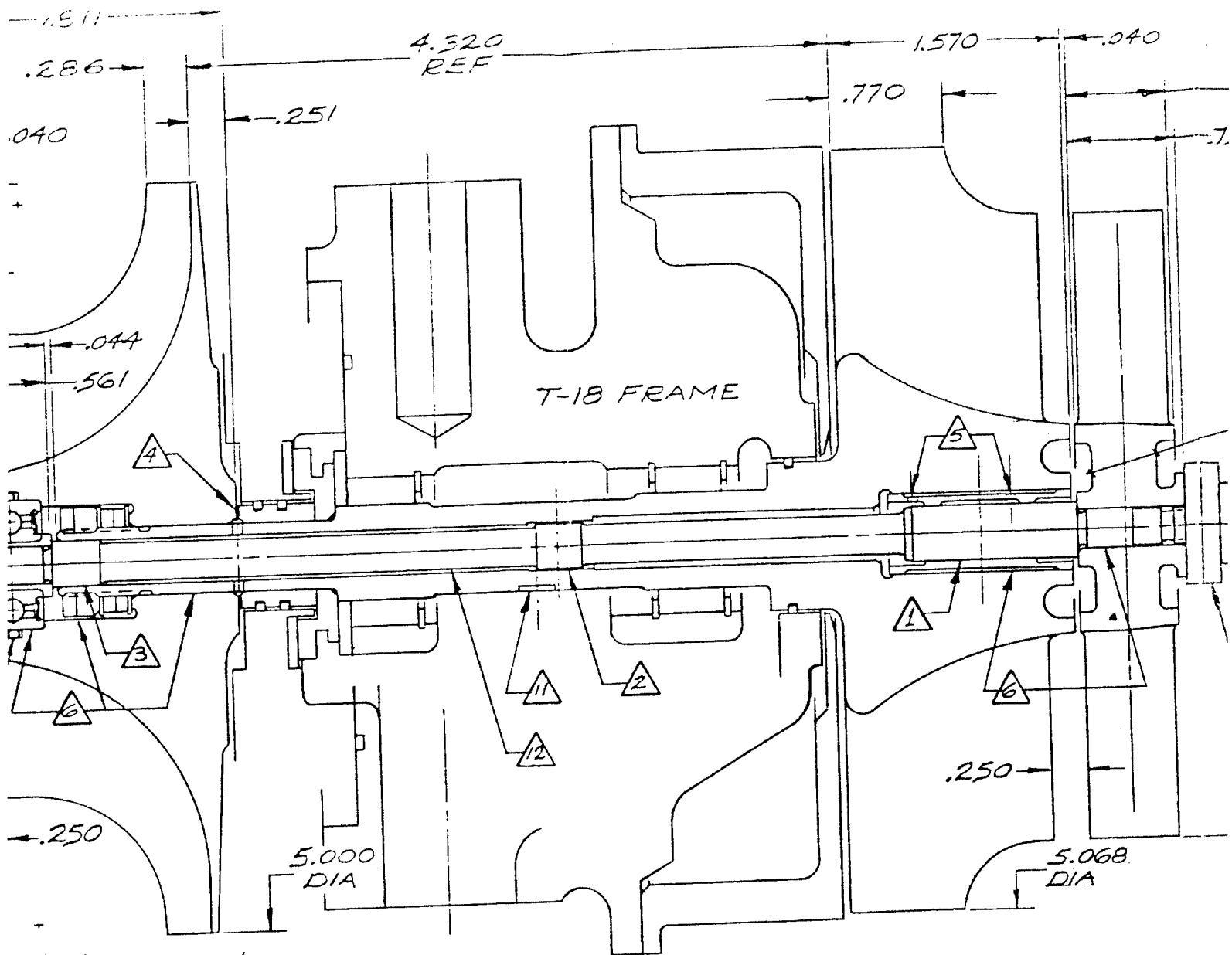
ated to allow low

to allow passing thru

minimize air flow

centrifuge.

speed spin to hold

ing weight and

oft compliance and

earing

⑩ "O" ring to resist outer race rotation when bore grows
⑪ Radial rotor speed indication.
⑫ .25 dia. shaft: first bending critical < 10,000 RPM, shear stress < 10,000 psi, torsional critical well below rotor blade frequency & shaft weight ≅ 11.0% of rotating weight to ease balance problem
⑬ Axial rotor speed indication.

②

9 FRAME

1.570 — .040
.770
.700
.750

5
7
1
2
6
8

.250
4.181 DIA
5.068 DIA
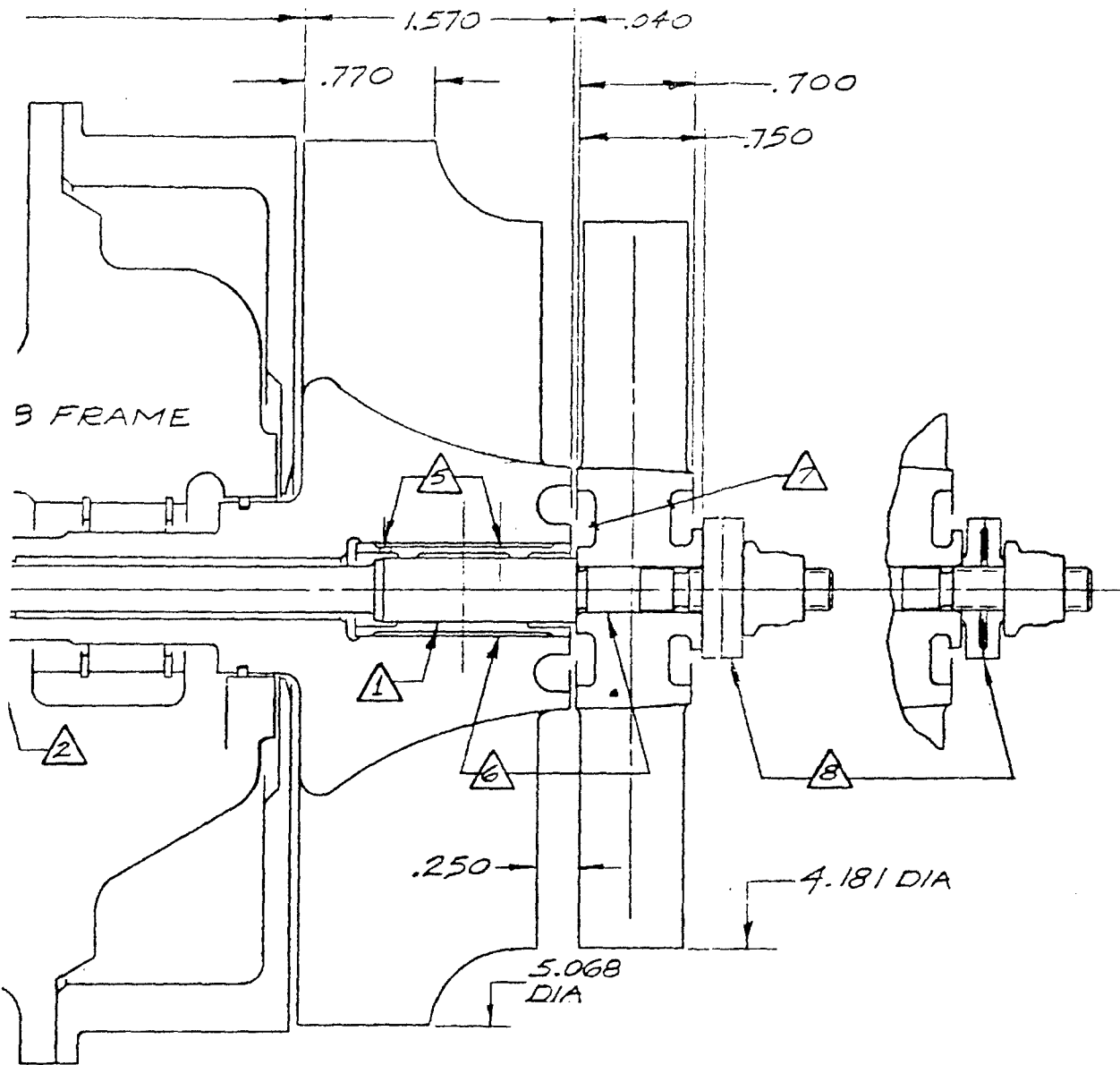
: outer race rotation when bore grows
peed indication.
': first bending critical < 10,000 RPM,
< 10,000 psi, torsional critical well below
equency & shaft weight ≅ 11.0% of
it to ease balance problem
eed indication.

Figure 9.   Detailed layout of twin-spool
turbocharger rotating assemblies

③

Graphitar
Journal
Bearing
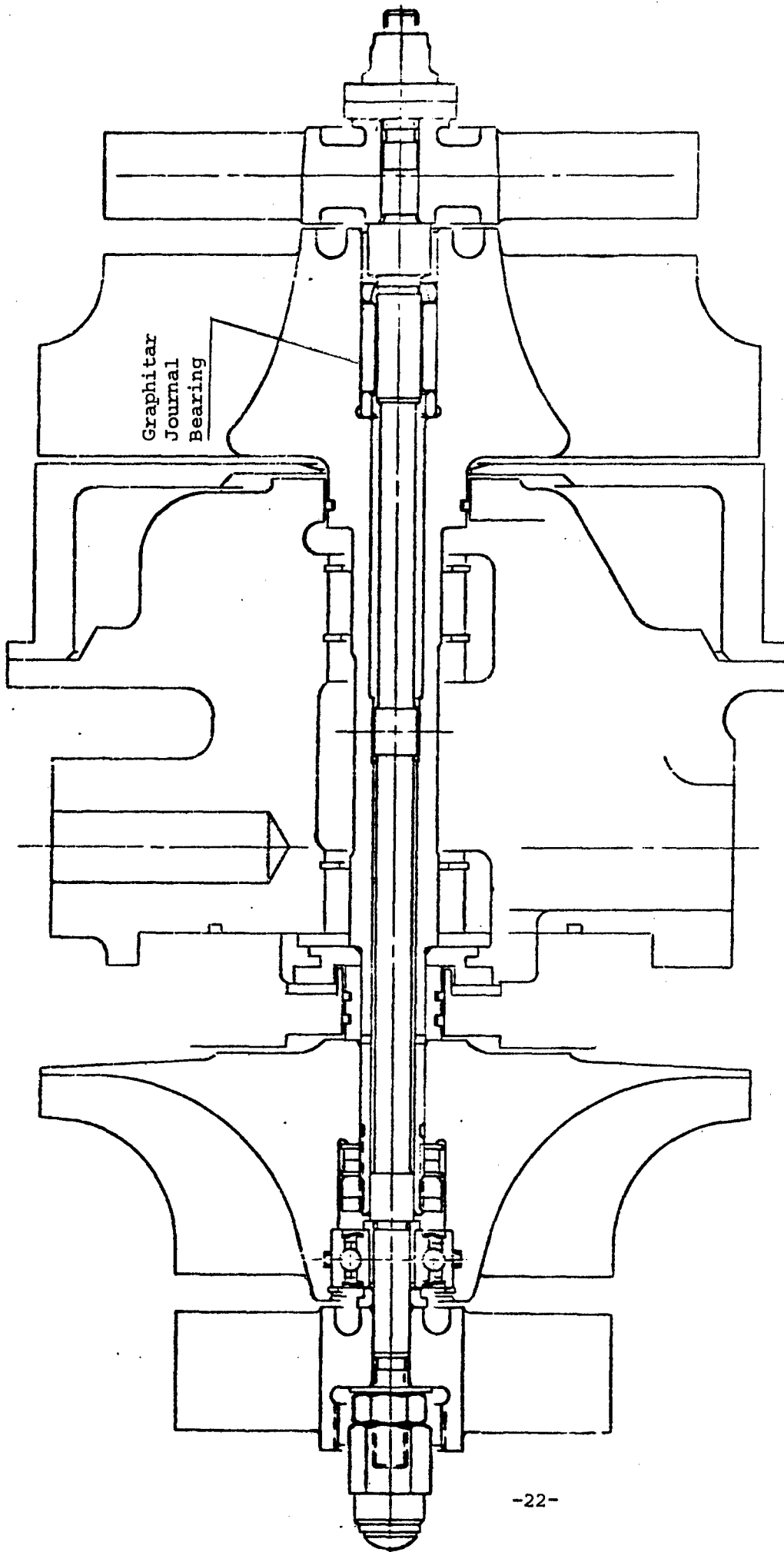
Figure 10. Modified twin-spool turbocharger using Graphitar journal bearing at turbine end

-22-

4.2 Principal Rotating Components

The four principal rotating components of the twin-spool turbocharger are i) the compressor inducer, ii) the radial compressor impeller, iii) the radial turbine rotor and iv) the turbine exducer and are presented conceptually in Figure 11. The aerodynamic design of these components involved the blending of the following considerations:

A) Solidity - (From Reference 3) Closer blade spacing (with respect to chord length) means that a given blade can operate over a wider range of inlet flow angles without separation. In addition, closer spacing means that the flow angle leaving a blade-to-blade passage (flow calculations are assumed to be average values for a given cross section) exhibits smaller variation across the blade passage and is more likely to exit parallel to the blade exit angle. In the instance where blade spacing, s, is fixed (i.e., when cutting an inducer or exducer from existing wheel designs) the solidity of the element is obtained by increasing the blade chord length, C, thereby improving the C/s ratio.

B) Blade angles - The blade angles of the principal components are optimized to satisfy the following criterion:

i) Leading edge blade angles are adjusted to minimize incident angle of attack on a given stage with emphasis placed on achieving near zero angle of attack at the lug (low engine RPM) condition for best efficiency in that range of operation.

ii) Trailing edge blade angles are adjusted a) for the inducer, to create sufficient loading (increased turning of airflow by the inducer means increased work done by the inducer stage) commensurate with exducer power output to achieve the reduced inner shaft speed desired and b) for the exducer, to achieve near zero exit swirl at reduced rotational speed, again with emphasis on optimization at lug operating conditions.

C) Wheel diameters - The diameters of the principal components are selected as follows:

i) The inducer diameter directly affects inlet annular flow area and, likewise, inducer inlet blade-to-blade passage area. This diameter is made just large enough to provide the required flow area to pass the rated (maximum power) engine airflow.

ii) The radial compressor wheel exit diameter is chosen to be consistent with the given airflow requirements as well. Suitability for a given range of airflow means the definition of an optimum blade-to-blade channel flow area, a function of overall wheel diameter (and blade height), with emphasis for optimization placed at the lug (low flow) condition. In practice, the ratio of exit diameter to inducer diameter may vary from about 1.4 to 1.9:1.

iii) The tip diameter of the radial turbine wheel is selected to achieve the optimum U/C_O ratio of 0.71 at design conditions, again with emphasis placed on low flow (i.e., lug engine speed) performance. The parameter U/C_O is the ratio of turbine tip speed to ideal (isentropically expanded) exhaust gas spouting velocity.

iv) The turbine exducer diameter is made as large as possible

to minimize axial gas exit losses. In conventional designs,

this would cause a large positive gas exit swirl; but, by

virtue of reduced exducer speed made possible by the twin-

spool concept, gas exit swirl is held to near zero values

at design conditions.

D) Efficiency - The primary design approach for the twin-spool turbo-

charger is to obtain i) optimum efficiency and performance at lug

engine conditions to obtain maximum boost pressure and ii) only

that efficiency and performance at the rated engine condition to

generate the (combustion-limited) rated boost pressure.

The results of the aerodynamic design, presented in Table 1, were

generated using a rather sophisticated computer program written to perform the

difficult and tedious task of matching the two twin-spool shafts. To be more

specific, this computer program determines the available turbine horsepower (for

both the radial and exducer sections) as a function of the split turbine geometry

and then determines the resultant compressor speed (for both the radial and

inducer sections) to absorb this horsepower, again as a function of the split

compressor geometry. The program uses several iterative techniques until the

horsepowers, speeds and flow conditions for the inducer/exducer sections and the

radial sections are matched.

Fabrication of the twin-spool turbocharger rotating components was

accomplished by a) axially splitting the inducer and radial compressor impeller

each from separate TMS 5", 40° backswept cast aluminum impellers and b) axially

splitting the radial turbine rotor and exducer sections each from separate

AiResearch T18A85 turbine wheels. Figure 12 presents photographs of the semi-finished inducer and exducer sections, while Figures 13 and 14 present photographs of the radial turbine and radial compressor wheels, respectively.

4.2.1 Spin Testing

The function of spin testing was to intentionally stress the bores of critical rotating components to yield by spinning them to 10 percent over rated speed. Following spin testing, the bore is then final machined. This process is done to eliminate further yielding in service thereby holding critical bore dimension more accurately and also to avoid low cycle fatigue.

Figure 15 is a photograph which shows the complete spin test hardware package, with radial turbine wheel installed, ready for testing in the TMS test facility. Features of the spin test hardware package include the following:

1) T18 bearing capsule (with floating sleeve bearings) modified for magnetic speed pickup access to the turbine shaft.

2) T18 turbine housing modified for cold-air testing.

3) Protective sling material surrounding bearing capsule and turbine housing.

4) Containment shield which fits in place of standard compressor housing.

5) Turbine trap downstream of turbine housing to capture high energy fragments should turbine failure occur.

6) Accelerometer to monitor dynamics of rotating assembly.

The radial turbine rotor was installed into the bearing test capsule with an artificial compressor inpeller secured in the "stack-up" (for overall assembly balance) and was successfully spun to 83,000 RPM. The radial

-26-

compressor impeller and turbine exducer were tested as well by mating each
to separate T18 turbine rotors with shafts modified to accept the respective
undersized bores. These components were both tested to 83,000 RPM which
corresponds to 10 percent and 15 percent over rated speed for each wheel,
respectively. During all tests minimal vibration was observed and no indication
of bore distortion was detectable.

Following spin tests, all components were final machined and
are presented in the photograph in Figure 16. Figure 17 presents a photograph
of the assembled (first design) twin-spool turbocharger with compressor and
turbine housings removed.

4.3 Compressor Diffuser and Housing

Figure 18 presents a photograph of the TMS adjustable 21-vane diffuser/backplate system. This diffuser was chosen for use with the twin-spool turbocharger because:

1. Data from airflow testing shows that this diffuser is capable of providing both the range and the efficiency needed to match or extend the operating envelope currently available with the NTC-475 engine with the originally-equipped twin-turbo package.

2. The adjustability of the diffuser allows for fine-tuning of the engine/turbo system during actual dyno testing. By having control over the diffuser throat area, the optimum balance between good engine lug performance and control of boost pressure at the rated condition may be obtained without the need to obtain and/or fabricate new hardware. The initial throat area for the diffuser was set at 1.6 in^2.

3. The diffuser was available and has been proven to be a valuable developmental tool.

In addition, an AiResearch torus style compressor housing was obtained and modified to a) match the shroud contour of the twin-spool compressor section and b) interface with the TMS adjustable diffuser/backplate system described above.

4.4   Turbine Nozzles and Housing

Calculations to match the correct exhaust manifold pressure to engine exhaust flow characteristics of the NTC-475 diesel engine resulted that the effective turbine nozzle area should be 2.91 in^2.   In an AiResearch turbine housing for use with a 5.1 inch diameter turbine wheel, this translates into the parameter A/R = 1.14.   The AiResearch nozzleless, volute style turbine housing is preferred because it has been shown to provide good engine lug performance due to its ability to recover exhaust gas pulse energy at low engine speeds.   Consequently, the AiResearch nozzleless volute, A/R = 1.14, was obtained and modified to match the shroud contour and exducer size of the twin-spool turbocharger.
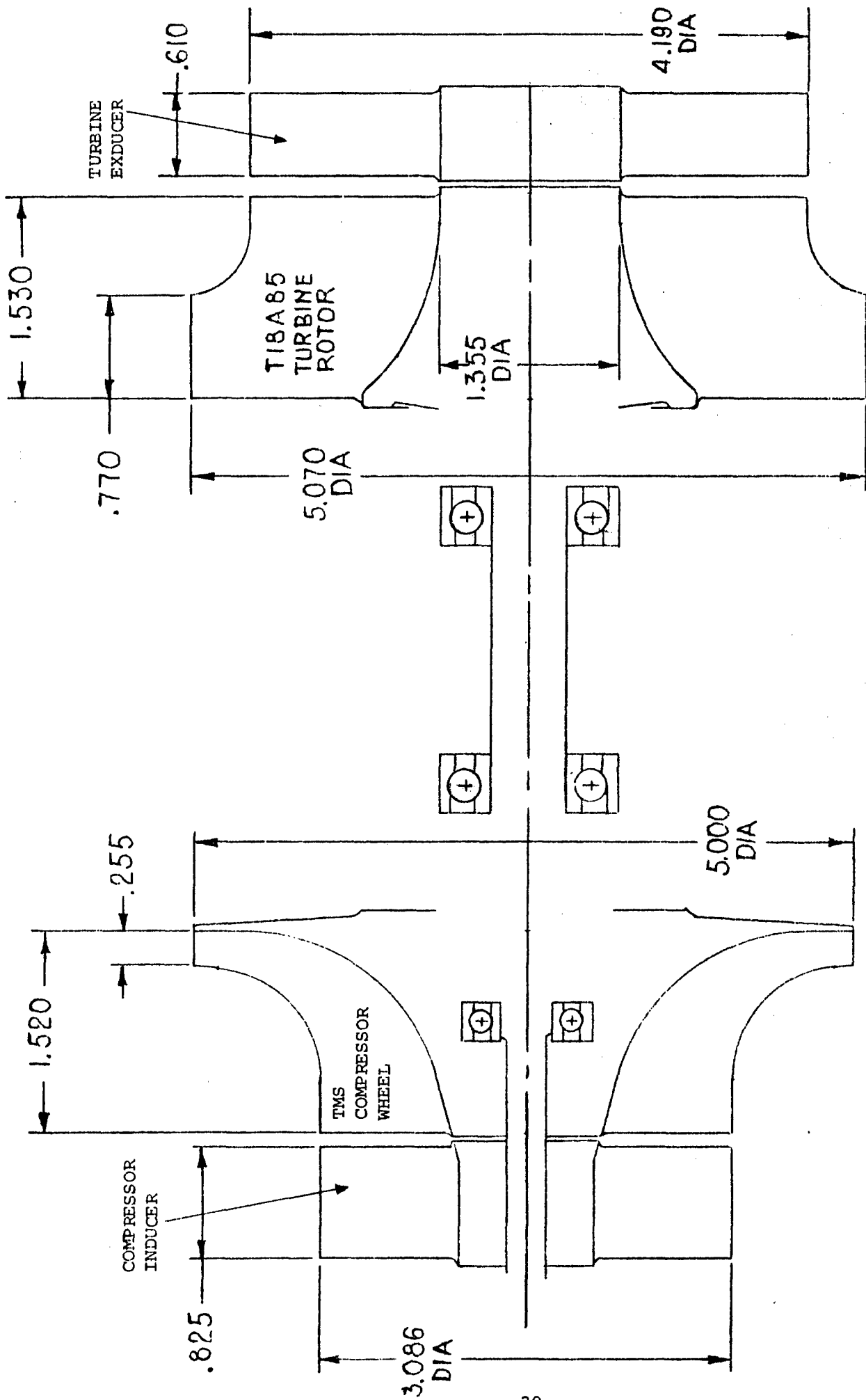
FULL SIZE

Figure 11. Twin-spool compressor and turbine wheel designs (using AID T18A85 turbine rotors and TMS 5" OD compressor wheels)

Labels within figure:

TURBINE EXDUCER

.610

4.190 DIA

1.530

T18A85 TURBINE ROTOR

1.355 DIA

.770

5.070 DIA

5.000 DIA

.255

1.520

TMS COMPRESSOR WHEEL

COMPRESSOR INDUCER

.825

3.086 DIA

Compressor Inducer Section

Diameter..................... 3.026 in.
Inlet Annular Area......... 6.39 in.^{2}
RMS Radius................. 1.128 in.
Inlet Blade Angle.......... 36.5 deg.
Inlet Channel Area......... 3.39 in.^{2}
Exit Blade Angle........... 69 deg.
Exit Channel Area.......... 5.09 in.^{2}
Number of Blades........... 10

Radial Compressor Section

Inlet Diameter............. 3.026 in.
Inlet RMS Radius........... 1.144 in.
Inlet Blade Angle.......... 49 deg.
Inlet Channel Area......... 4.59 in.^{2}
Exit Diameter.............. 5.00 in.
Exit Blade Angle........... 50 deg.
Exit Channel Area.......... 3.10 in.^{2}

Radial Turbine Section

Inlet Diameter............. 5.086 in.
Exit Diameter.............. 4.214 in.
Exit RMS Radius............ 1.578 in.
Exit Blade Angle........... 36.5 deg.
Exit Channel Area.......... 8.18 in.^{2}

Turbine Exducer Section

Inlet Diameter............. 4.214 in.
Inlet Blade Angle.......... 36.0 deg.
Exit Diameter.............. 4.214 in.
Exit RMS Radius............ 1.560 in.
Exit Blade Angle........... 53.5 deg.
Exit Channel Area.......... 6.48 in.^{2}

Compressor Housing and Diffuser

Diffuser Throat Area.... 1.60 in.^{2}
Number of Vanes......... 21
Housing Type............ Torus

Turbine Housing

Housing Type............ AID Nozzleless
                         Volute
Effective Nozzle Area... A/R=1.14

Where:

1) all angles are measured at the RMS radius
2) all compressor blade angles are given with respect to the tangential direction
3) all turbine blade angles are given with respect to the axial direction

Table 1. Key physical parameters of the twin-spool turbocharger first aerodynamic design
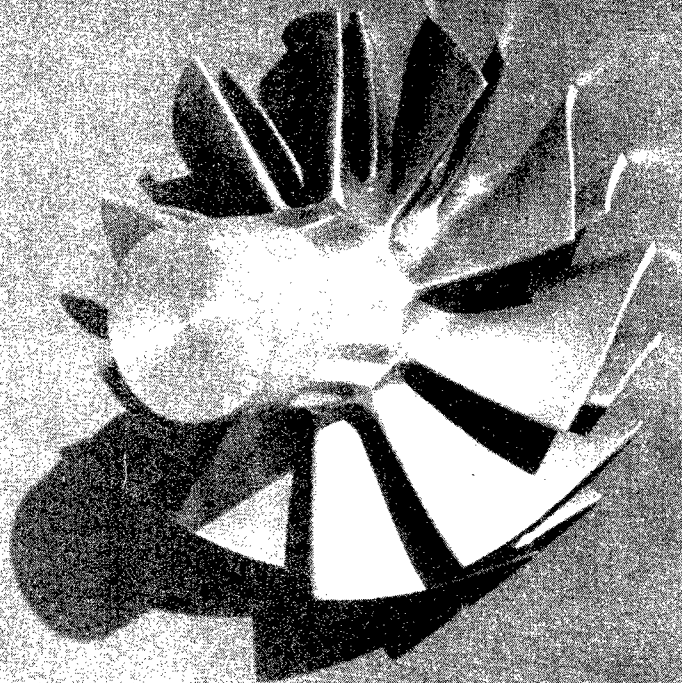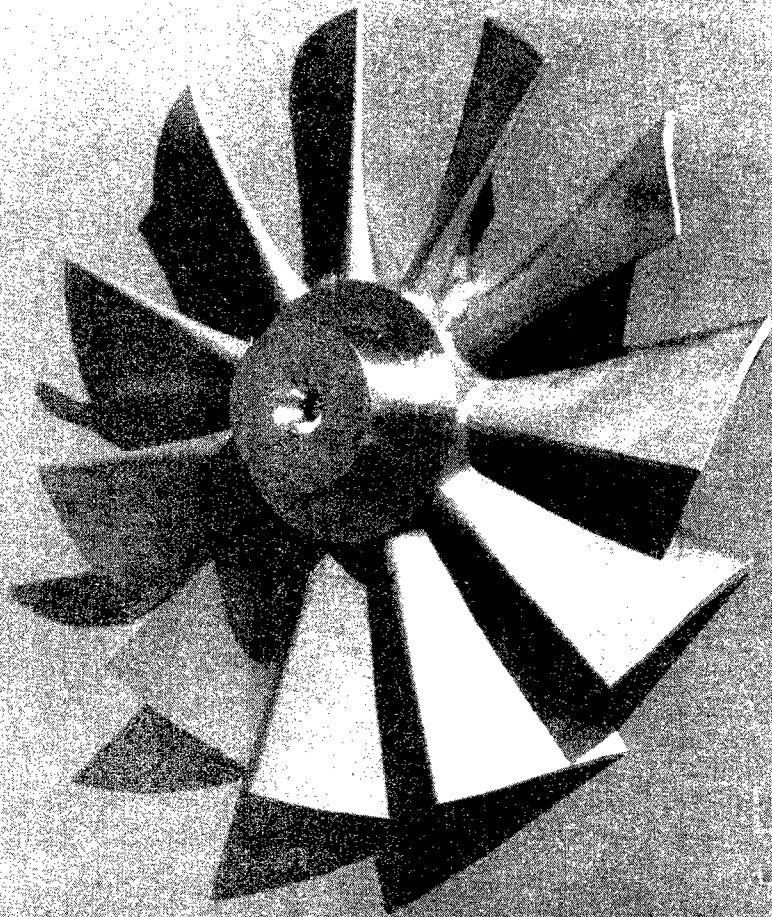
Figure 12. Photograph of inducer and exducer sections

-32-
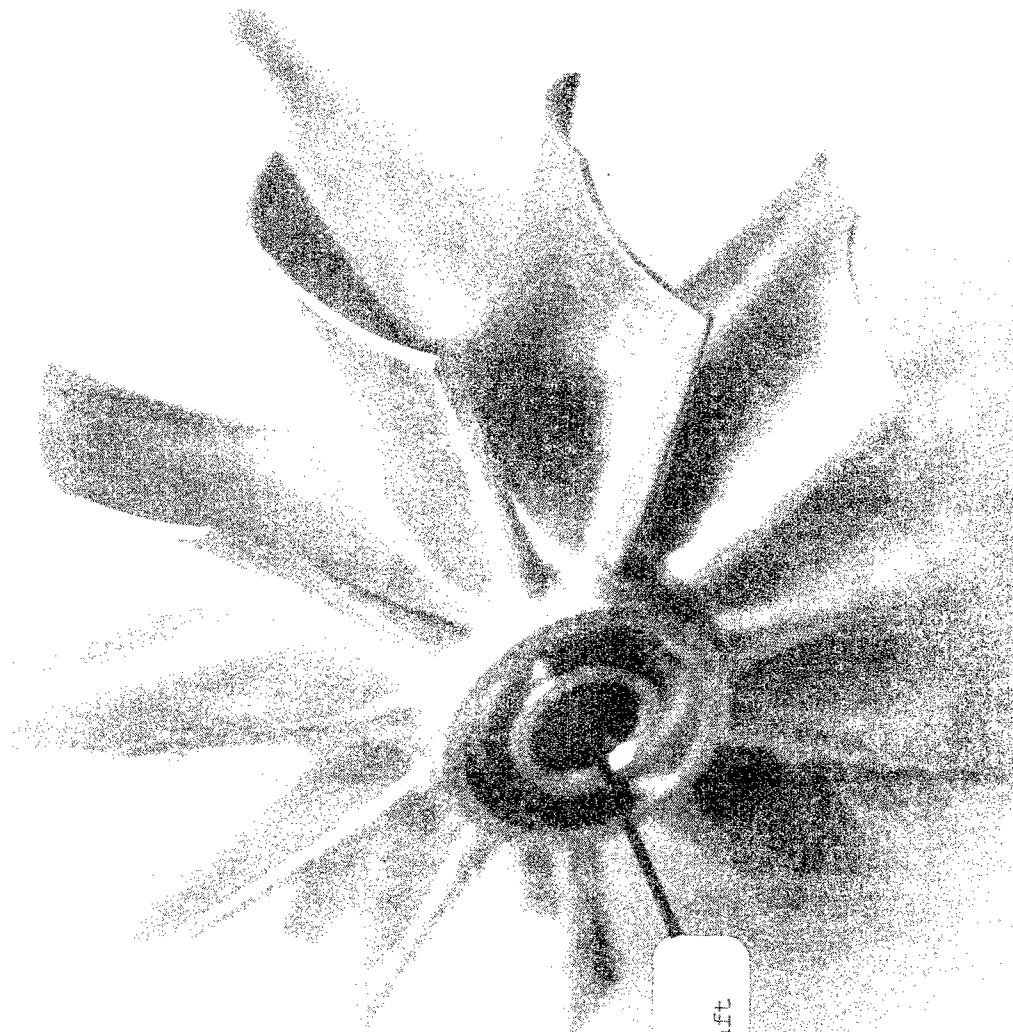
Hollow
turbine shaft

Figure 13. Twin-spool turbocharger radial turbine wheel
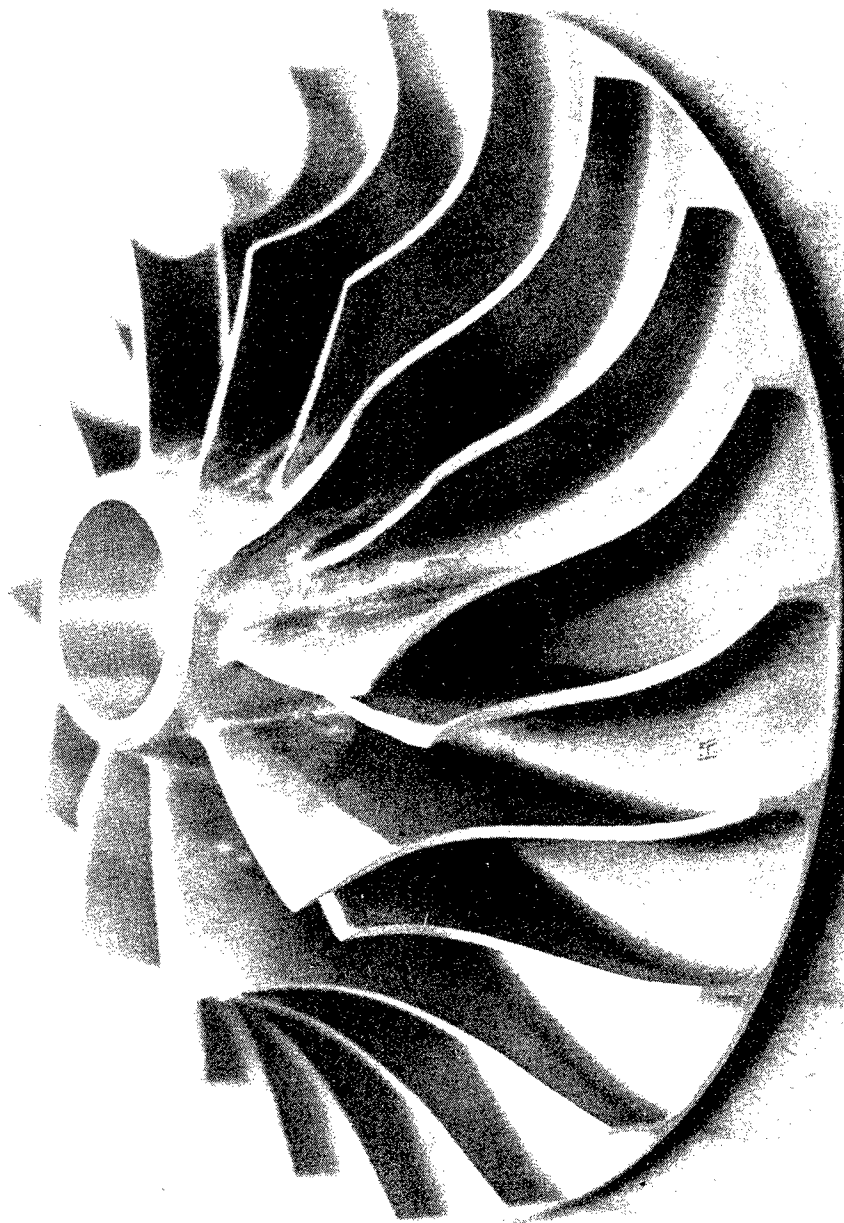
Figure 14. Twin-spool turbocharger radial compressor wheel

Turbine trap
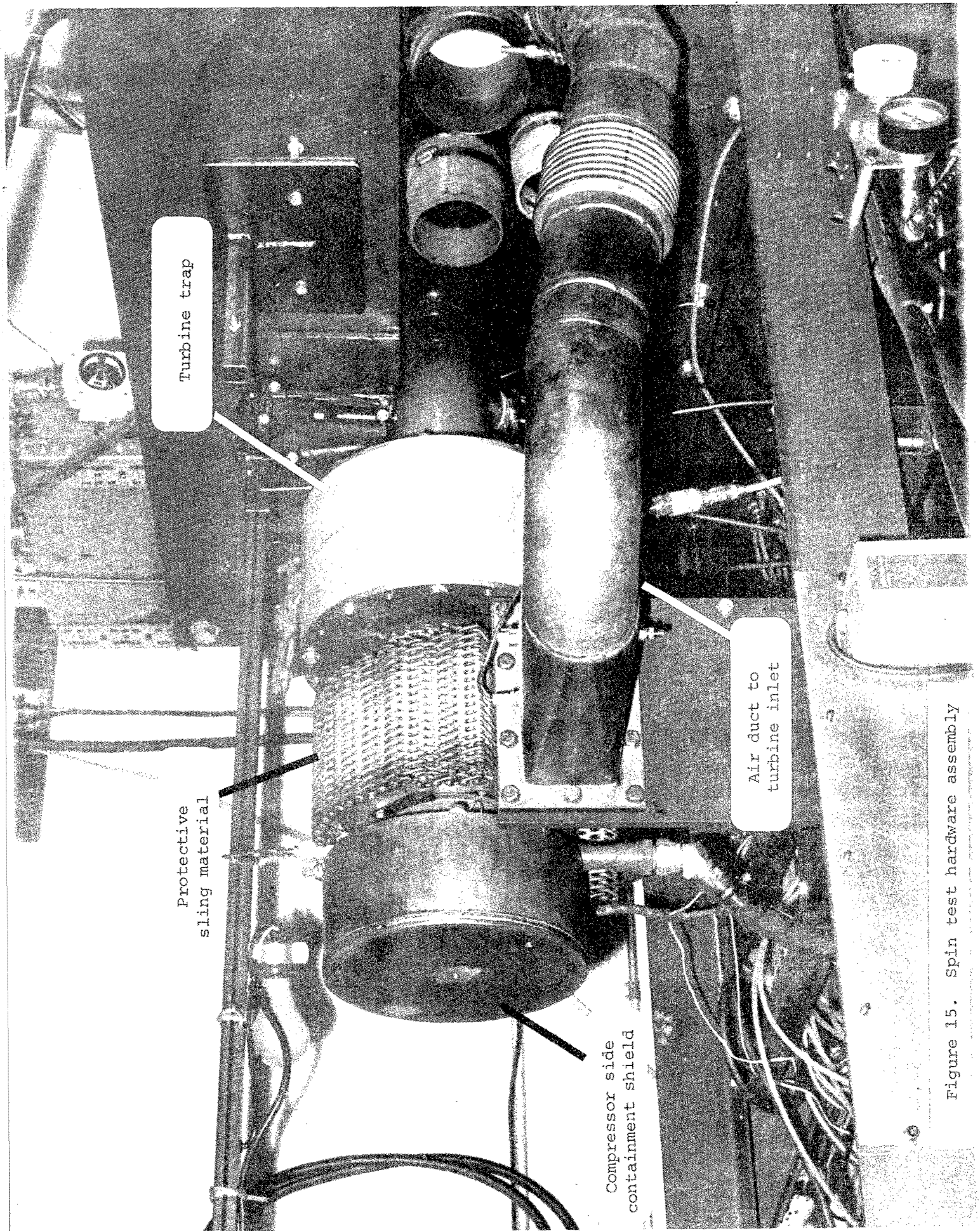
Protective sling material

Air duct to turbine inlet

Compressor side containment shield

Figure 15. Spin test hardware assembly

Radial
Compressor

Inner
Shaft

Inducer

Radial
Turbine

Outer
Shaft

Exducer
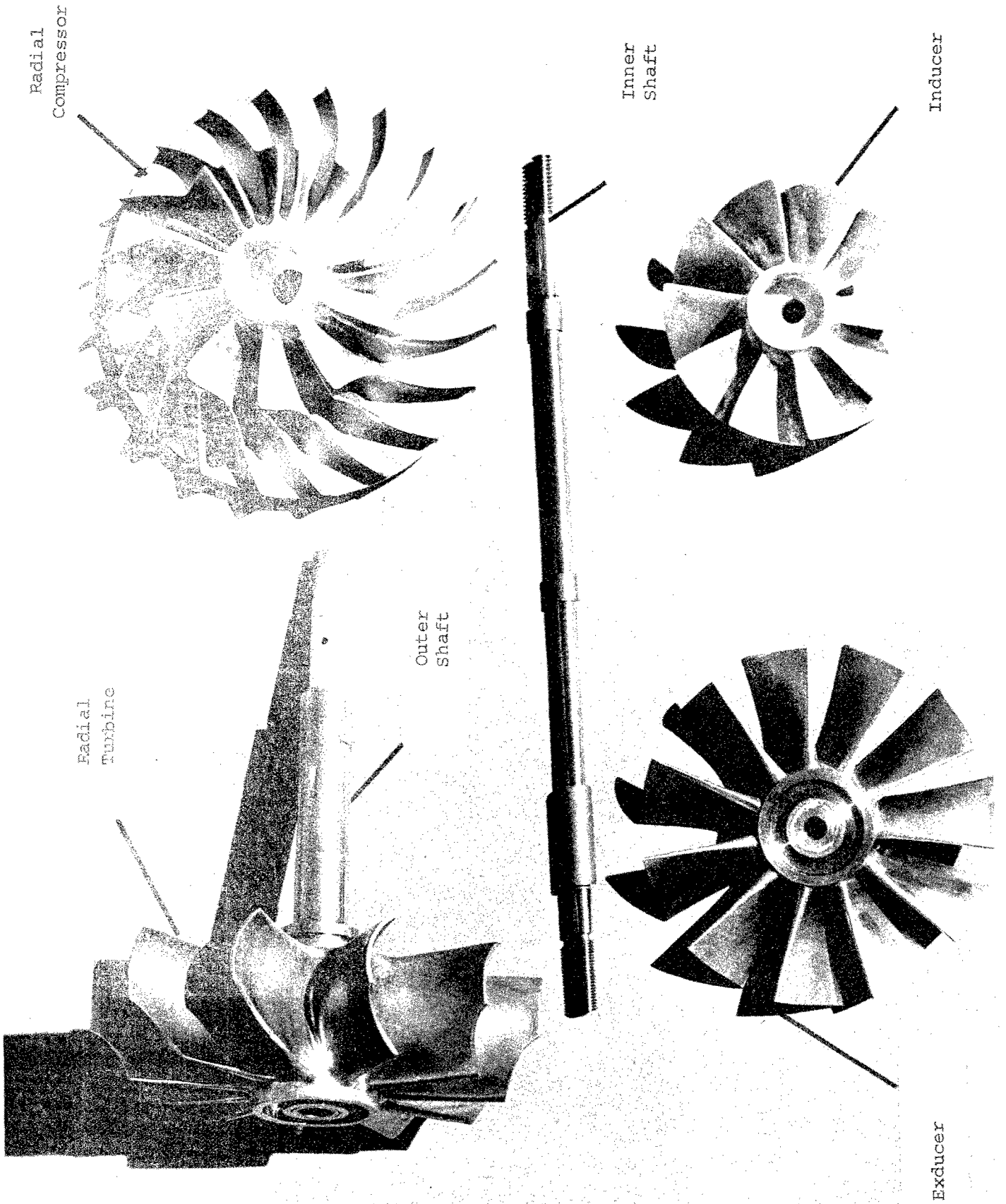
Figure 16. Finished rotating components of twin-spool turbocharger

-36-

Radial
Compressor Wheel

Inducer

Bearing
Housing

Turbine
Heat Shield

Exducer

Radial
Turbine Rotor
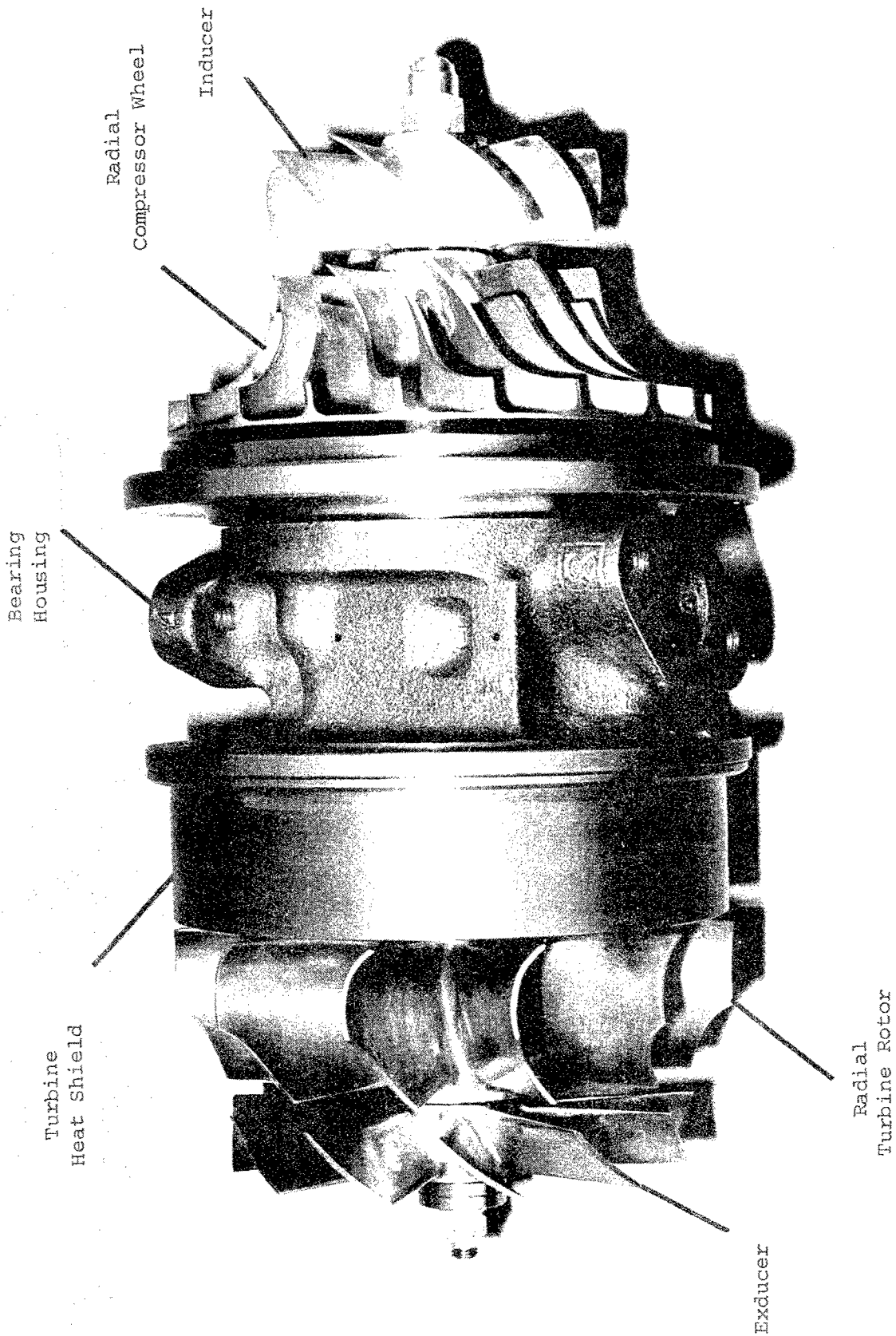
Figure 17. Photograph of assembled twin-spool turbocharger rotating assembly

-37-
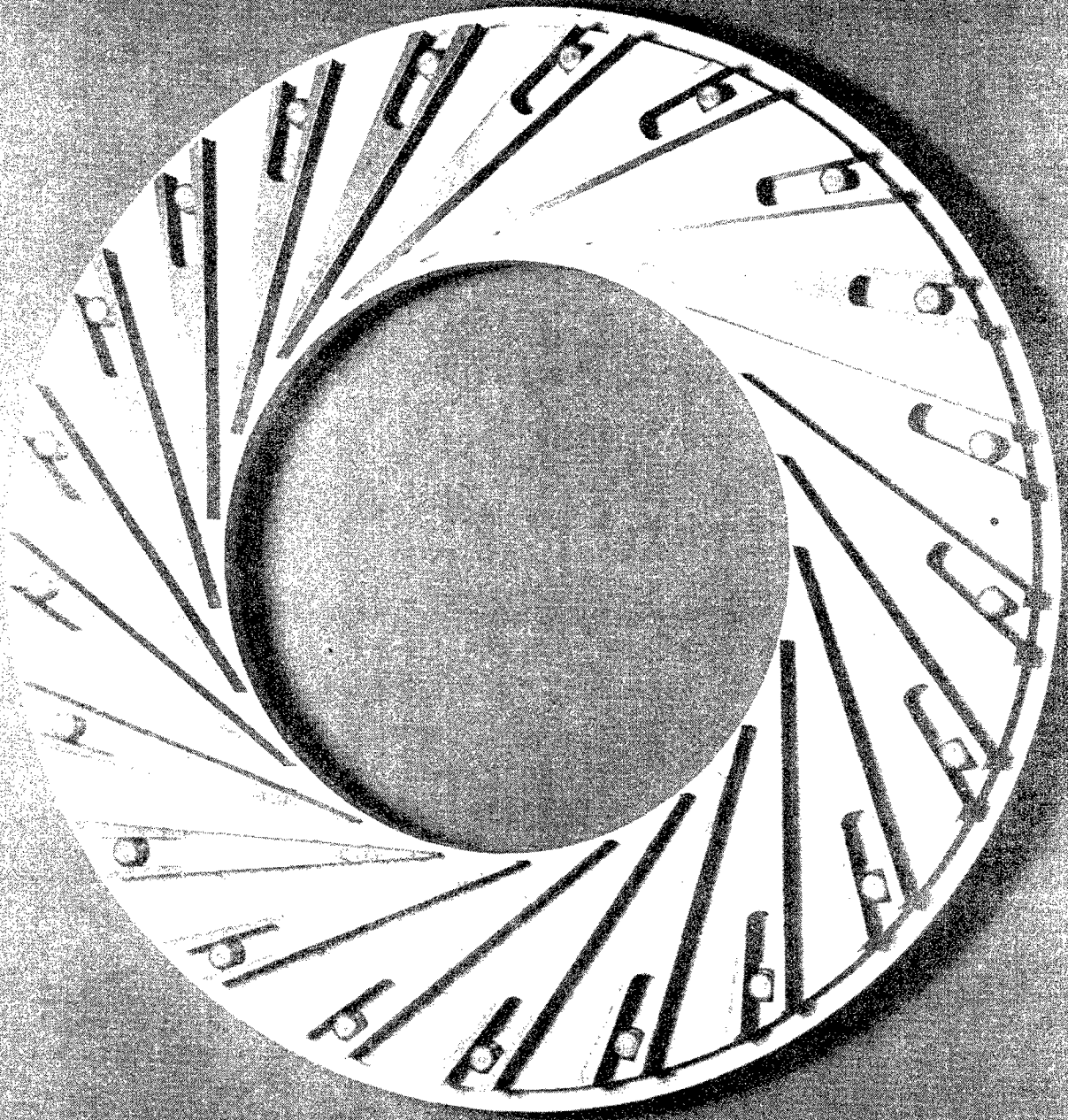
Figure 18. TMS adjustable vaned diffuser system

5.0 EXPERIMENTAL PROGRAM

5.1 Baseline Engine Testing

5.1.1 Baseline Engine Selections

A survey of engines suitable for twin-spool turbocharger development resulted in the selection of the Cummins NTC-475 diesel engine. The reasons for this choice were: 1) the Cummins 855 diesel presently is in production, 2) the 475 hp Cummins 855 diesel is an advanced, high efficiency engine with the very respectable BSFC of .34 lb/bhp hr and 3) the 475 hp Cummins 855 diesel utilizes two broad range, high efficiency series turbochargers. Figure 19 presents a photograph of the Cummins NTC-475 twin-turbo diesel engine.

The use of the two series turbochargers on the 475 hp Cummins 855 diesel is a direct result of the need for high torque at the low engine speed (lug) conditions. Using dual series turbochargers reduces the pressure ratio requirement of each compressor--and the range of most centrifugal compressors is significantly increased as the pressure ratio requirement is reduced.

Now, as has already been stated in the Program Objective, the specific goal of this program will be to obtain the approximate 475 hp Cummins 855 diesel engine performance by using the single twin-spool turbocharger in place of the existing dual series turbochargers. It is anticipated that this one-for-two turbocharger replacement will reduce the space and weight requirements of the turbocharger systems of high output military diesel engine applications.

5.1.2 Manufacturer's Performance Specifications

Table 2 presents engine performance data for the NTC-475 diesel engine, as supplied by the Cummins Engine Company. Figures 20 and 21 present some of this data in plotted form. Important data gleaned from Table 2 and Figures 20 and 21 are:

1. The engine torque increases from 1188 lb ft at rated engine speed of 2100 RPM to a maximum of 1430 lb ft at lug engine speed of 1400 RPM.

2. The optimum engine BSFC is about .34 lb/bhp hr and occurs from about 1300 RPM to about 1800 RPM.

3. The intake manifold pressure and the exhaust manifold pressure decrease from 89" Hga to 71" Hga and from 86" Hga to 53" Hga, respectively, in going from 2100 RPM rated engine speed to 1300 RPM lug engine speed.

4. The F/A ratio and the exhaust manifold temperature increase from .032 to .044 and from $1120^{\circ}F$ to $1200^{\circ}F$, respectively, in going from 2100 RPM rated engine speed to 1300 RPM lug engine speed.

The Cummins data indicates that the engine is firing pressure limited above 1400 RPM, but boost pressure limited below 1400 RPM. Furthermore, it appears that the boost pressure limitation below 1400 RPM results from limited availability of turbine-to-compressor power which, with fixed turbine nozzle geometry and without wastegate, can only be improved upon by 1) increasing F/A ratio and, therefore, exhaust gas temperature (EGT) and/or 2) improving the compressor and turbine efficiencies. As noted in Item 4 above, the first technique has been used; however, it is the second technique which must be addressed in order to improve engine lug performance.

5.1.3 Engine Test Set-Up

Figure 22 presents a photograph of the NTC-475 engine mounted on the TMS diesel engine dyno test bed. Tasks undertaken to prepare for engine baseline testing included the following:

1. Motor mounts were fabricated to secure the NTC-475 engine to the dyno test bed.

2. An engine-to-dyno flywheel adapter was fabricated in order to connect with the General Electric TG25H 500 hp eddy current dynamometer. The engine mounts were adjusted for optimum driveshaft alignment (dual Zurn Amerigeor couplings were employed).

3. The engine inlet duct system, complete with bellmouth flowmeter, air cleaner and adjustable butterfly valve (for inlet pressure correction) was connected to the engine's first stage compressor inlet.

4. The test facility exhaust system (i.e., muffler and building exit plumbing) was connected to the engine.

5. The test facility fuel system, which includes main reservoir, feed pump, filter, recirculation tank and Cox rotameter, was connected to the engine.

6. The test facility water cooling system was connected to the engine.

7. A (60-tooth) sprocket-gear assembly was adapted to the engine crankshaft and magnetic probes installed in order to monitor engine RPM.

8. Electrical hook-ups to the engine, including starter and fuel control circuits, were completed.

9. The engine, turbochargers and related support systems were fully instrumented for pressures, temperatures, speeds and flow rates. A detailed listing of the instrumentation appears in Table 3.

10. Calibration of the dyno console safety shut-down system

   was done to the following specifications:

   Min. Oil Press   ---- 20 psig

   Max. Oil Temp   ---- 220°F

   Max. Coolant Temp   ---- 200°F

   Max. Blowby Press   ---- 14 in. H_2O

   Max. Engine Speed   ---- 2200 RPM

11. The General Electric TG25H dynamometer was calibrated

   over the torque range of 0 to 1500 ft. lbs.

5.1.4 Test Procedure

Table 4 is presented to show the engine operating points that were set for the NTC-475 baseline test. At each of the six engine speeds shown, torque was adjusted by increments of 300 lbs. ft. until the maximum torque for the given speed was obtained. This test plan yielded 29 engine operating points from which baseline data was collected.

For each of the operating conditions, the set speed was held constant by varying the dynamometer load as fuel flow was adjusted to produce the desired torque output. In addition, the inlet air control valve was adjusted to maintain the constant inlet reference pressure of 28.4 in Hga. Data was collected for non-critical measurements (i.e., support system measurements not related to engine/turbo performance) while stabilization of important pressures and temperatures occurred. Once steady-state conditions were verified, critical data was collected and the next set point was established.

5.1.5 Test Data Reduction

An engine performance map was generated along with supplemental curves which help to analyze engine/turbocharger performance for the NTC-475 engine.

Existing compressor, turbine and engine computer programs were used to calculate the critical turbocharger and engine performance from the test data.

5.1.6 Baseline Engine Test Results and Discussion

The "raw" test data and reduced test results for the NTC-475 engine baseline test are presented in tabular form in Appendix B. For analysis and comparison studies, the reduced test data has been plotted and is presented in Figures 23 through 27. The important results gleaned from the test data are as follows:

1) The maximum BHP and BMEP obtained in the baseline engine tests (see Figure 23) were quite close to the values supplied/specified by Cummins. The maximum BHP of 475 hp, as specified by Cummins, was obtained at 2100 RPM and maximum torque of 1194 lb. ft.

2) The very respectable BSFC (see Figure 24) of about .34 lb/hp-hr, as specified by Cummins, was obtained at 1500 RPM and maximum torque of about 1450 lb. ft. (see Figure 22).

3) The peak boost pressure (see Figure 25) of about 87-89 in. Hga and the peak airflow of about 1.5 lb./sec., both as specified by Cummins, were obtained at 2100 RPM and maximum torque of 1194 lb. ft.

4) Both the AiResearch T18A85 and Holset HC3-5 turbochargers demonstrated (generally) increasing efficiencies (see Figures 26, 27 and Appendix A) in going from 2100 RPM rated engine speed to 1300 RPM lug engine speed. This is exactly

what is needed to a) give optimum diesel engine (lug) performance at low speeds while b) limiting boost pressure at high (rated) speeds.

5) The exceptional increase in the Holset turbocharger efficiency at lug was due in large part to the following good design practice:

a) The turbine U/C_o (see Appendix B), at the maximum torque condition, increased from about .57 at 2100 RPM rated speed to about .65 at 1300 RPM lug speed. The optimum U/C_o for best turbine efficiency is about .71.

b) The turbine gas exit swirl angle (see Appendix B), at the maximum torque condition, changed from about -14° at 2100 RPM rated speed to about -2° at 1300 RPM lug speed. The optimum swirl angle is 0°.

c) The indicated compressor efficiency (see Figure 27), at the maximum torque conditions, increased from about 69 percent at 2100 RPM rated speed to about 78 percent at 1300 RPM lug speed.

d) The apparent turbine efficiency (see Appendix B) at the maximum torque condition, increased from about 55 percent at 2100 RPM rated speed to about 67 percent at 1300 RPM lug speed.

The above turbocharger data results, most notably for the the Holset HC3-5, indicated that the baseline turbocharger system was suitably designed to give good lug speed performance while limiting rated speed boost

-44-

pressures. It should be noted that the ample airflow range capability of the turbocharger system is a direct result of the relatively low pressure ratio requirement placed upon each compressor stage -- that is, 1.77:1 and 1.94:1 maximum for the T18A85 and HC3-5, respectively. The maximum pressure ratio required of a <u>single</u> compressor stage replacing the two compressor stages turns out to be about 3.1:1 where the same wide compressor range, in conventionally designed compressors, would be difficult to achieve. The TMS, advanced twin-spool compressor concept, however, was thought to be capable of this combined pressure ratio and still give (or extend) the broad (torque) range available with the originally equipped turbocharger system.

5.1.7 Baseline Turbocharger Bench Tests

In order to further assess turbocharger performance characteristics of the NTC-475 twin-turbo engine, each turbocharger was removed from the engine and individually bench tested. (A complete description of turbocharger bench test set-up and procedure is presented in Sections 5.2.1 and 5.2.2.) Bench testing was carried out using the same airflow measurement equipment (calibrated venturi and manometer) as used in the NTC-475 baseline test so that accurate and complete compressor maps could be obtained for the two turbocharger stages.

Figures 28 and 29 present the resultant compressor maps for the T18A85 and HC3-5, respectively. Also shown on these maps are the engine operating lines which were determined experimentally in the NTC-475 baseline engine test. Important results which are obtained from these figures are as follows:

1) The T18A85 compressor (see Figure 28) is operated near the center of its range with the majority of the operating envelope lying within the 73 percent efficiency island. With the NTC-475 operating at maximum torque, the compressor efficiency increases from about 70 percent to about 74 percent as the engine speed is changed from 2100 RPM to 1300 RPM.

2) The HC3-5 compressor efficiency (see Figure 29) increases from about 67 percent to about 74 percent as engine speed is changed from 2100 RPM to 1300 RPM. This trend, which is apparent in both the T18A85 and HC3-5 compressors, is exactly what is desired to a) give optimum diesel lug performance while b) limiting boost pressure at the rated condition.

3) The HC3-5 compressor is operated very close to the compressor instability limit or "surge line" at the engine speed of 1300 RPM. While operation of the compressor close to this region has no detrimental effect, it does mean that lug performance at engine speeds lower than 1300 RPM would not be possible.

The above findings reaffirm the suitability of the originally-equipped two-stage turbocharger system to give good lug speed torque performance, albeit limited to 1300 RPM engine speed. Improvements which were felt to be feasible and beneficial to the lug speed torque performance of the NTC-475 over and above that which the originally-equipped turbo system provided were:

1) Elimination of heat and pressure loss normally found between turbine stages of multi-stage systems.

2) Improvement of overall turbine efficiency by a) recovering more of the available exhaust gas pulse energy across a single turbine stage and b) minimizing turbine exducer leaving losses with the use of the twin-spool split exducer concept.

3) Improvement of compressor range and efficiency with the use of the twin-spool compressor resulting in a broader torque range than was presently available.
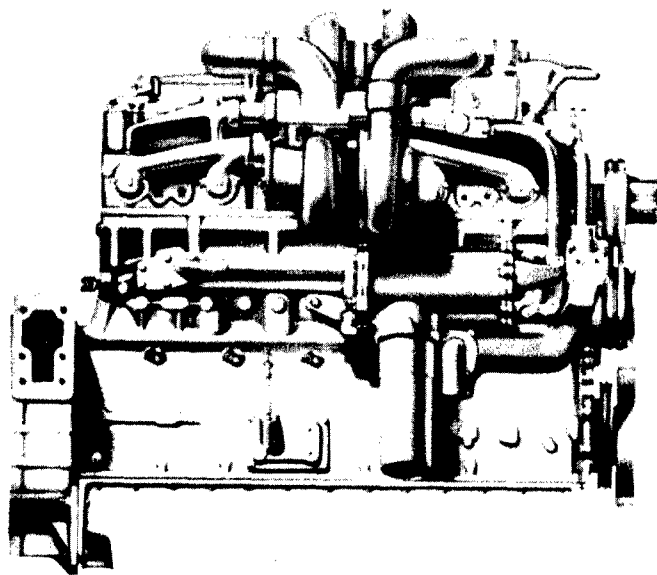
Figure 19. Photograph of 475 HP Cummins 855 diesel engine

RPM	Torque Lb. Ft.	H.P.	BMEP	Fuel Rate Lb/Hr	$\dot{m}$ Lb$_m$/Sec	F/A	Intake Map, "Hga	Intake Manifold Temp, °F	Vol. Eff.	BSFC	Exh. Man. Temp, °F	Exh. Man. Press, "Hga
2100	1188	475	209	170	1.455	.032	89	198	.933	.358	1120	86.3
1900	1285	465	227	160	1.288	.035	87	190	.922	.344	1140	79.3
1700	1365	442	241	150	1.121	.037	84	190	.929	.340	1160	71.3
1500	1420	406	250	n.a.	.972	.039	79	190	.970	.340	1160	62.3
1400	1430	380	251	n.a.	.870	.042	76	185	.967	.340	1170	58.3
1300	1420	351	250	120	.763	.044	71	180	.963	.341	1200	53.3

Table 2. Engine performance data for 475 hp Cummins 855 diesel engine
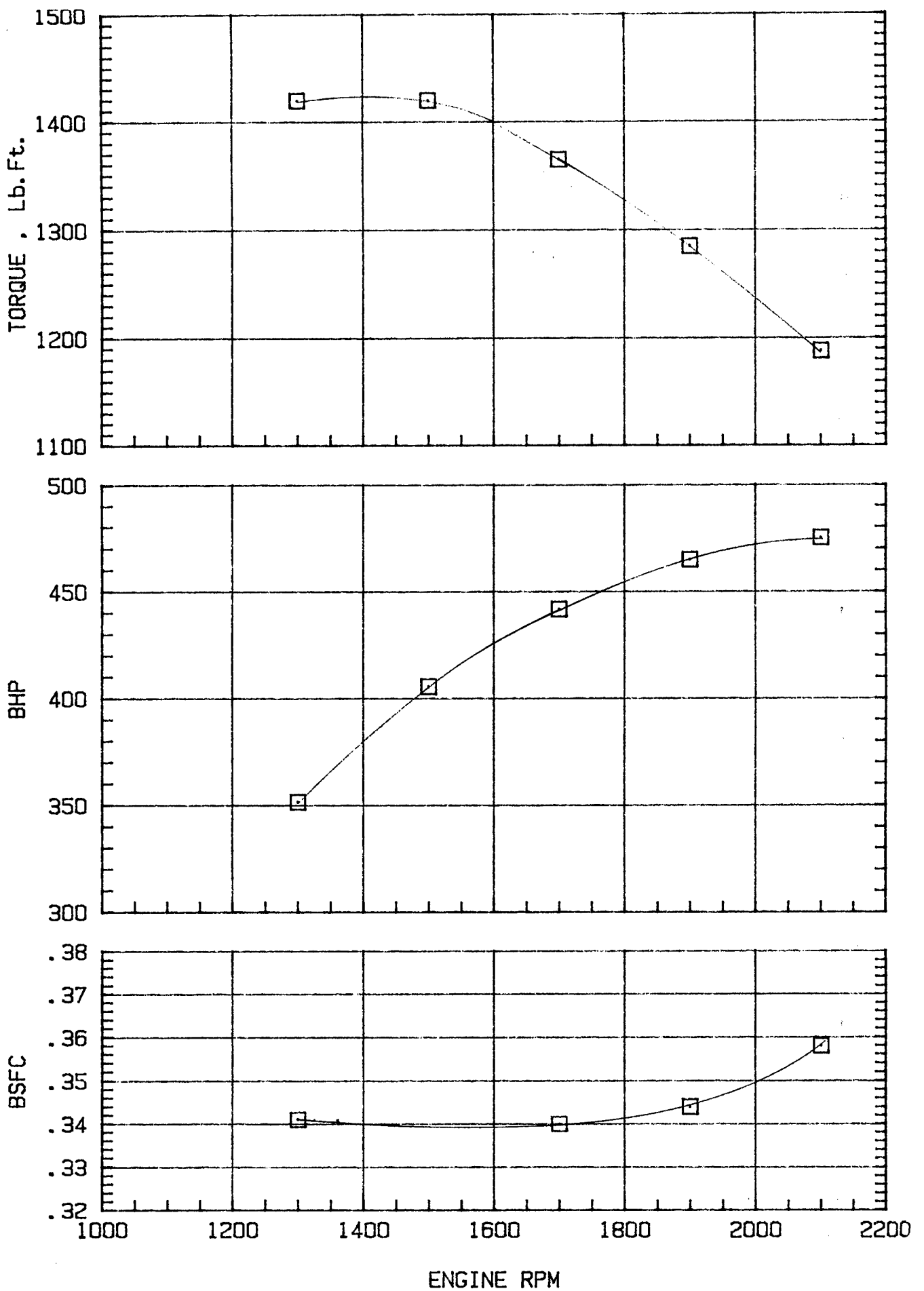
Figure 20. Performance Curves for Cummins NTC-475 B.C. III Diesel Engine
C.P.L. #586
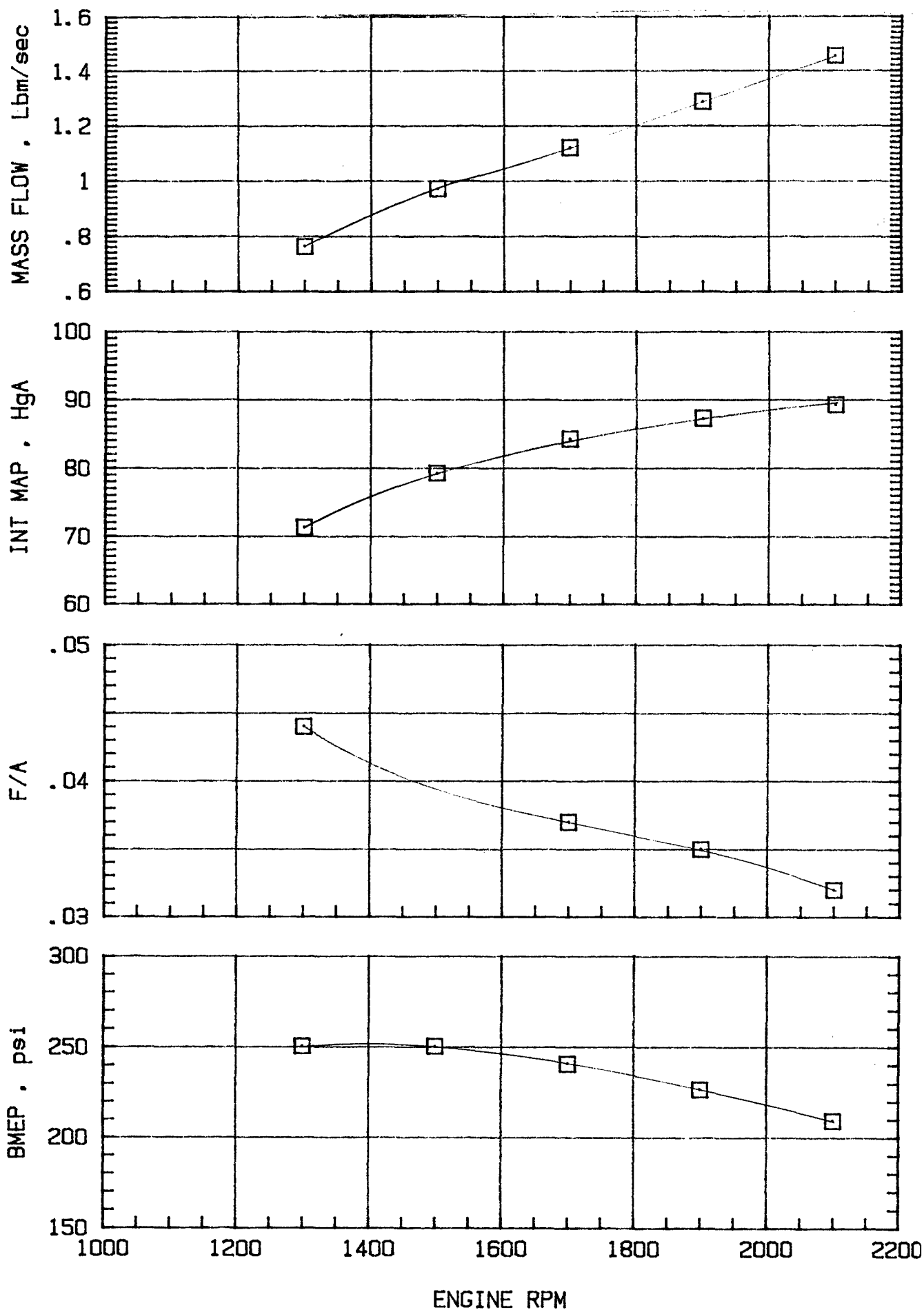
Figure 21. Performance Curves for Cummins NTC-475 B.C. III Diesel Engine
C.P.L. #586
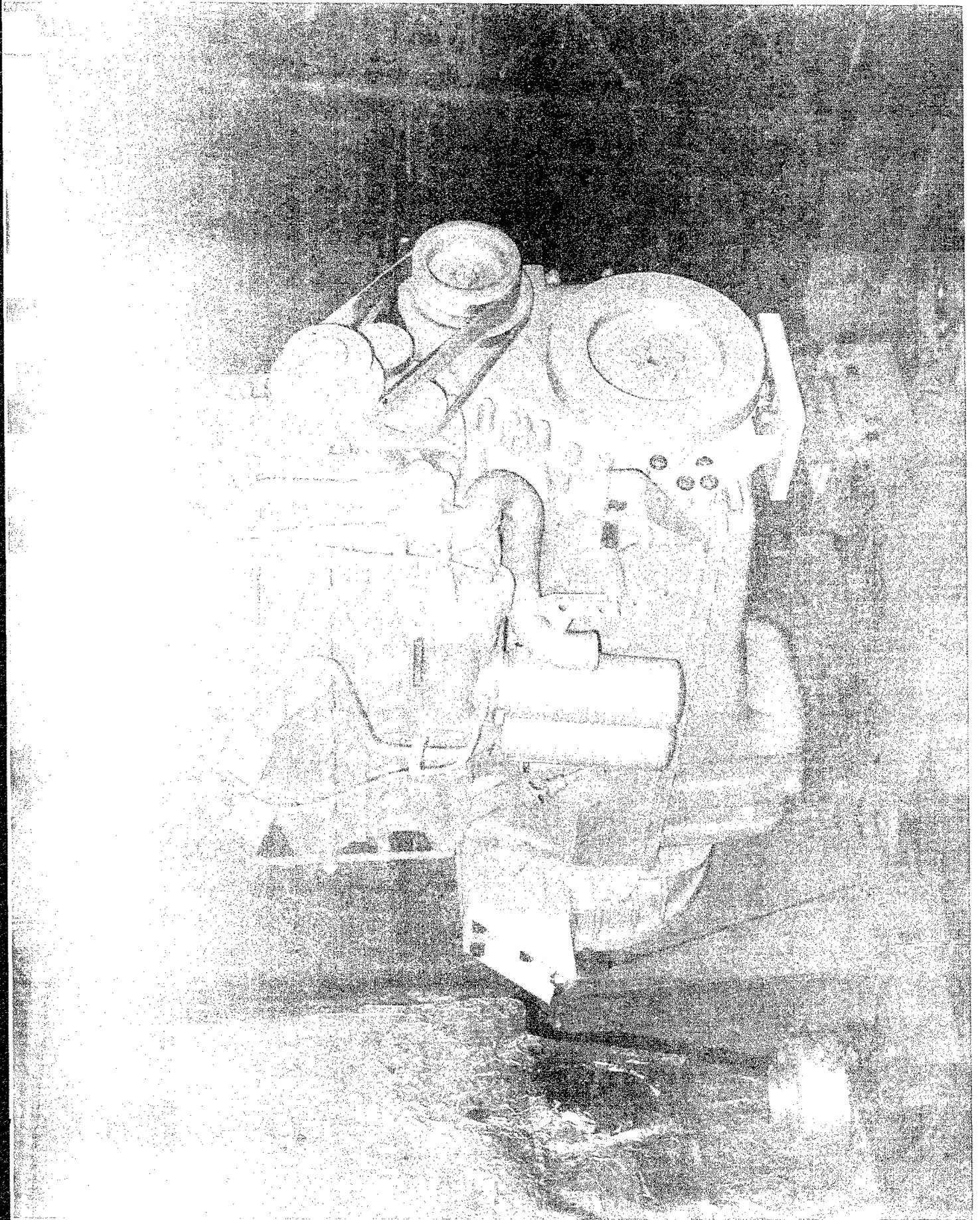
Figure 22. Photograph showing Cummins NTC-475 engine mounted on test stand

TABLE 3

NTC-475 BASELINE TEST INSTRUMENTATION LIST

ITEM	FUNCTION	SENSOR	QTY	RANGE	READOUT
TURBOCHARGER SYSTEM					
Temperatures					
1	Ambient	Thermocouple	1	-200 – 2500°F	Doric Digital Trendicator
2	T18 Compressor Inlet	Thermocouple	1	-200 – 2500°F	Doric Digital Trendicator
3	T18 Comp. out/HC3 Inlet	Thermocouple	1	-200 – 2500°F	Doric Digital Trendicator
4	HC3 Compressor Exit	Thermocouple	1	-200 – 2500°F	Doric Digital Trendicator
5	Intake Manifold	Thermocouple	1	-200 – 2500°F	Doric Digital Trendicator
6	HC3 Turbine Inlet	Thermocouple	2	-200 – 2500°F	Doric Digital Trendicator
7	HC3 Turbine Exit	Thermocouple	1	-200 – 2500°F	Doric Digital Trendicator
8	T18 Turbine Inlet	Thermocouple	1	-200 – 2500°F	Doric Digital Trendicator
9	T18 Turbine Exit	Thermocouple	1	-200 – 2500°F	Doric Digital Trendicator
Pressures					
10	Ambient	Barometer	1	0 – 40 in. Hga	Visual
11	Venturi Throat $\triangle$P	Static Tap	1	0 – 14 in. H_2O	Incline Manometer
12	T18 Comp. Inlet $\triangle$P	Total Probe	1	0 – 60 in. H_2O	Manometer
13	T18 Impeller Exit	Static Tap	1	0 – 75 psia	Kollsman
14	T18 Comp. Exit	Total Probe	1	0 – 75 psia	Kollsman
15	HC3 Impeller Exit	Static Tap	1	0 – 75 psia	Kollsman
16	HC3 Comp. Exit	Total Probe	1	0 – 75 psia	Kollsman
17	Intake Manifold	Static Tap	1	0 – 75 psia	Kollsman
18	Intake Manifold	Static Tap	1	0 – 150 in. Hga	Kollsman
19	HC3 Turbine Inlet	Total Probe	1	0 – 150 in. Hga	Kollsman
20	HC3 Turbine Inlet	Total Probe	1	0 – 75 psia	Kollsman
21	HC3 Turbine Exit	Static Tap	1	0 – 75 psia	Kollsman

(Continued)

TABLE 3 (CONT.)

ITEM	FUNCTION	SENSOR	QTY	RANGE	READOUT
22	T18 Turbine In	Total Probe	1	0 - 75 psia	Kollsman
23	T18 Turbine Exit	Static Tap	1	0 - 75 psia	Kollsman
Speeds					
24	HC3 Turbocharger RPM	Magnetic Pickup	1	0 - 1,000,000	Anadex Digital Counter
25	T18 Turbocharger RPM	Magnetic Pickup	1	0 - 1,000,000	Anadex Digital Counter
ENGINE/DYNO INSTRUMENTATION					
26	Engine Torque	Hagen Load Cell	1	0 - 120 Hga	Pennwalt Pressure Gauge
27	Engine RPM	Magnetic Pickup	1	0 - 10,000	Anadex Digital Counter
28	Fuel Flow	Cox Rotometer	1	20 - 280 Lb/Hr	Visual
29	Oil Temperature	Thermocouple	1	$-200 - 2000^{\circ}F$	Howell Digital Indicator
30	Oil Temperature	Thermocouple	1	$0 - 300^{\circ}F$	API Instruments Meter
31	Oil Pressure	Static Tap	1	0 - 60 psi	ACCO Helicoid Gauge
32	Blowby Pressure	Static Tap	1	$0 - 20$ In. H_2O	Dwyer Magnehelic
33	Water Out Temperature	Thermocouple	1	$0 - 300^{\circ}F$	API Instruments Meter
34	Water In Temperature	Thermocouple	1	$-200 - 2000^{\circ}F$	Howell Digital Indicator
35	Water Out Pressure	Static Tap	1	0 - 60 psi	ACCO Helicoid Gauge
36	Water In Pressure	Static Tap	1	0 - 60 psi	ACCO Helicoid Gauge
37	Fuel In Temperature	Thermocouple	1	$-200 - 2000^{\circ}F$	Howell Digital Indicator
38	Fuel In Pressure	Static Tap	1	0 - 100 psi	ACCO Helicoid Gauge
39	Fuel In Pressure	Static Tap	1	0 - 200 psi	U.S. Gauge Bourdon Tube
40	Dyno Water Temperature	Thermocouple	1	$-200 - 2000^{\circ}F$	Howell Digital Indicator
41	Dyno Water Pressure	Static Tap	1	0 - 100 psi	Duragauge Bourdon Tube
42	Dyno D.C. Amperes	Static Tap	1	0 - 10	General Electric Meter
43	Dyno D.C. Volts	Static Tap	1	0 - 150	General Electric Meter
44	Load Cell Air Pressure	Static Tap	1	0 - 100 psi	U. S. Gauge Bourdon Tube

RPM	TORQUE SETTING , lbs. ft.				
1300	300	600	900	1200	1420
1400	300	600	900	1200	1430
1500	300	600	900	1200	1420
1700	300	600	900	1200	1365
1900	300	600	900	1200	1285
2100	300	600	900	1188	-----

TABLE 4

ENGINE BASELINE TEST OPERATING POINTS
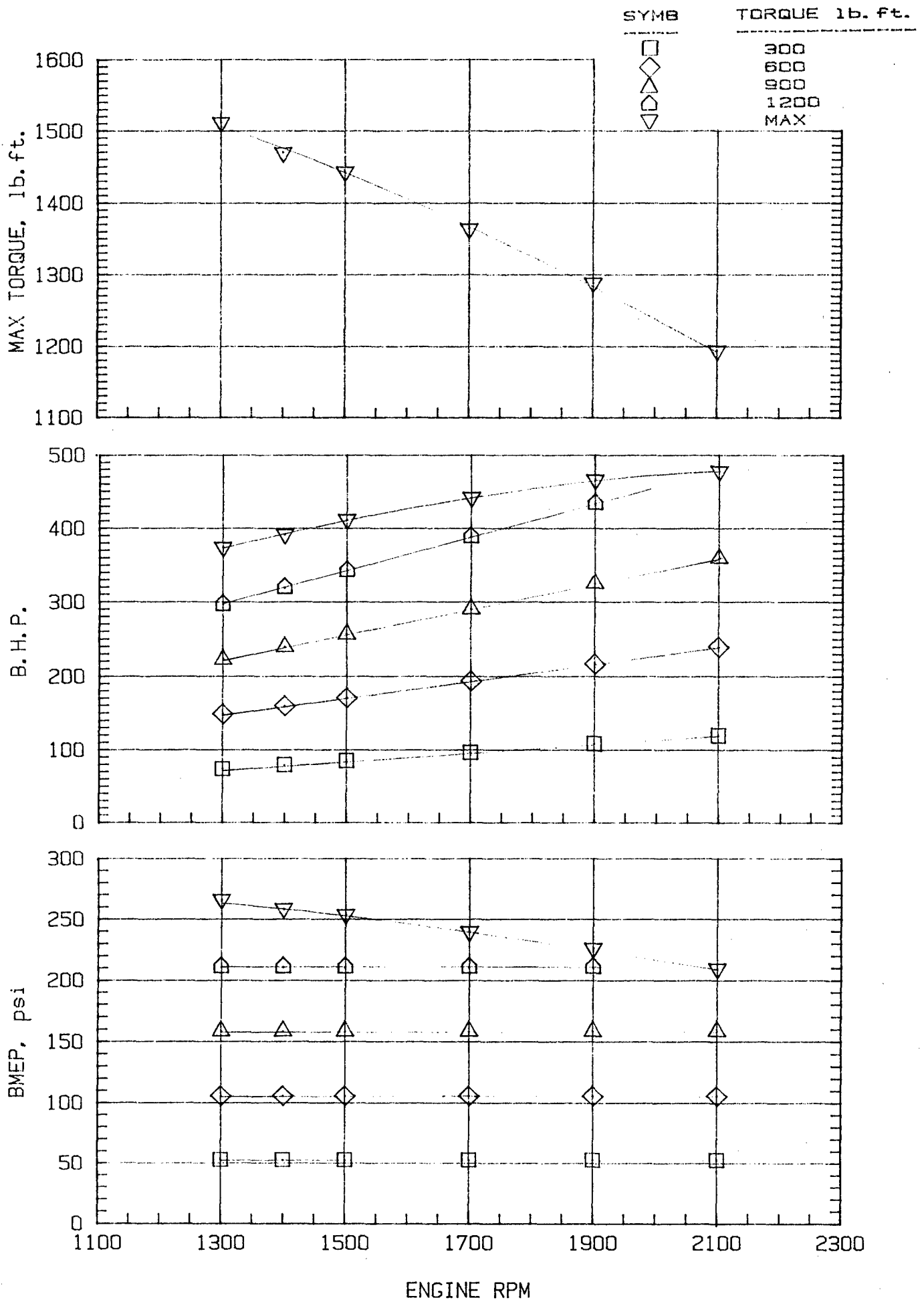
Figure 23. Engine test results: Cummins NTC-475 baseline engine performance
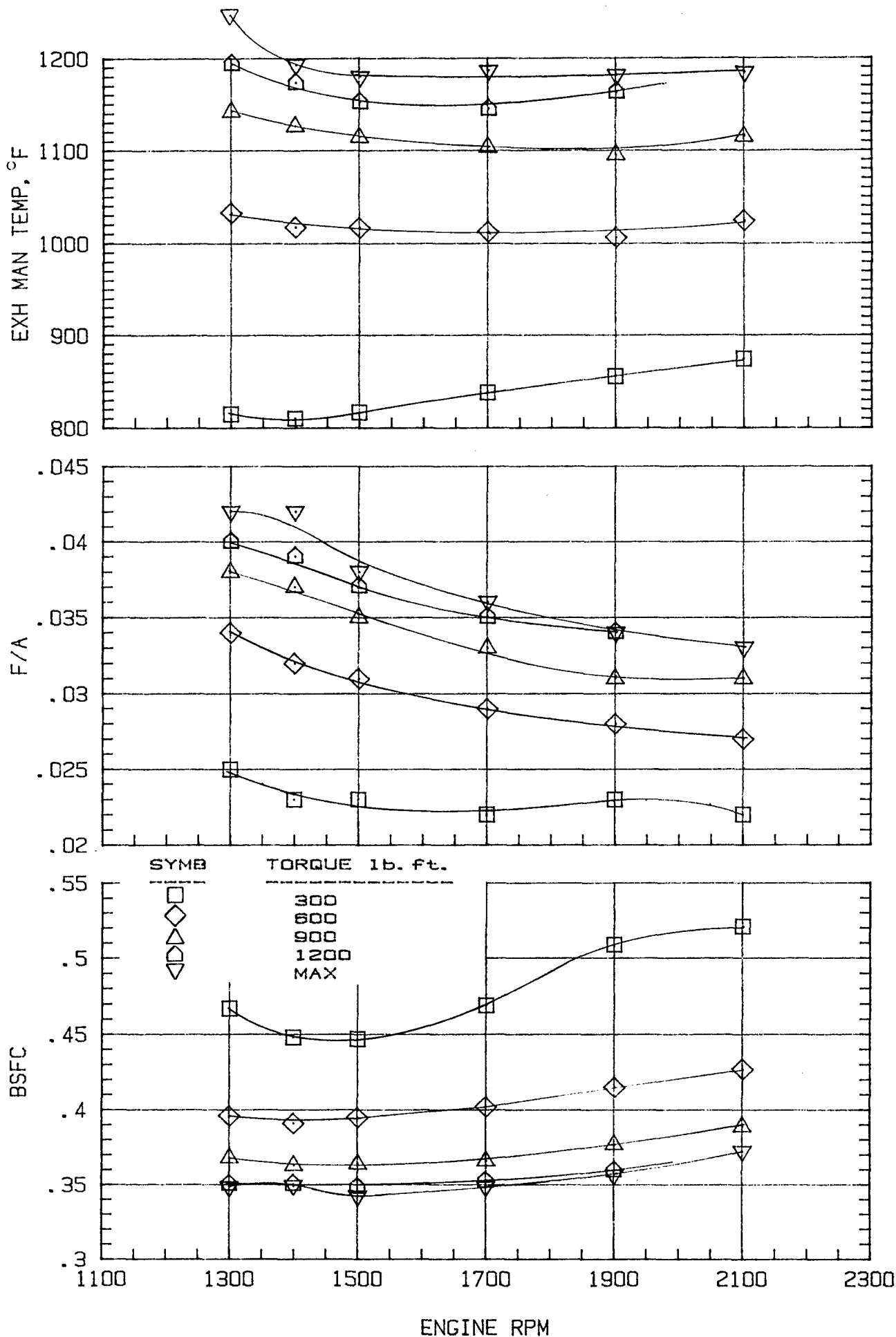
Figure 24. Engine test results: Cummins NTC-475 baseline engine performance
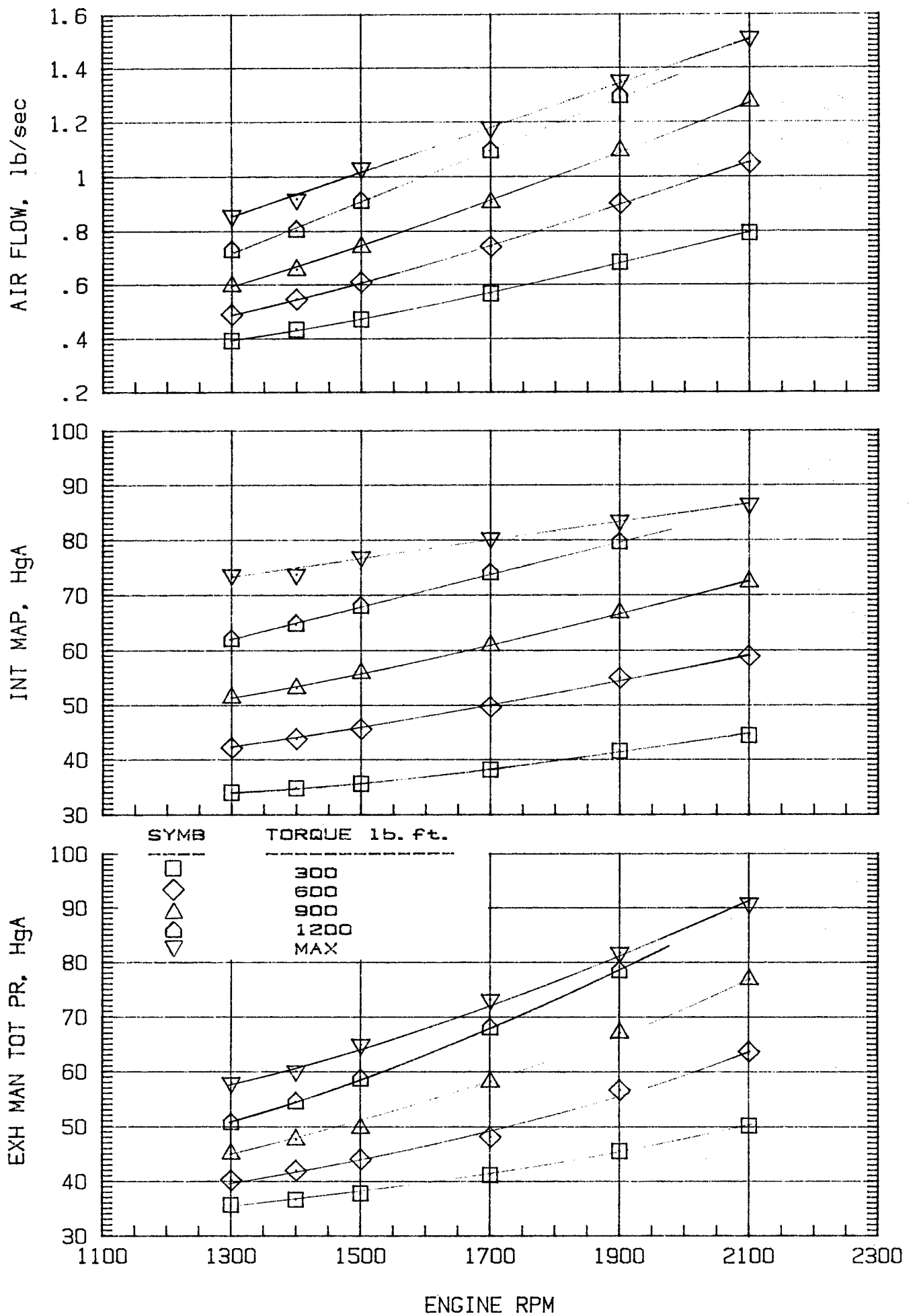
Figure 25. Engine test results: Cummins NTC-475 baseline engine performance
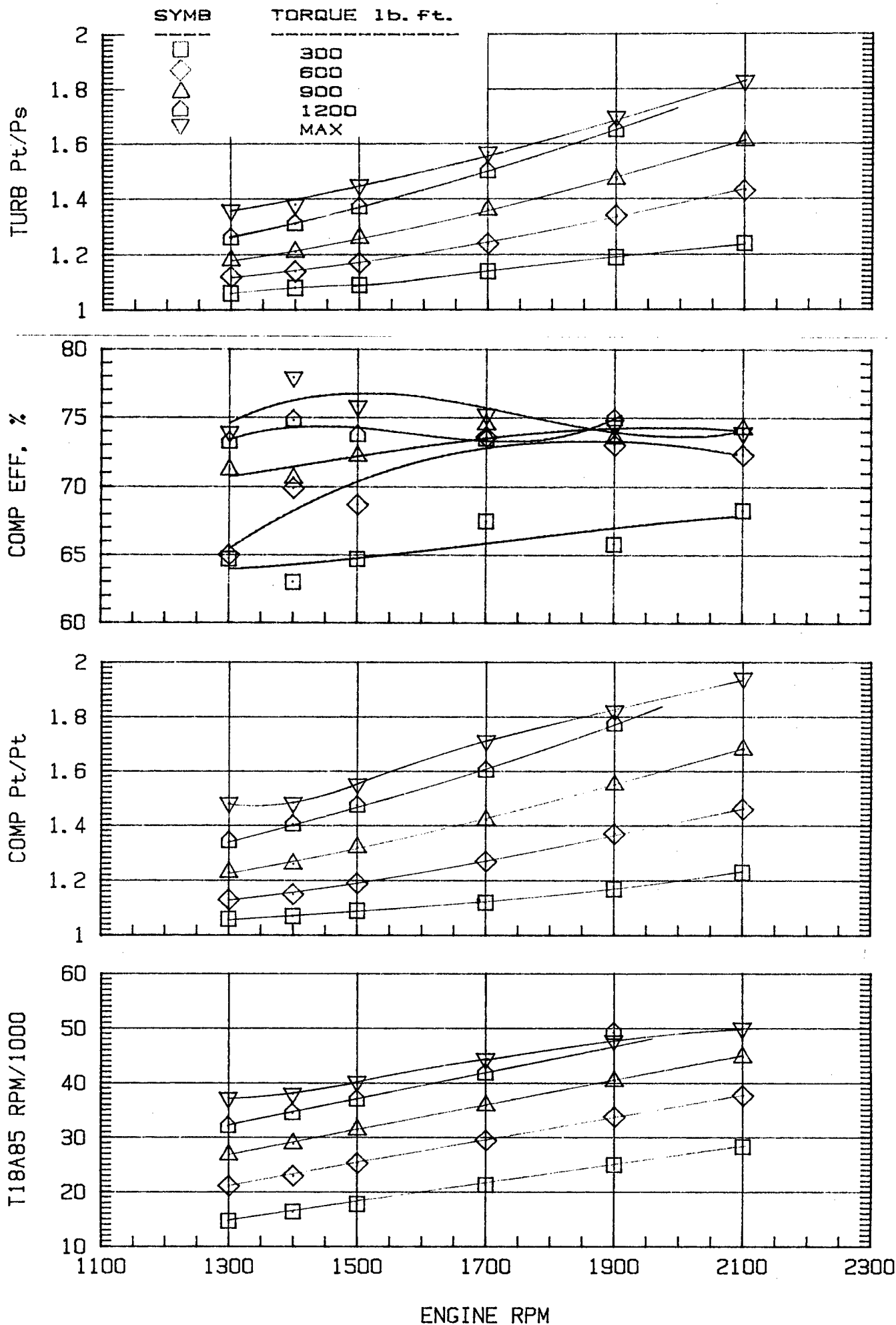
Figure 26. Engine test results: AiResearch T18A85 turbocharger performance
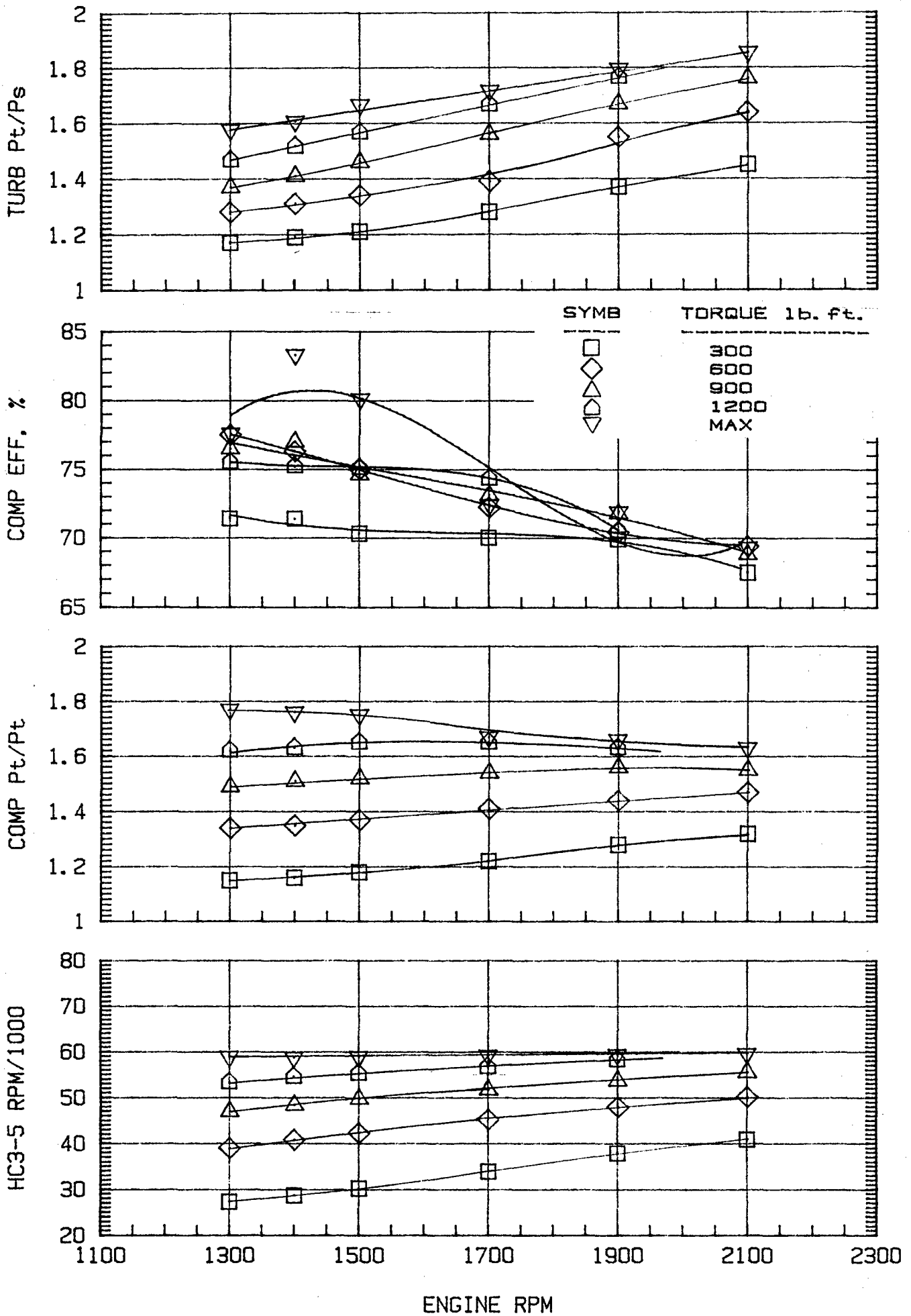
Figure 27. Engine test results: Holset HC3-5 turbocharger performance
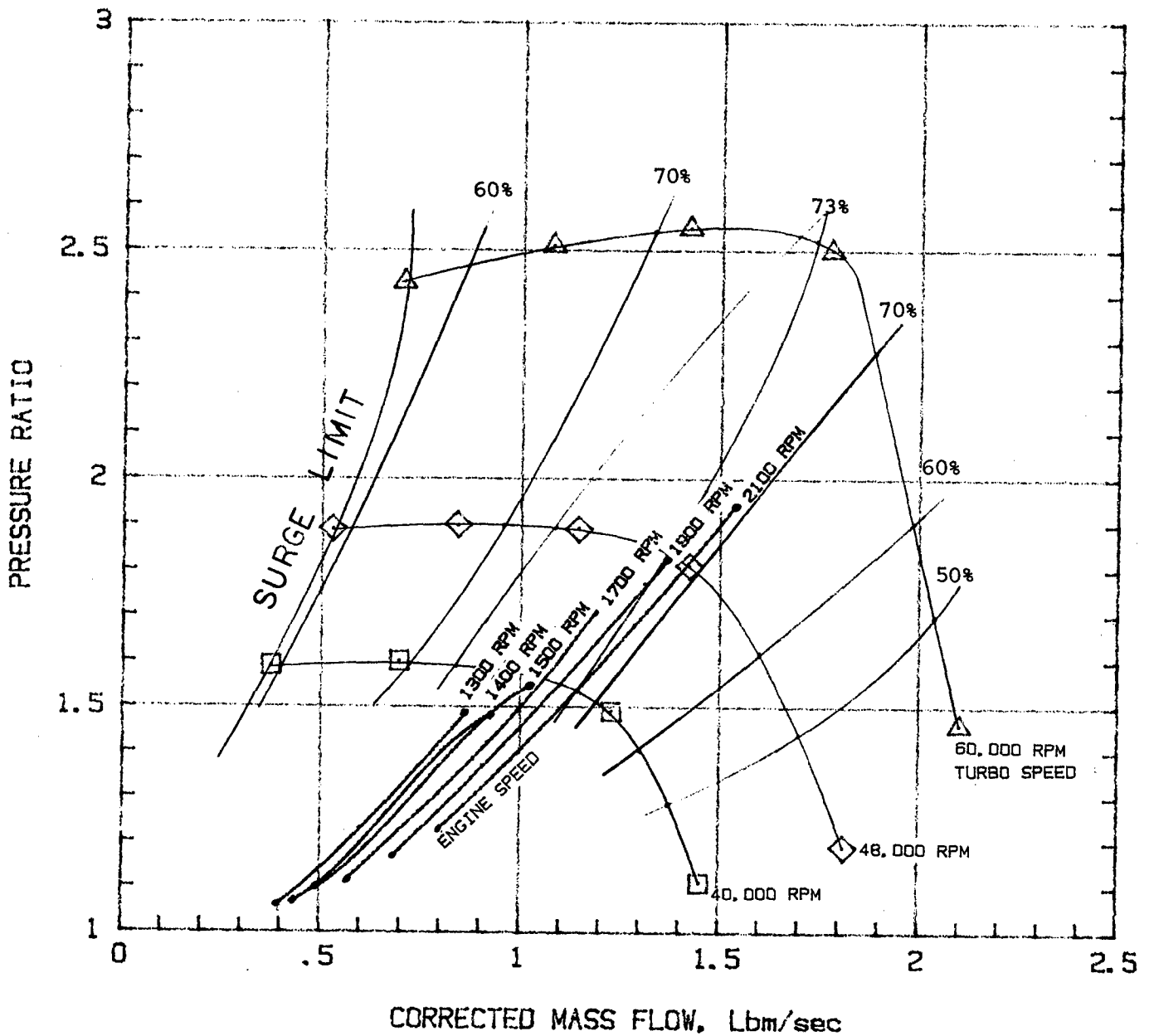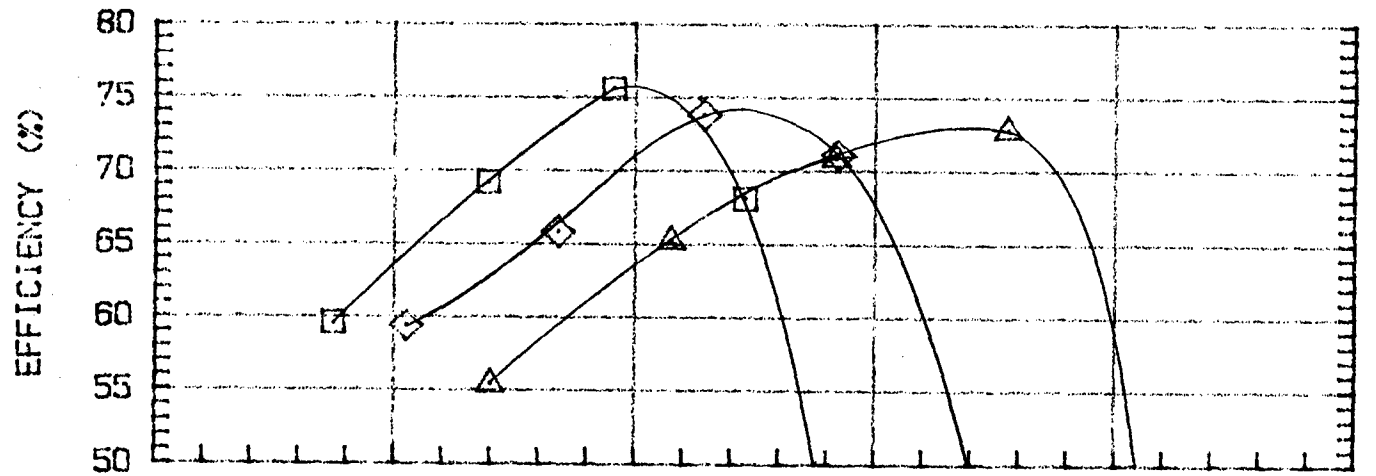
Figure 28. Compressor map of T18A85 turbocharger with NTC-475 engine operating
lines included
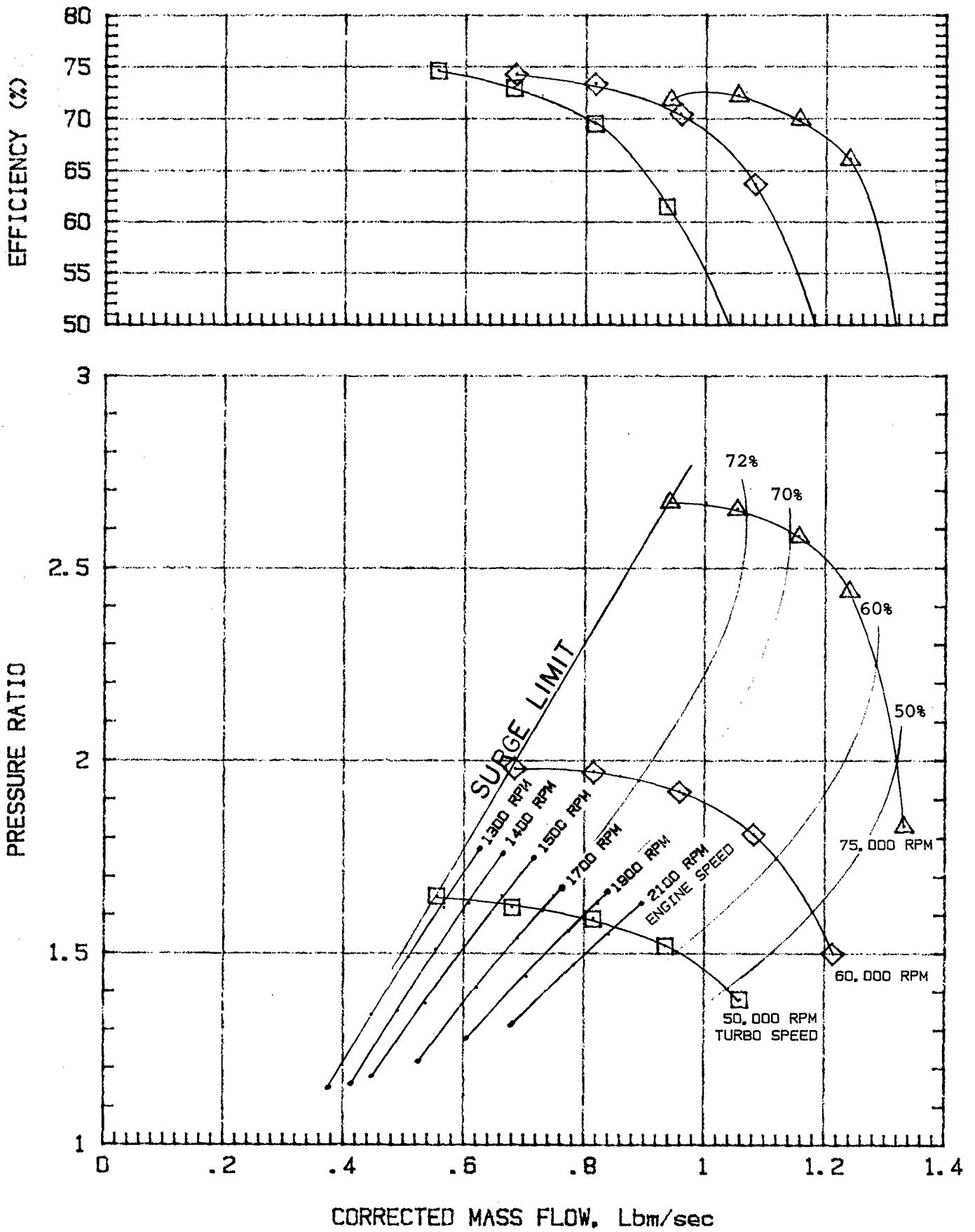
Figure 29. Compressor map of HC3-5 turbocharger with NTC-475 engine operating lines

5.2 First Design Twin-Spool Turbocharger Bench Testing

5.2.1 Bench Test Set-Up

Figure 30 presents a photograph of the first design twin-spool turbocharger installed in the TMS bench test facility. Features of the bench test apparatus include:

1. Variable air supply for driving turbine. Tests may be run with "cold" air (100 to 350°F) or with hot air (600 to 1400°F) to simulate engine exhaust properties.

2. Remotely adjustable compressor back-pressure valve. Mass flow may be varied at constant compressor speed so that compressor performance data may be collected over the range from surge to choke.

3. Dedicated turbo oil supply. Pumped oil is heated or cooled as required, filtered and regulated to provide controlled pressure and temperature oil to the turbocharger.

4. Safety shutdown system which turns off the turbine drive air supply in the event of i) low oil pressure at the bearing capsule inlet, ii) high oil temperature at the bearing capsule outlet and iii) excessive gas temperature at the turbine inlet.

5. Complete instrumentation of pressures, temperatures and speeds, as outlined in Table 5.

5.2.2 Bench Test Procedure

The turbine drive air system was started slowly and the turbocharger run at low speed while checks were made to determine that mechanical

operation was normal (with close attention given to monitored vibration) and that all instrumentation was functioning properly.

Twin-spool compressor performance was measured by setting a predetermined corrected radial section speed and collecting data at a number of airflow settings across the compressor range from surge to choke. Corrected radial section speed is defined as follows:

$$N_{corr} = \frac{N_{radial\ section\ actual}}{\sqrt{T_{comp\ inlet}/545°R}}$$

For each of the airflow settings tested, steady-state conditions were verified (stabilization of key pressures and temperatures observed) before data was collected. At the completion of a given "speed-line", the compressor discharge valve was opened fully and the turbine drive airflow increased until the turbocharger was accelerated to the next corrected speed.

As before, close attention was given to the monitored vibratory characteristics and also the sound of the turbocharger to avoid operation at any obvious critical speed condition.

5.2.3 First Design Twin-Spool Turbocharger Bench Test Results

and Performance Analysis

Figure 31 presents the compressor performance map of the twin-spool turbocharger resulting from bench testing at the corrected radial section speeds of 20,000, 25,000, 30,000, 35,000, 40,000 and 48,000 RPM. (Testing at speeds above 48,000 RPM was not feasible due to the occurrence of high vibratory characteristics.) As shown in the compressor map, peak compressor efficiency increased from 59 percent to about 70 percent as the speed was varied from 20,000 to 48,000 RPM. In addition, the peak pressure ratio attained

was 1.84:1. The inclusion of the NTC-475 diesel engine constant speed operating lines serves to show the suitability of the twin-spool compressor section to satisfy the airflow range requirements of that engine and indicates 1) correct sizing of compressor inducer diameter and 2) appropriate diffuser throat area setting. The broad range shown, however, would normally be expected to decrease with increasing rotor speed (and, hence, higher pressure ratio) operation. Figures 32 and 33 present additional curves obtained from the data and from which the following important results are noted:

1) The inducer speed, as shown in Figure 32, ran about 10 percent to 20 percent higher than that of the radial compressor wheel. Inducer speed varied as a function of compressor airflow with peak overspeed typically occurring near the midpoint between choke and surge for a given constant speed line.

2) Work done by the inducer on the airflow, as shown in Figure 32, varied mostly between 28 and 36 percent of the total work done by the whole compressor. This excessive amount of inducer work was a direct result of the inducer overspeed condition and was felt to contribute to the low overall compressor efficiencies presented in Figure 31.

3) The pressure ratio developed by the inducer varied from about 1.03:1 to 1.16:1, primarily as a function of absolute inducer speed and only secondarily as a function of compressor airflow.

4) The inducer blade leading edge angle of attack, as shown in Figure 33, varied from about 8 to 22 degrees, and was a

direct result of the inducer overspeed condition noted in Item 1 above.

5) The radial compressor blade leading edge angle of attack, as shown in Figure 33, varied mostly between -25 and -37 degrees. This also was a direct result of the inducer overspeed condition which, in effect, imparted an excessive positive tangential velocity component to the airflow thereby turning the airflow beyond what was required for a smooth transition into the radial compressor stage.

6) The turbine exducer gas exit swirl angle varied from about 47 to 67 degrees, as shown in Figure 33. The large positive swirl was, again, a result of the inner shaft overspeed condition which gave rise to an abnormally large positive tangential component to the absolute gas exit velocity.

Analysis of the inner shaft overspeed condition encountered on these tests indicated that the following factors were involved:

1) Testing conducted with the cold-flow turbine inlet condition (100-300°F) led to poor radial turbine performance due to decreased radial turbine efficiency, which in turn led to surplus energy production in the turbine exducer stage. One of the losses that can be experienced in a radial turbine occurs when there is a mismatch between the tangential speed of the radial blade tips and the velocity of the gas approaching the blade tips. The parameter U/C_0 is a measure of this relationship between the incoming gas and the turbine tip speed.

U is the turbine tip speed in feet per second, and C_0 is the spouting velocity which is defined as the velocity the gas would achieve if expanded isentropically from turbine inlet conditions to ambient conditions. The ideal value of U/C_0 for best turbine efficiency is 0.71. As shown in Figure 33, the values of U/C_0 resulting from the twin-spool turbocharger bench tests varied between about .85 and .95. For these values of U/C_0, an efficiency loss of up to 20 percent was reasoned to have been present.

2) Another source of loss in the radial turbine can be blade exit leaving loss caused by large amounts of gas swirl in the same direction as wheel rotation. This condition can be caused by a) insufficient exit blade angle, b) excessive exit channel flow area, c) gas flow that exits the radial turbine passage that does not travel parallel to the turbine blade surface. It was felt that the design of the radial turbine wheel could be improved by extending the exit blading length by about 0.4 inches. In doing so, an increase of the solidity of the radial turbine section would be achieved with a concurrent increase of the exit blade angle and decrease of the exit channel area.

Mechanically, the design was plagued by high vibrations particularly at the turbine end. The turbine air bearing did not work satisfactorily, the Everlube 811 coating tended to wear off and all bearing surfaces on the turbine end

showed high wear. Many fixes were tried; some helped, but it appeared that rated rotor speeds were going to be very difficult to achieve.

It became apparent at this point in the program that a new mechanical design and a modified aerodynamic design were required.

COMPRESSOR
EXIT

VIBRATION
TRANSDUCER

TURBINE
EXHAUST

AIR METERING
BELLMOUTH

TWIN-SPOOL
TURBOCHARGER

OIL COOLER AND
FILTER ASSEMBLY
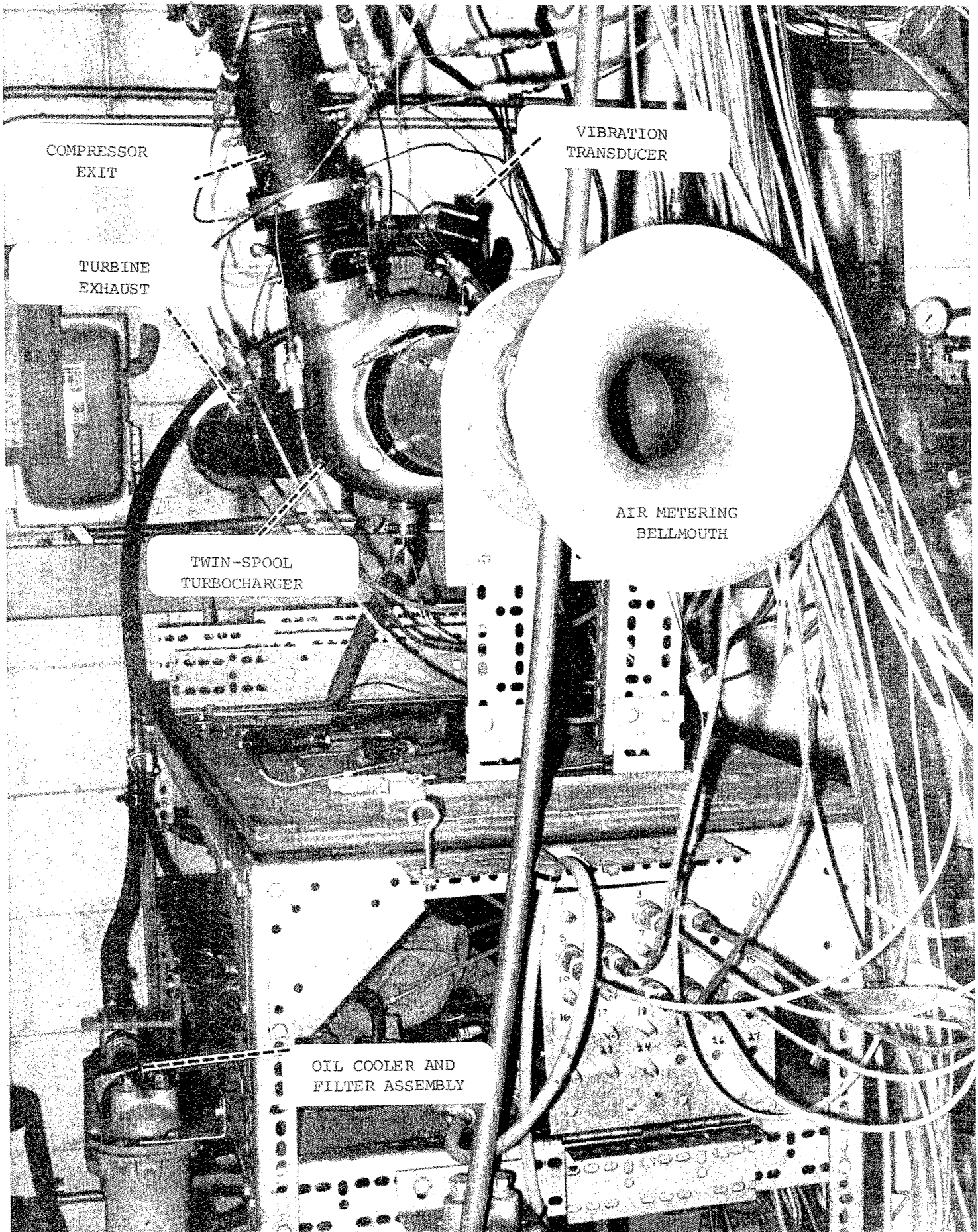
Figure 30.   Photograph showing twin-spool turbocharger test set-up

TABLE 5

TWIN-SPOOL TURBOCHARGER BENCH TEST
INSTRUMENTATION LIST

ITEM	FUNCTION	SENSOR	QTY	RANGE	READOUT
Temperatures					
1	Compressor inlet	Thermocouple	1	-200 to 2000°F	Howell Digital Indicator
2	Compressor inlet total	Thermocouple	1	-200 to 2000°F	Howell Digital Indicator
3	Shroud inlet	Thermocouple	1	-200 to 2000°F	Howell Digital Indicator
4	Inducer out total	Thermocouple	1	-200 to 2000°F	Howell Digital Indicator
5	Compressor outlet total	Thermocouple	2	-200 to 2000°F	Howell Digital Indicator
6	Turbine inlet	Thermocouple	2	-200 to 2000°F	Howell Digital Indicator
7	Turbine out	Thermocouple	1	-200 to 2000°F	Howell Digital Indicator
8	Turbine out total	Thermocouple	1	-200 to 2000°F	Howell Digital Indicator
9	Oil inlet	Thermocouple	1	-200 to 2000°F	Howell Digital Indicator
10	Oil out	Thermocouple	1	-200 to 2000°F	Howell Digital Indicator
Pressures					
11	Ambient	Barometer	1	0 to 40 in.Hga.	Visual
12	Venturi	Static tap	1	0 to 60 in. H_2O	Manometer
13	Compressor inlet	Total probe	1	0 to 60 in. H_2O	Manometer
14	Inducer 1/8" up	Static tap	1	0 to 200 in Hga.	Kollsman
15	Inducer 1/8" down	Static tap	1	0 to 200 in Hga.	Kollsman
16	Compressor 1/8" up	Static tap	1	0 to 200 in Hga.	Kollsman
17	Compressor 1/8" down	Static tap	1	0 to 200 in Hga.	Kollsman
18	Compressor tip	Static tap	4	0 to 100 psia.	Kollsman
19	Diffuser channel	Total probe	5	0 to 100 psia.	Kollsman
20	Compressor out	Total probe	2	0 to 100 psia.	Kollsman
21	Turbine in	Total probe	2	0 to 100 psia.	Kollsman
22	Turbine out	Static tap	1	0 to 100 psia.	Kollsman
23	Turbine out wedge	Total probe	1	0 to 3 psig.	Dwyer
Speeds					
24	Radial wheels	Magnetic pickup	1	0 to 1,000,000	Anadex Digital Counter
25	Axial wheels	Magnetic pickup	1	0 to 1,000,000	Anadex Digital Counter
Vibration					
26	Turbocharger	Vibration transducer	1	0 to 600 mv.	Tektronix Scope
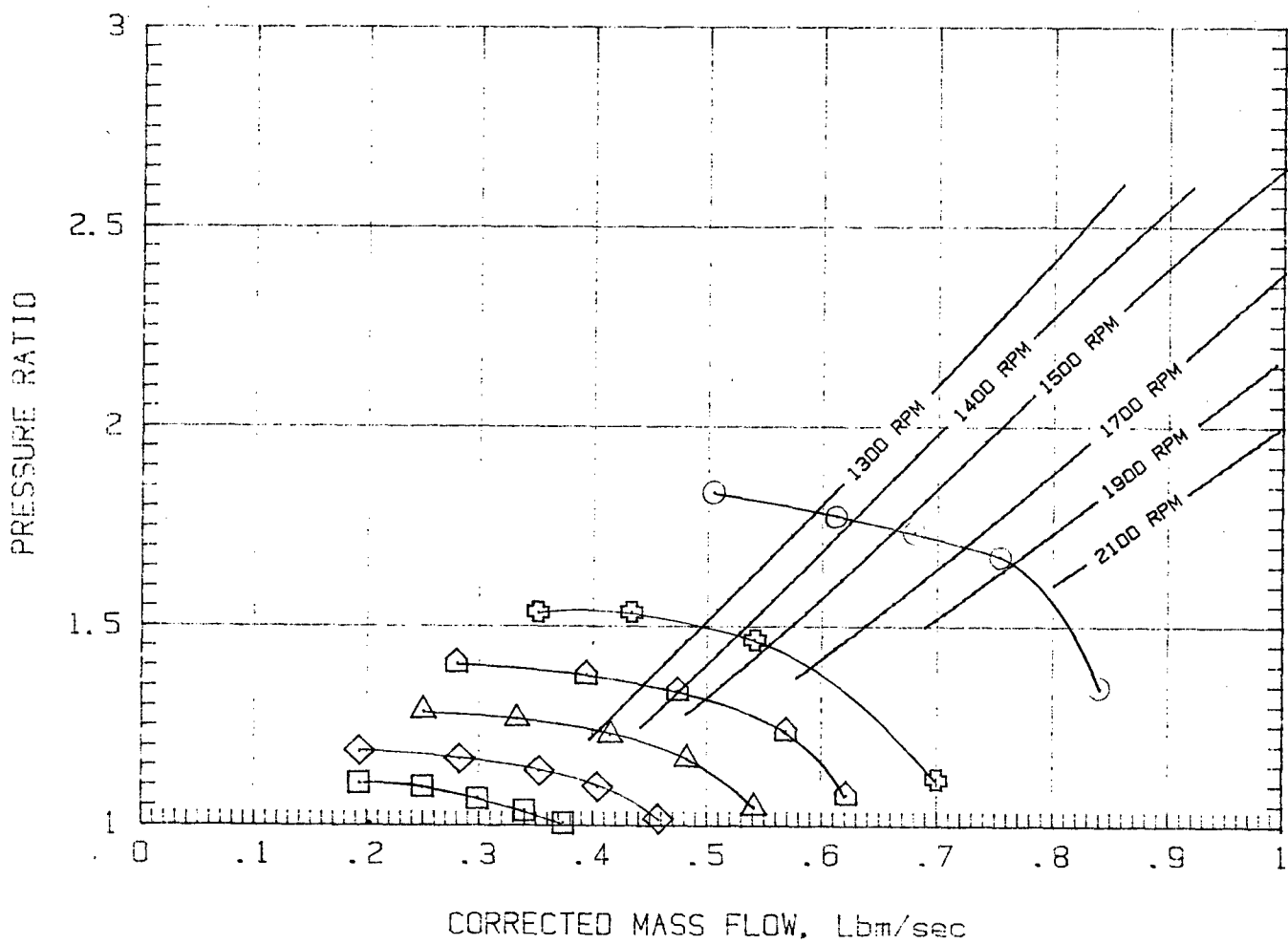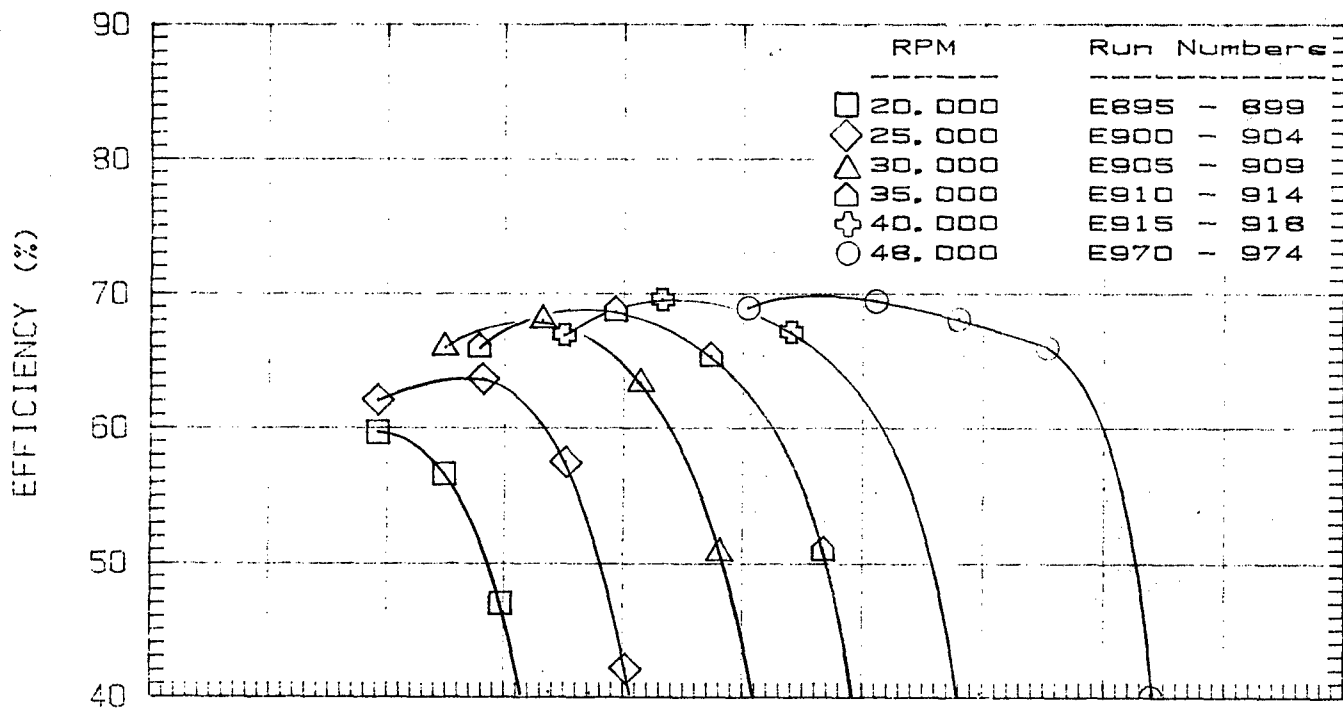
Figure 31. Twin-spool turbocharger low speed compressor map (combustor off)
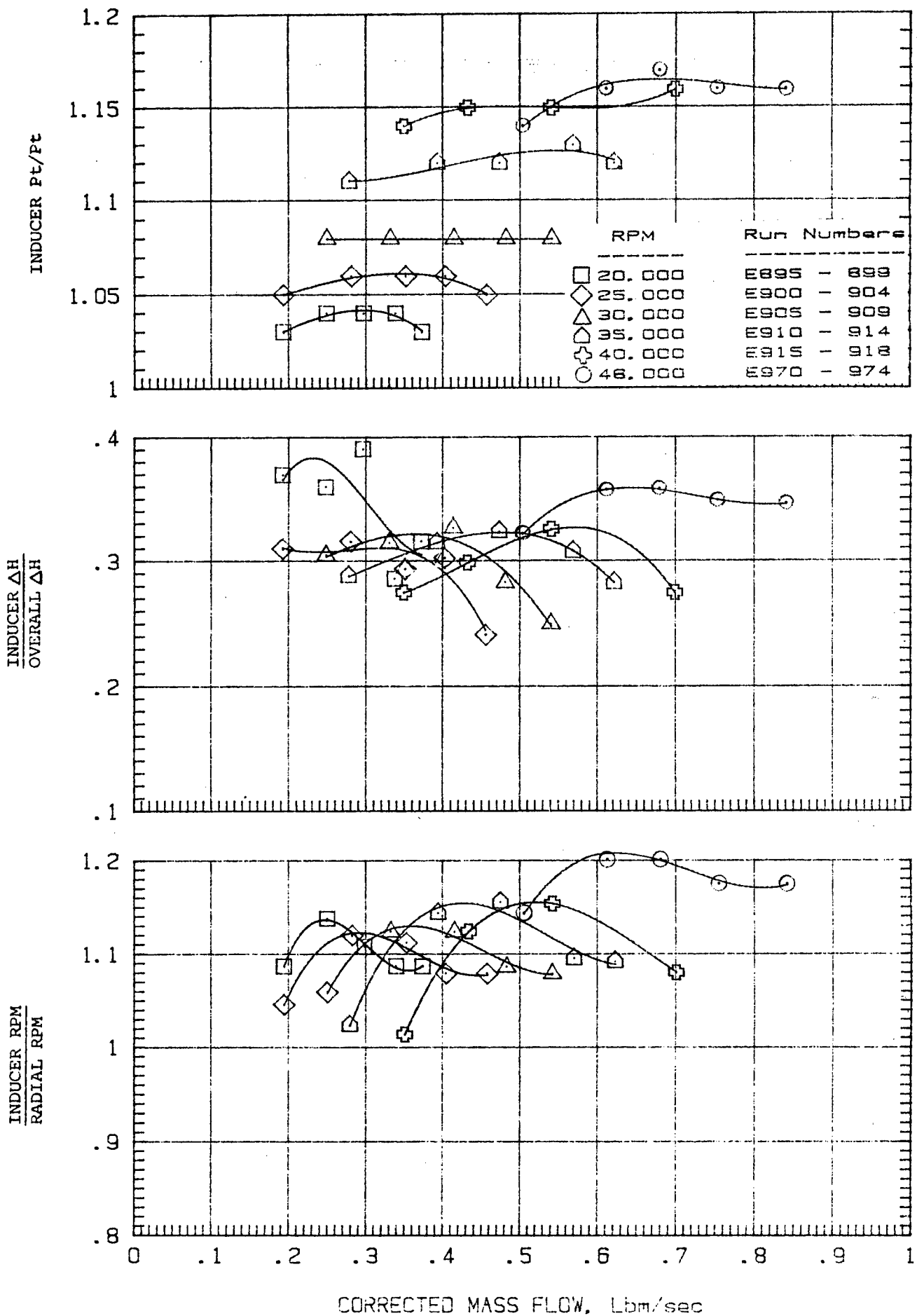
Figure 32. Variation of inducer speed/radial speed ratio, inducer work/radial section work and inducer pressure ratio as a function of corrected airflow
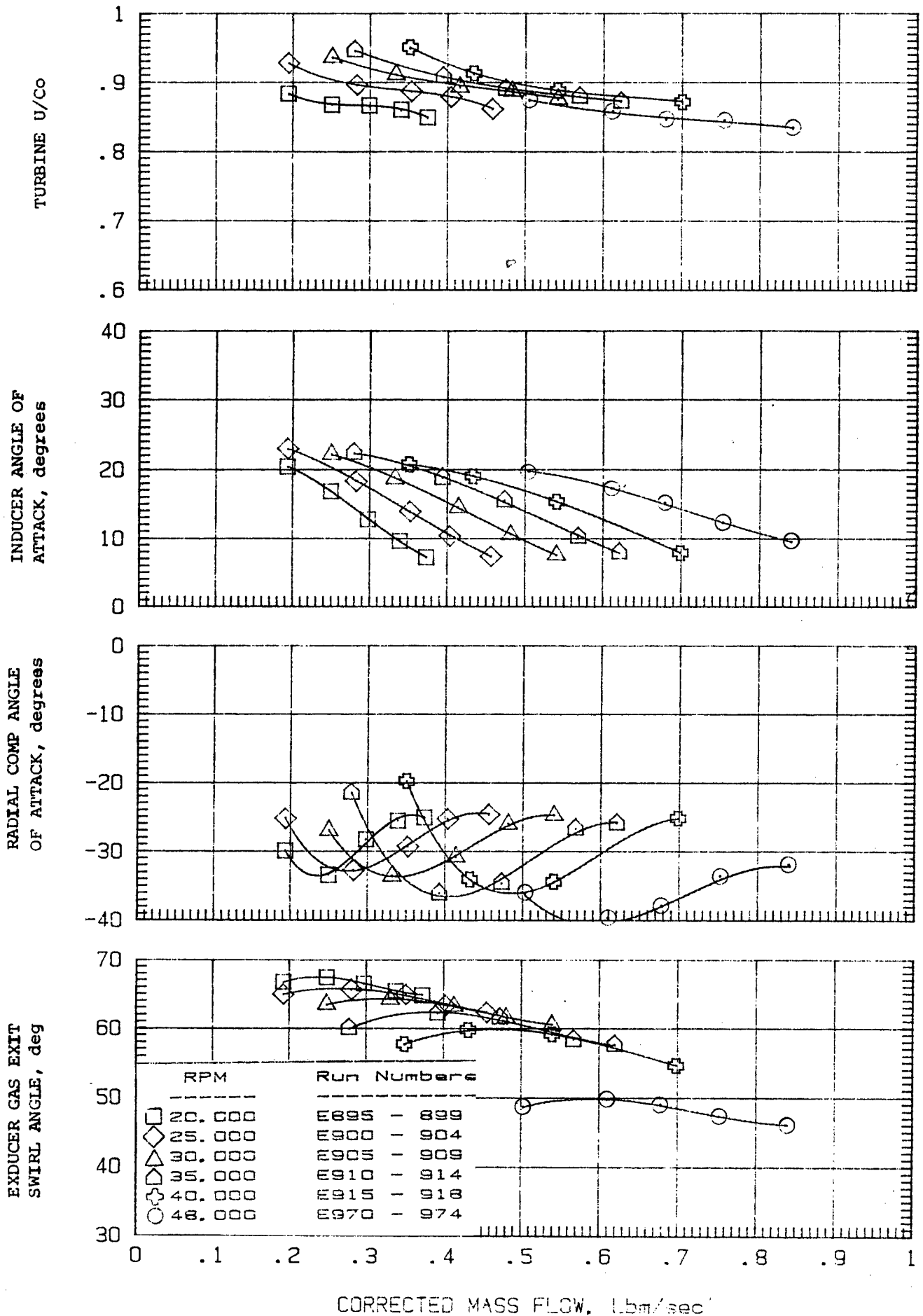
Figure 33. Variation of exducer gas exit swirl angle, radial compressor angle of attack, inducer angle of attack and turbine U/C_O as a function of corrected airflow

6.0 HARDWARE DESIGN AND FABRICATION - SECOND DESIGN TWIN-SPOOL TURBOCHARGER

6.1 Bearing System

Figure 34 presents a layout drawing of the second design twin-spool turbocharger. This alternate bearing system was developed for the twin-spool turbocharger in order to separate the dynamics of the inner and outer shafts thereby avoiding the obstacle of bearing coupled shaft-to-shaft imbalance and vibration difficulties. The principal features of the new bearing system were as follows:

i) The outer shaft of the twin-spool turbocharger was made to a slightly larger diameter than previously used and was installed in a bearing system which featured axially preloaded angular contact ball bearings and a radially preloaded damper system which located the bearing outer races. This ball bearing system had been previously fabricated, developed and tested (approximately 1000 hours of operation) and was of proven reliability. The necessary parts to build the complete bearing capsule were already on hand.

The ball bearing system was chosen to reduce the amount of radial shaft excursion to a minimum so that accurate inner-to-outer shaft concentricity could be achieved under dynamic conditions thereby avoiding shaft-to-shaft contact.

ii) The inducer end of the inner shaft was supported by a pair of permanently lubricated ball bearings installed in a bearing capsule which was attached to the compressor housing through rigid struts. The permanently lubricated bearings were preferred in the

compressor end of the turbocharger to avoid the presence of an
oil supply and drain system within the induction system which
could pose a hazard with diesel engine operation should an oil
leak occur.

The pair of bearings were located radially by preloaded damper
springs acting on the outer races and were preloaded in the axial
direction as well to eliminate all radial and end play between
the inner and outer bearing races. These bearings served to
locate the inner shaft axially as well as radially within the twin-
spool turbocharger.

iii)   The exducer end of the inner shaft was supported by a single
ball bearing which was (radially) spring-damper mounted within a
bearing capsule which was rigidly supported by the turbine
housing. Lubrication and cooling for the un-shielded ball bearing
was accomplished by flowing an air/oil mist into the bearing
capsule and through the bearing itself during operation.

iv)   Fabrication of new components was kept to a minimum. The
principal components to be fabricated were a new inner shaft,
inner shaft compressor end and turbine end bearing capsules and
related support structures, adapting hardware to mate above support
structures to the compressor and turbine housings and miscellaneous
fasteners and seals.

6.2 Aerodynamic Components

Table 6 presents the key physical parameters relating to the principal
aerodynamic components used in the new twin-spool turbocharger. Figure 35 presents

a photograph of the new rotating elements, complete with new inner shaft, in preliminary assembled form. Specific changes made to these components (with respect to the first design) were as follows:

Compressor Inducer

The compressor inducer diameter was increased by 0.060 inches along with a concurrent increase in blade-to-blade passage flow area.

Radial Compressor Impeller

The radial compressor impeller inlet diameter was increased by 0.060 inches as well. The exit backswept angle was decreased from 40 degrees to 25 degrees to increase the overall impeller work factor (due to increased net tangential component of exit airflow) thereby optimizing for best compressor efficiency at (engine) lug conditions.

Radial Turbine Rotor

The radial turbine exit diameter was decreased from 4.18 inches to 3.78 inches, with a concurrent decrease in exit channel area from 8.18 in^2 to 5.55 in^2. In addition, the exit blade angle was changed from 37 degrees to 51 degrees. These changes were made to increase the rearward tangential component of the channel exit gas velocity, thereby producing less positive gas exit swirl than previously attained and hence improving radial turbine efficiency. This change was also thought to increase the blade-to-blade solidity of the radial turbine rotor to the point where flow separation and recirculation would be avoided.

Turbine Exducer

The inlet diameter of the turbine exducer was decreased to 3.92 inches to provide a smooth entry for flow leaving the radial turbine section. The exit diameter of the exducer section was kept the same as previously used (4.18 inches)

to minimize axial exit leaving losses, and a diametral expansion angle of 24 degrees was used between the respective diameters. The original exit blade angle of 53.5 degrees and exit channel area of 6.48 in.^{2} were retained, as both were deemed appropriate to produce near zero exit swirl for the reduced exducer speed which was expected.

Compressor Housing and Diffuser

The compressor housing and adjustable vane diffuser assembly, as used previously in the twin-spool turbocharger, was modified to accept mounting of the new inner shaft bearing capsule within the compressor housing inlet duct. The diffuser throat area was set at 1.6 in^2.

Turbine Housing and Nozzles

A divided volute with adjustable vane turbine nozzle assembly was selected for use with the new twin-spool turbocharger design. This housing was selected because:

1) The effect of exhaust gas pulse recovery may be enhanced with the use of a turbine housing which has a divided volute. A divided volute, when used in conjunction with a split exhaust manifold of the type used on the NTC-475, serves to separate the exhaust pulses of the front three cylinders from those of the rear three cylinders. The benefit of this arrangement is to provide a smaller volume into which a given exhaust pulse will expand, thereby preserving the magnitude of the pulse which can be delivered to the turbine.

2) The use of adjustable turbine nozzles allows for fine-tuning of the engine/turbo system when actual engine testing has begun. By having control over the nozzle throat area, the optimum balance

between good engine lug performance and control of boost pressure
at the rated condition may be obtained without the need to obtain
and/or fabricate new hardware.

3) The divided volute/adjustable nozzle system required no fabrica-
tion (as it had been developed during a previous effort) and
required only simple modification to accept mounting of the new
inner shaft bearing capsule within the turbine housing exit duct.

Figure 36 presents a photograph of the partially assembled (second
design) twin-spool turbocharger. As shown in the photograph, the radial turbine
wheel and compressor wheel have been installed into the TMS ball bearing capsule.
In addition, the modified compressor and turbine housings have been fitted with
their respective inner shaft bearing capsules. Figure 37 presents a photograph of
the completed twin-spool turbocharger as viewed from the compressor inducer and
turbine exducer ends, respectively. As part of the final assembly procedure,
the following parameters were measured and/or adjusted to ensure proper turbocharger
operation:

Radial compressor shroud clearance.............. 0.014 in.

Radial turbine shroud clearance................. 0.038 in.

Outer shaft end play............................ 0.002 in.

Outer shaft rotating eccentricity............... $T.I.R. \leq 0.0006$ in.

Inducer to compressor housing concentricity..... Centering checked and verified

Exducer to turbine housing concentricity........ Centering checked and verified

Inner shaft end play............................ 0.003 in.

Inner shaft rotating eccentricity
    inducer end center.......................... $T.I.R. \leq 0.0004$ in.
    exducer end center.......................... $T.I.R. \leq 0.0004$ in.

Compressor diffuser vane height................. 0.250 in.

Compressor diffuser throat area................. $A_d = 1.60$ in.^{2}

Turbine nozzle throat area...................... $A_n = 2.89$ in.^{2}

①
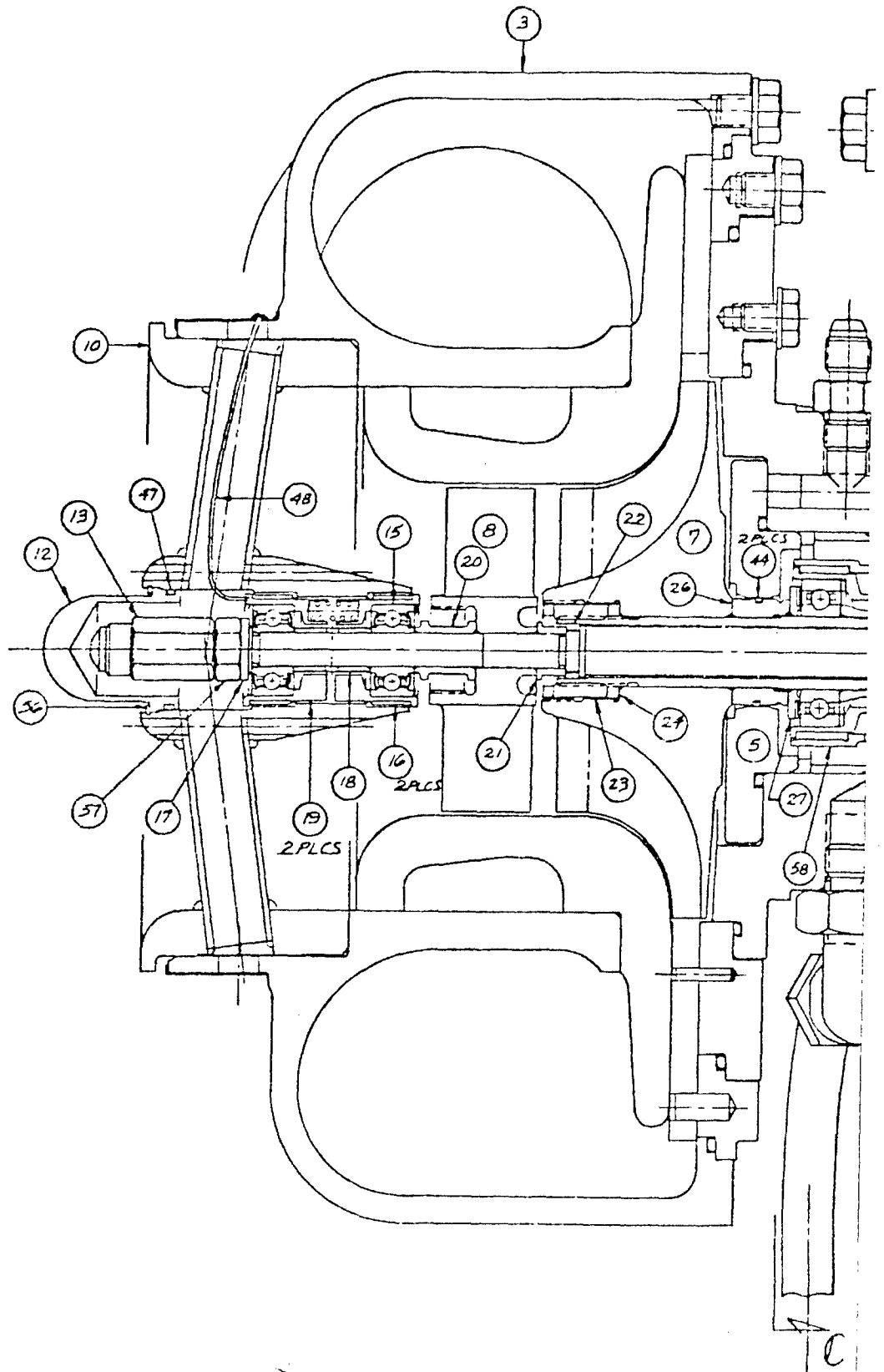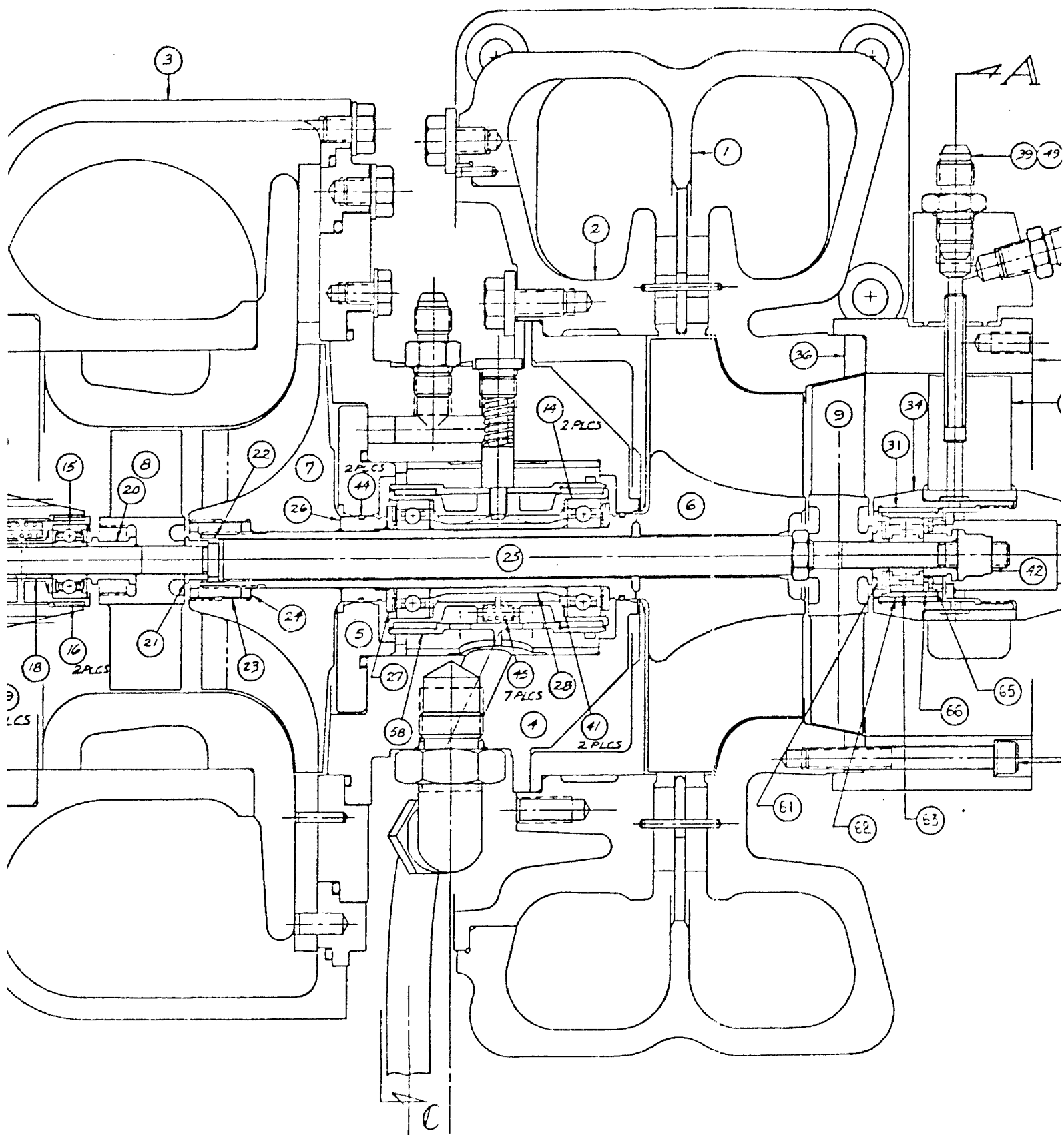
Figur

Figure 34A - PARTS LIST

F/N	Part No.	Req.	Description
1	TAC-129-20B-1	1	Turbine volute
2	-2	1	Turbine volute insert
3	-3	1	Compressor housing
4	-4	1	Bearing housing
5	-5	1	Bearing housing cover
6	-6	1	Radial turbine rotor
7	-7	1	Radial impeller
8	-8	1	Inducer
9	-9	1	Exducer
10	-10	1	Axial compressor bearing housing
11			
12	-12	1	Axial compressor bearing housing closure
13	-13	1	5/16-18 unc magnetic nut
14	103T/103H	2	Barden ball bearing
15	38 SST x 2	2	Barden ball bearing
16	TAC-129-20B-16	2	Axial compressor damper ring
17	-17	1	Axial compressor washer
18	-18	1	Inducer bearing spacer
19	-19	2	Axial compressor spring carrier
20	-20	1	Inducer spacer
21	-21	1	Axial shaft seal retainer
22	-22	1	Axial shaft seal ring
23	-23	1	Impeller nut
24	-24	1	Impeller washer
25	-25	1	Axial rotor shaft
26	-26	1	Thrust spacer
27	-27	2	Slinger - radial shaft bearing
28	-28	1	Radial shaft bearing spacer
31	-31	1	Axial turbine damper ring
32	-32	3	Axial turbine expansion joint pin
33	-33	1	Axial turbine bearing housing nut
34	-34	1	Axial turbine bearing carrier

(Continued)

F/N	Part No.	Req.	Description
35	TAC-129-20B-35	1	Axial turbine spider
36	-36	1	Axial turbine spacer
37	-37	1	Axial turbine ring
38	-38	1	Oil/air in adaptor - axial turbine
39	NZSB1801600D	1	Lee oil jet in fitting Ph213-417-8844
40	TAC-129-20B-40	2	Expansion joint pin adaptor
41	-41	2	Radial rotor bearing shim
42	ESNA Z1825-054	1	Axial turbine shaft nut
43	¼-20x2.25 cres.	6	Socket head bolts - Ref. F/N 37
44	Piston ring, R.M.#118032	2	Radial turbine/compressor seal ring
45	C0180-026-0620M	7	Assoc.Spring-3 axial comp/4 rad. rotor
46	8-C5BU-S	1	Parker fitting or equiv.
47	2-022 (.989 x .070)	1	Parker "O" ring or equiv.
48		1	Thermocouple
49	10061-04-5-0	1	Fluorocarbon seal Ph 213-594-0491
50	10-24 x 1.75	4	Socket head bolts - Ref. F/N 10
51	TAC-129-20B-51	2	F/N 40/32 Assem.
52	-52	1	F/N 38/32 Assem.
53	3-8 (.644 x .087)	1	Parker "O" ring or equiv. Ref. F/N 46
54	¼-20x1.25 cres.	2	Socket head bolts Ref. F/N 54
55	¼-20x1.00 cres.	4	Socket head bolts Ref. F/N 51
56	Spirolox - RR-115	1	F/N 12 retainer ring
57	TAC-129-26	1	5/16 unc nut
58	Existing part	1	Radial element rotor damper ring carrier
59	PB00900FFBP	1	Metal "O" ring
60	PB005339FFBP	1	Metal "O" ring
61	TAC-129-20C, F/N 61	1	Slinger washer
62	TAC-129-20C, F/N 62	1	Sleeve
63	38SSTX2	1	Barden ball bearing
64	TAC-129-20C, F/N 64	1	Spacer
65	TAC-129-20C, F/N 65	1	Retainer
66	F0846-008	1	Finger spring washer - Assoc. Spring Corp.

Compressor Inducer Section

```
Diameter................ 3.086 in.
Inlet Annular Area...... 6.75 in.²
RMS Radius.............. 1.152 in.
Inlet Blade Angle....... 40 deg.
Inlet Channel Area...... 4.20 in.²
Exit Blade Angle........ 69 deg.
Exit Channel Area....... 5.20 in.²
Number of Blades........ 10
```

Radial Compressor Section

```
Inlet Diameter.......... 3.086 in.
Inlet RMS Radius........ 1.164 in.
Inlet Blade Angle....... 52 deg.
Inlet Channel Area...... 5.00 in.²
Exit Diameter........... 5.00 in.
Exit Blade Angle........ 65 deg.
Exit Channel Area....... 3.225 in.²
```

Radial Turbine Section

```
Inlet Diameter.......... 5.086 in.
Exit Diameter........... 3.780 in.
Exit RMS Radius......... 1.423 in.
Exit Blade Angle........ 51.0 deg.
Exit Channel Area....... 5.551 in.²
```

Turbine Exducer Section

```
Inlet Diameter.......... 3.920 in.
Inlet Blade Angle....... 31.0 deg.
Exit Diameter........... 4.181 in.
Exit RMS Radius......... 1.560 in.
Exit Blade Angle........ 53.5 deg.
Exit Channel Area....... 6.48 in.²
```

Compressor Housing and Diffuser

```
Diffuser Throat Area.... 1.60 in.²
Number of Vanes......... 21
Housing Type............ Torus
```

Turbine Housing and Nozzle

```
Nozzle Throat Area...... 2.89 in.²
Number of Vanes......... 2 x 18 = 36
Housing Type............ Divided Volute
```

Where:

1) all angles are measured at the RMS radius
2) all compressor blade angles are given with respect to the tangential direction
3) all turbine blade angles are given with respect to the axial direction

Table 6. Key physical parameters of the second twin-spool turbocharger aerodynamic design

Exducer

Radial Compressor Wheel

Radial Turbine
Rotor and Shaft

Ball Bearing
Journal Areas

Inducer
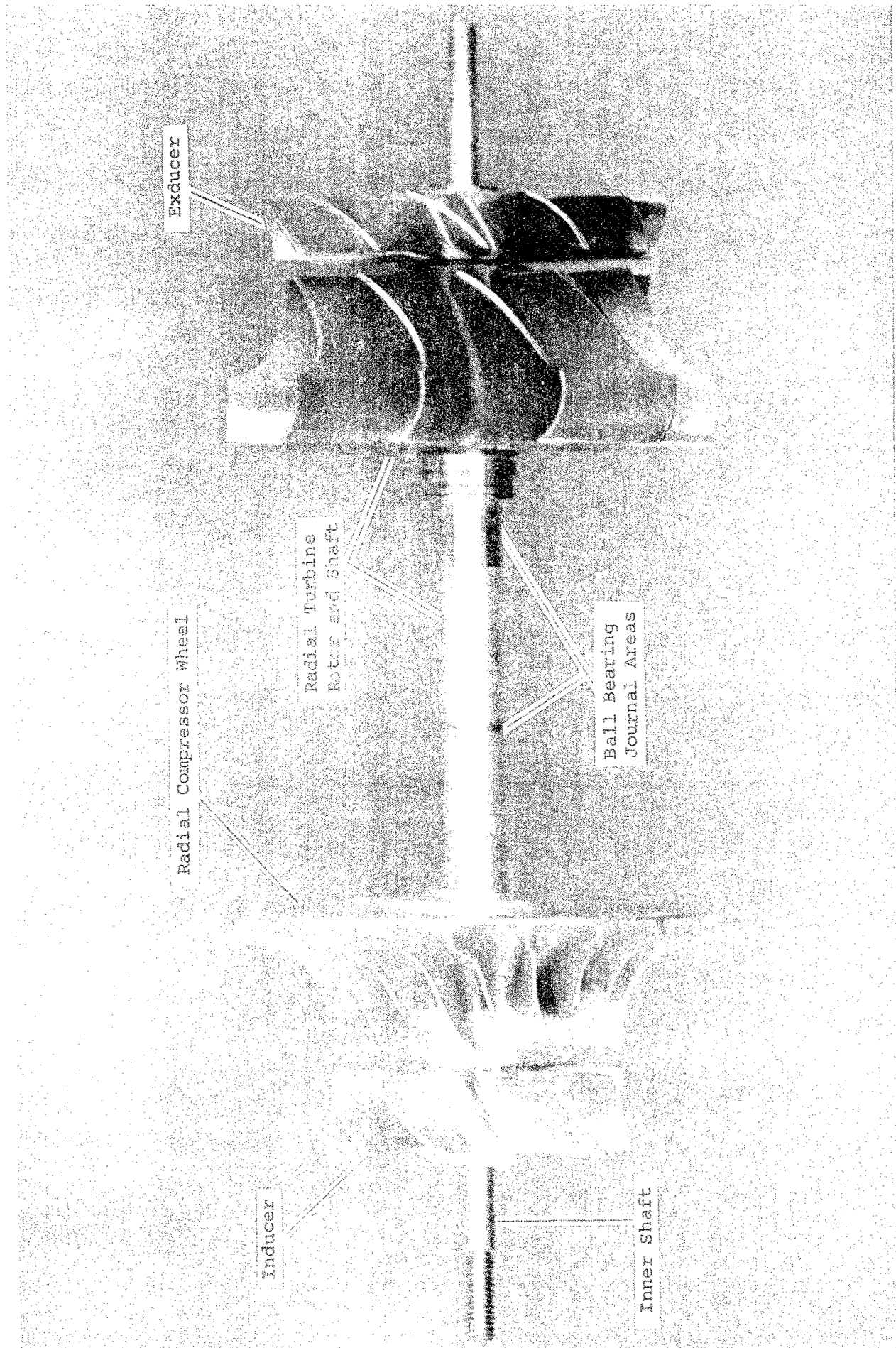
Inner Shaft

Figure 35. Preliminary assembly of inner and outer shaft rotating elements for new twin-spool turbocharger

Figure 36. Completed radial section bearing capsule assembly, along with turbine and compressor housings both equipped with inner shaft bearing capsules

Divided Volute Turbine
Housing w/Adjustable Nozzles

Radial Section
Speed Pickup

Oil Out

Compressor Housing
w/Vaned Diffuser
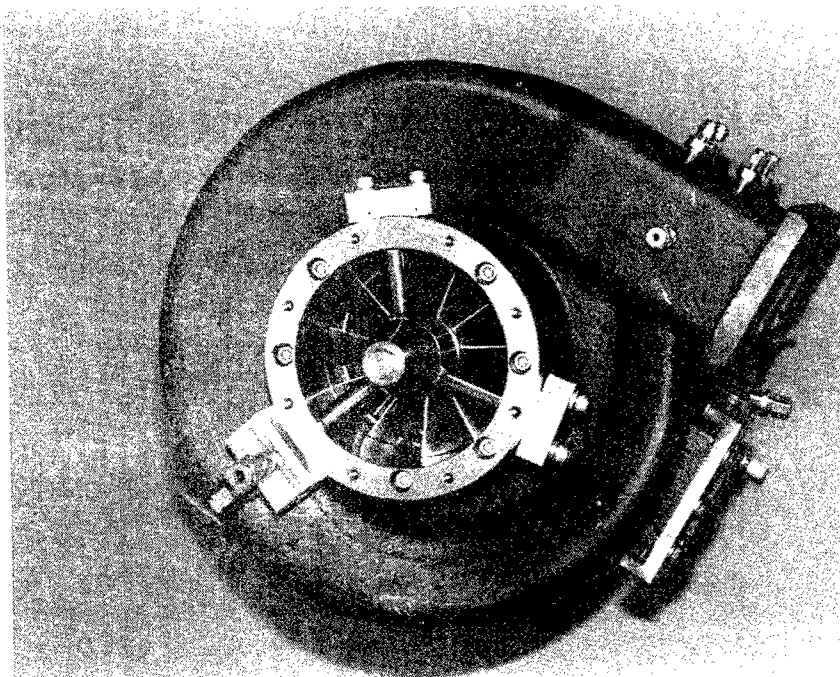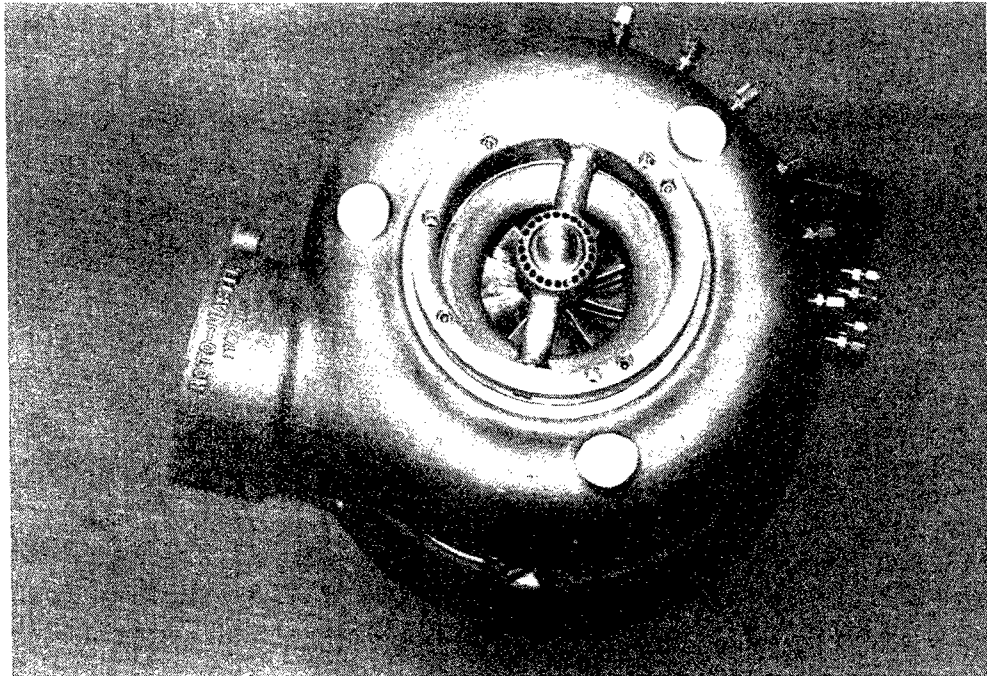
Figure 37. Assembled new twin-spool turbocharger as viewed
from compressor and turbine ends, respectively

7.0 EXPERIMENTAL PROGRAM - SECOND DESIGN TWIN-SPOOL TURBOCHARGER

7.1 Bench Testing

Figure 38 presents photographs of the (second design) twin-spool turbocharger installed in the TMS bench test facility. A complete description of bench test apparatus, set-up and test procedure appear in Sections 5.2.1 and 5.2.2 of this report.

7.1.1 Second Design Twin-Spool Turbocharger Bench Test Results

and Performance Analysis

Initial low speed operation of the (second design) twin-spool turbocharger was found to be free of significant vibration or mechanical interaction between the inner and outer shafts. Continued testing was conducted over a range of airflows at the corrected radial compressor speeds of 48,000, 60,000 and 72,000 RPM without any mechanical anomalies.

Presented in Figure 39 is the twin-spool compressor map resulting from the collected bench test data. The highlights of the compressor performance results, as shown in Figure 39, are as follows:

CORRECTED SPEED	MAX. PRESS. RATIO	MAXIMUM EFFICIENCY	AIRFLOW RANGE (SURGE TO W_{corr} @ 60% EFF.)
48,000 RPM	1.88/1	76%	.60 to .88 lbm/sec
60,000 RPM	2.56/1	74.4%	.78 to 1.17 lbm/sec
72,000 RPM	3.50/1	72%	1.05 to 1.51 lbm/sec

Also shown in Figure 39 are the engine operating speed lines for the Cummins NTC-475 twin-turbo diesel engine (as determined through baseline engine testing and presented in Section 5.1 of this report). These curves, as shown on the compressor map, serve to demonstrate the apparent suitability

of the twin-spool compressor section to meet or exceed NTC-475 baseline engine
performance requirements in the following ways:

1) Engine low speed operation (1300 RPM operating line is
shown) was sufficiently far away from the compressor low
flow surge limit that engine lugging capability (high
torque, low speed) appeared to be achievable at an even
lower engine RPM than originally possible.

2) Compressor efficiency at the 1300 RPM operating line varied
between 74 and 76 percent. This high efficiency helps to
extend high intake manifold pressure operation to lower
engine speeds (increased compressor efficiency reduces
turbine power requirements and allows higher radial section
speeds) and was expected to extend engine lugging capability.

3) Compressor range was sufficiently wide to accommodate full
rated engine power (at 2100 RPM) with no change in diffuser
area setting required. Compressor efficiency at full
engine power was expected to be about 67 percent, which
calculations showed to be ideal to prevent over-boosting of
the intake manifold pressure at that condition.

4) Maximum radial compressor speed at rated engine power was
estimated to be about 74,000 RPM. Previous experience with
the ball bearing rotor suspension being used had shown that
reliable and lengthy operation could be expected at this speed.

Further results are shown in Figure 40 which presents curves of
a) inducer angle of attack, b) radial compressor angle of attack, c) inducer to
radial compressor section speed ratio, d) inducer work done to overall compressor

-87-

work ratio, e) exducer exhaust swirl angle and f) turbine U/C_o ratio all as a function of corrected compressor airflow. It should be noted that for the test results presented here, the 48,000 RPM data was collected using cold drive air on the turbine side and that the 60,000 and 72,000 RPM data was collected using hot (900 to 1200°F) drive air on the turbine and was, therefore, more representative of results to be expected during engine operation of the twin-spool turbocharger. Using 60,000 and 72,000 RPM as a basis, the important results to be observed from Figure 40 are summarized below:

ITEM	RESULT	COMMENT
Inducer Angle of Attack	10.8 to -3.6 degrees	Low enough to avoid inducer stall, enhances inducer efficiency.
Radial Compressor Angle of Attack	6.3 to -5.0 degrees	Flow virtually aligned with blade leading edge. Ideal for best efficiency.
$\dfrac{\text{Inducer RPM}}{\text{Radial RPM}}$	74 to 78% approx.	Result of split wheel power balance. Ideal result to produce above effects.
$\dfrac{\text{Inducer } \triangle H}{\text{Overall } \triangle H}$	10 to 15% typical	Split wheel power balance. Ideal values.
Exducer Exhaust Swirl Angle	+6 to +10 degrees	Result of slowed exducer. Values are good for best overall turbine efficiency.
Turbine U/C_o	.66 to .69 dimensionless	Ratio of turbine tip speed to turbine spouting velocity. A value of .707 is optimum for maximum efficiency.

Concurrent with wide compressor range and good low-flow efficiency, the turbine section of the twin-spool turbocharger exhibited favorable performance as well. The ratio of radial section tip speed to exhaust gas spouting velocity, U/C_o, is a strong factor affecting turbine efficiency. The ideal value of 0.707

was effectively achieved during the 60,000 and 72,000 RPM tests. In addition, turbine exit gas swirl (for which large positive values, i.e., greater than 20 degrees, are known to deteriorate turbine performance) was observed to be within 6 to 10 degrees positive with respect to exducer rotation. In consideration of these factors, it was expected that the turbine section would have the efficiency necessary to provide the required power at low flows to capitalize on the wide range of the twin-spool compressor section.

The above results indicated that the new twin-spool turbocharger geometry had been optimized to the point where the range and efficiency would permit the twin-spool turbo to meet or exceed the performance of the two turbos currently used on the NTC-475. Further testing of the twin-spool turbocharger was then carried out on the NTC-475 diesel engine.
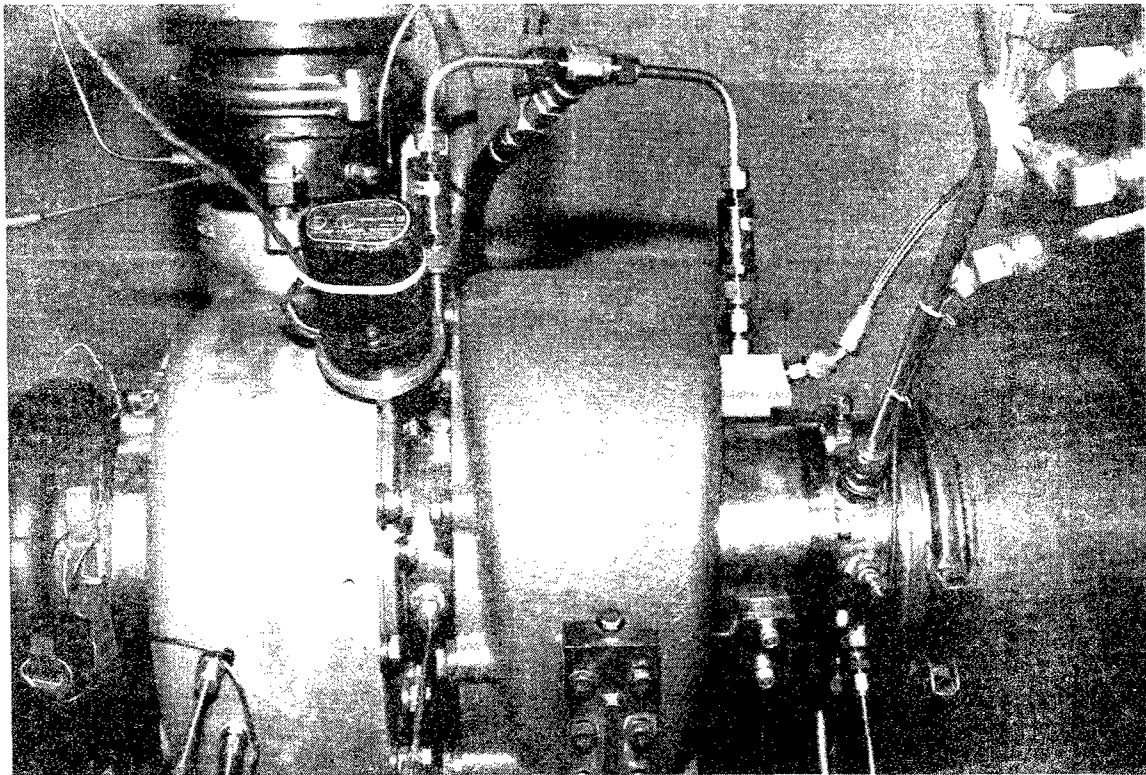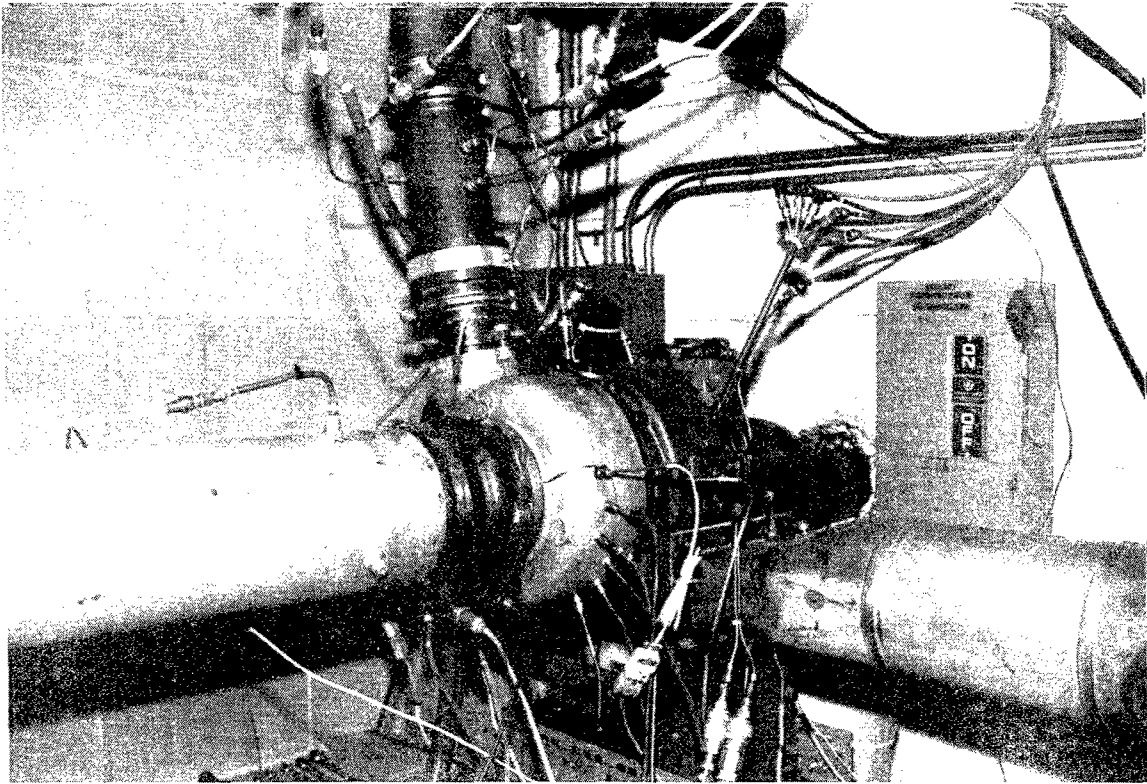
Figure 38. Completed installation of the twin-spool turbocharger in the
TMS turbo bench test facility

RPM	Run №.
□ 48,000	N13 – N15
◇ 60,000	N16 – N20
△ 72,000	N21 – N25

EFFICIENCY (%)

100
90
80
70
60
50
40

Cummins NTC-475
Baseline Engine
Operation Lines

N/√θ = 72,000 RPM

N/√θ = 60,000 RPM

N/√θ = 48,000 RPM

1300 RPM
1400 RPM
1500 RPM
1700 RPM
1900 RPM
2100 RPM

PRESSURE RATIO

5
4
3
2
1

0   .2   .4   .6   .8   1   1.2   1.4   1.6

CORRECTED MASS FLOW Lbm/sec
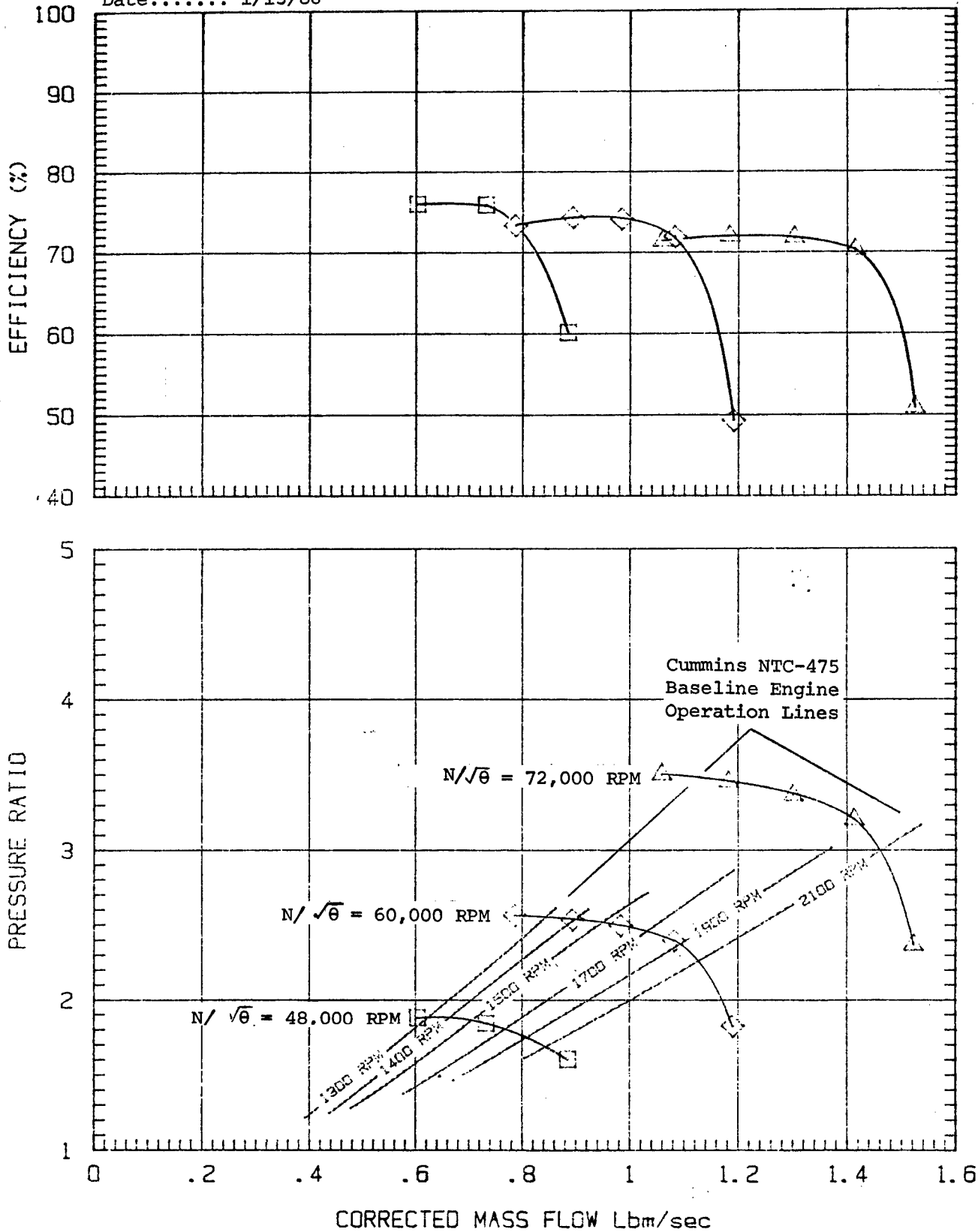
Figure 39. Compressor map showing performance results of twin-spool
turbocharger as a function of corrected compressor air flow.

-91-
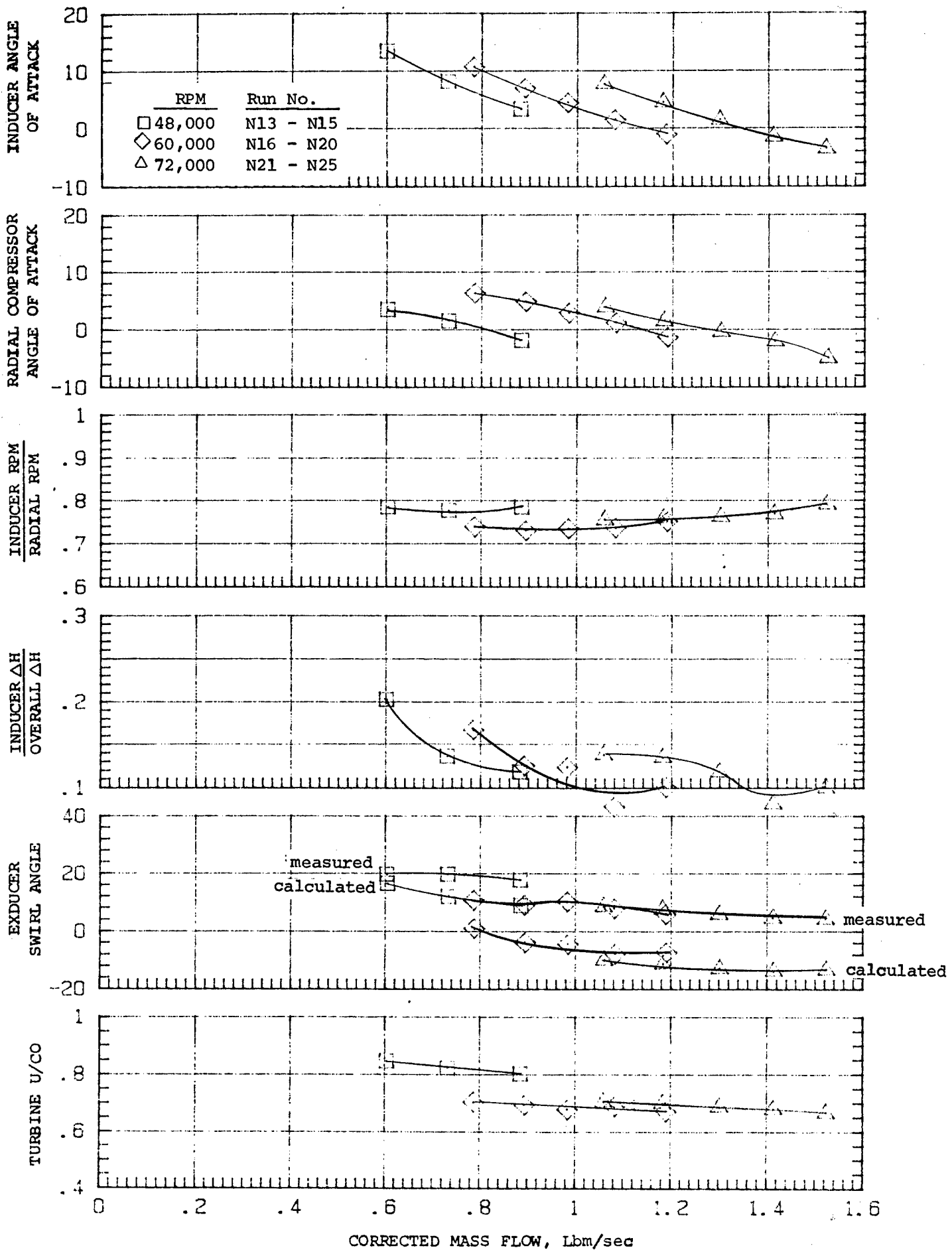
Figure 40. Various important parameters which affect twin-spool turbocharger performance as a function of corrected compressor airflow

7.2 Twin-Spool Turbocharger/Engine Testing

7.2.1 Engine/Turbocharger Test Set-Up

Figure 41 presents a photograph of the (second design) twin-spool turbocharger installation on the Cummins NTC-475 diesel engine. While the general engine test set-up is described in Section 5.1.3 of this report, specific preparations for twin-spool turbocharger/engine testing are described as follows:

1) The twin-spool turbocharger was mounted via the turbine volute inlet flange directly to the NTC-475 exhaust manifold outlet. The existing exhaust system (en route to muffler) was adapted to the twin-spool turbine outlet.

2) The engine inlet duct system was connected to the twin-spool compressor inlet. Fabrication and installation of new ducting was required to connect the twin-spool compressor outlet to the engine intake manifold.

3) The engine lubrication system was adapted to the twin-spool turbocharger so as to provide oiling for both the main (radial rotor shaft) bearing capsule and the inner shaft (turbine exducer end) bearing capsule. In addition, regulated bleed air (from the engine auxilliary compressor) was connected to the inner shaft bearing capsule air/oil mist mixing block inlet.

4) The twin-spool turbocharger was fully instrumented for pressures, temperatures, speeds and airflow rate. In addition, protective radiation shielding was placed on the engine exhaust manifold, turbine volute and exhaust pipe to protect the instrumentation lines from heat damage.

-93-

7.2.2 Test Procedure

Table 7 is presented to show the engine operating points that were set for the NTC-475 diesel engine/twin-spool turbocharger test. At each of the seven engine speeds shown, torque was adjusted by increments of 300 lbs-ft until the maximum torque for the given speed was obtained. This test plan yielded 33 engine operating points from which data was collected.

For each of the operating conditions, the set speed was held constant by varying dynamometer load as fuel flow was adjusted to produce the desired torque output. In addition, the inlet air control valve was adjusted to maintain the constant compressor inlet reference pressure of 28.4 inches of Hga Data was collected for non-critical measurements (i.e., support system measurements not related to engine/turbo performance) while stabilization of important pressures and temperatures occurred. Once steady state conditions were verified, critical data was collected and the next set point was established.

7.2.3 Test Data Reduction

An engine performance map was generated along with supplemental curves which serve to analyze engine/turbocharger performance. Specially designed twin-spool compressor and turbine and existing engine performance analysis computer programs were used to calculate the critical turbocharger and engine performance from the test data.

7.2.4 Twin-Spool Turbocharger/NTC-475 Engine Test Results and

Performance Analysis

Presented in Appendix A are the "raw" test data and reduced test results in tabular form. The reduced test data is also presented in several plots which are discussed as follows:

- Figure 42 presents BMEP and BHP as a function of engine speed and torque, and also presents maximum engine torque as a function of engine speed. Comparison with Figure 23, Section 5.1.6, shows that the maximum BHP and BMEP obtained in the twin-spool turbocharger/NTC-475 engine test closely match the results of the baseline engine test. The rated BHP of 475 hp was obtained at 2100 RPM rated engine speed and the maximum deviation occurred at 1300 RPM where BHP and BMEP varied by approximately 3 percent from baseline results.

- Figure 43 presents BSFC, F/A ratio and exhaust manifold gas temperature, all as a function of engine speed and torque. As can be seen there, the excellent BSFC of about 0.35 was obtained at 1400 RPM, at the maximum torque of 1476 lb/ft, which matches the baseline test results.

- Figure 44 presents exhaust manifold pressure, intake manifold pressure and engine airflow, all as a function of engine speed and torque. As shown in these curves, a peak boost pressure of 82.5 in. Hga and corresponding peak airflow of about 1.45 lb/sec were obtained at 2100 RPM rated engine speed, which fell within about 5 percent of baseline engine test results.

- Figure 45 presents compressor pressure ratio, compressor effi-ciency, radial compressor wheel angle of attack and inducer angle of attack, all as a function of engine speed and torque. In addition, Figure 46 presents cor-rected radial compressor RPM, ratio of inner to outer shaft speeds and ratio of work done by the inducer stage to total compressor work, all as a function of engine speed and torque. As can be seen in Figure 45, the twin-spool compressor section demonstrated increasing efficiency in going from 2100 RPM rated engine

-95-

speed (approximately 70 percent) to 1500 RPM lug engine speed (73 to 75 percent efficiency) and produced no less than 71 percent compressor efficiency at 1200 RPM at torque settings of 600 lb/ft and above. This maximization of compressor efficiency at lug engine speeds is exactly what is needed to a) give optimum engine low speed (lug) performance while b) avoiding engine over-boost at rated speed.

Further examination of Figure 45 shows that the maximum compressor efficiency, which occurred at 1500 engine RPM, coincides with the occurrence of near zero angles of attack on both the inducer and radial compressor sections (see upper curves). These aerodynamic parameters were a direct result of the twin-spool turbocharger split inducer/exducer design which produced the desired shaft-to-shaft power and speed ratios presented in Figure 46.

- Figure 47 presents turbine pressure ratio, turbine efficiency, turbine U/C_o and turbine exducer exit gas swirl, all as a function of engine speed and torque. These curves show that the overall twin-spool turbine section exhibited increasing efficiency from about 65 percent at 2100 RPM rated engine speed to about 80 percent at 1200 RPM lug speed. This is the desired result when designing for optimum engine lug performance and is attributed to the following factors:

a) Turbine U/C_o, at the maximum torque condition, increased from about 0.67 at 2100 RPM rated speed to about 0.71 at 1300 RPM lug speed. The optimum value of U/C_o, for best turbine efficiency, is 0.707.

b) Exducer gas exit swirl angle, at the maximum torque condition, varied from about -12 degrees (minus means opposite wheel rotation) at 2100 RPM to near zero swirl at 1300 RPM lug

speed. When zero exit swirl is achieved, tangential exit losses from the turbine can be avoided, thereby maximizing available turbine efficiency. The above was made possible through the design of the split inducer/exducer concept which allowed lower exducer rotational speeds, thereby preventing large positive values of exit swirl.

c) Exhaust pulse energy recovery in the twin-spool turbine, most notably at lower engine speeds where availability of pulse energy increases, served to enhance turbine efficiency by the extraction of extra work from the exhaust gas over and above that which steady-state, steady-flow calculations predict using time-averaging pressure and temperature measurements.

The above results demonstrate the suitability of the twin-spool turbocharger to provide good engine lug speed performance while limiting rated speed boost pressure. Presented in Figure 48 are the NTC-475 engine speed operating lines, as obtained through engine testing with the twin-spool turbocharger, superimposed on the compressor map of the twin-spool turbocharger (as determined through bench testing and presented in Section 7.1). This compressor map serves to demonstrate the ability of the twin-spool turbocharger to not only meet the range and pressure ratio requirements of the NTC-475 diesel engine from the original 1300 RPM lug engine speed to 2100 RPM rated engine speed but in addition extends the lug capability to 1200 RPM.
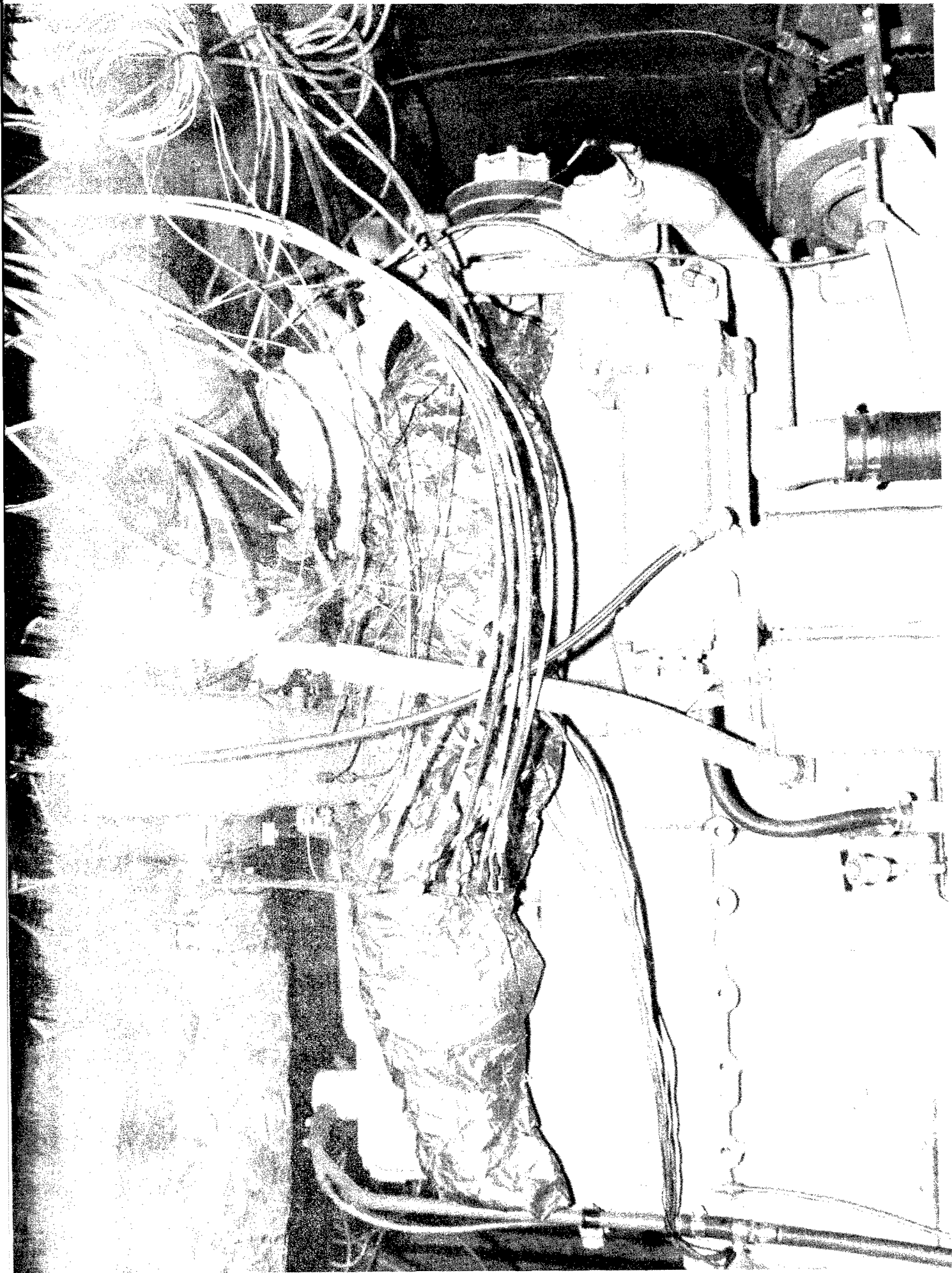
Figure 41. Installation of the twin-spool turbocharger on the Cummins NTC-475 diesel engine

RPM	TORQUE SETTING, Lbs. ft.				
1200	300	600	900	1200	-----
1300	300	600	900	1200	MAX
1400	300	600	900	1200	MAX
1500	300	600	900	1200	MAX
1700	300	600	900	1200	MAX
1900	300	600	900	1200	MAX
2100	300	600	900	MAX	-----

Table 7. Twin-spool turbo/NTC-475 engine operating points
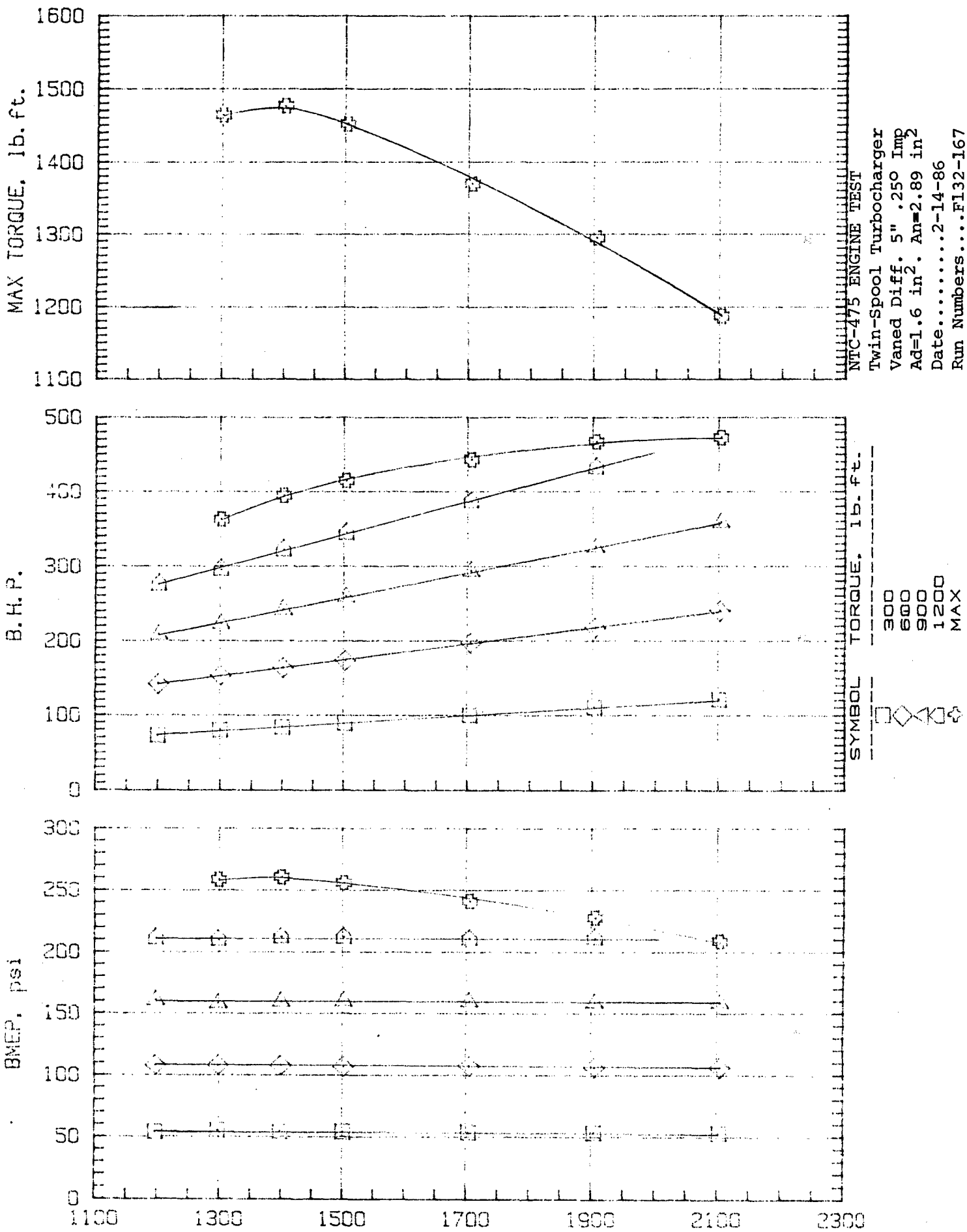
Figure 42. Variation of engine brake horsepower and brake mean effective pressure as a function of engine speed and toque, twin-spool turbochar ger / NTC-475 diesel engine test.
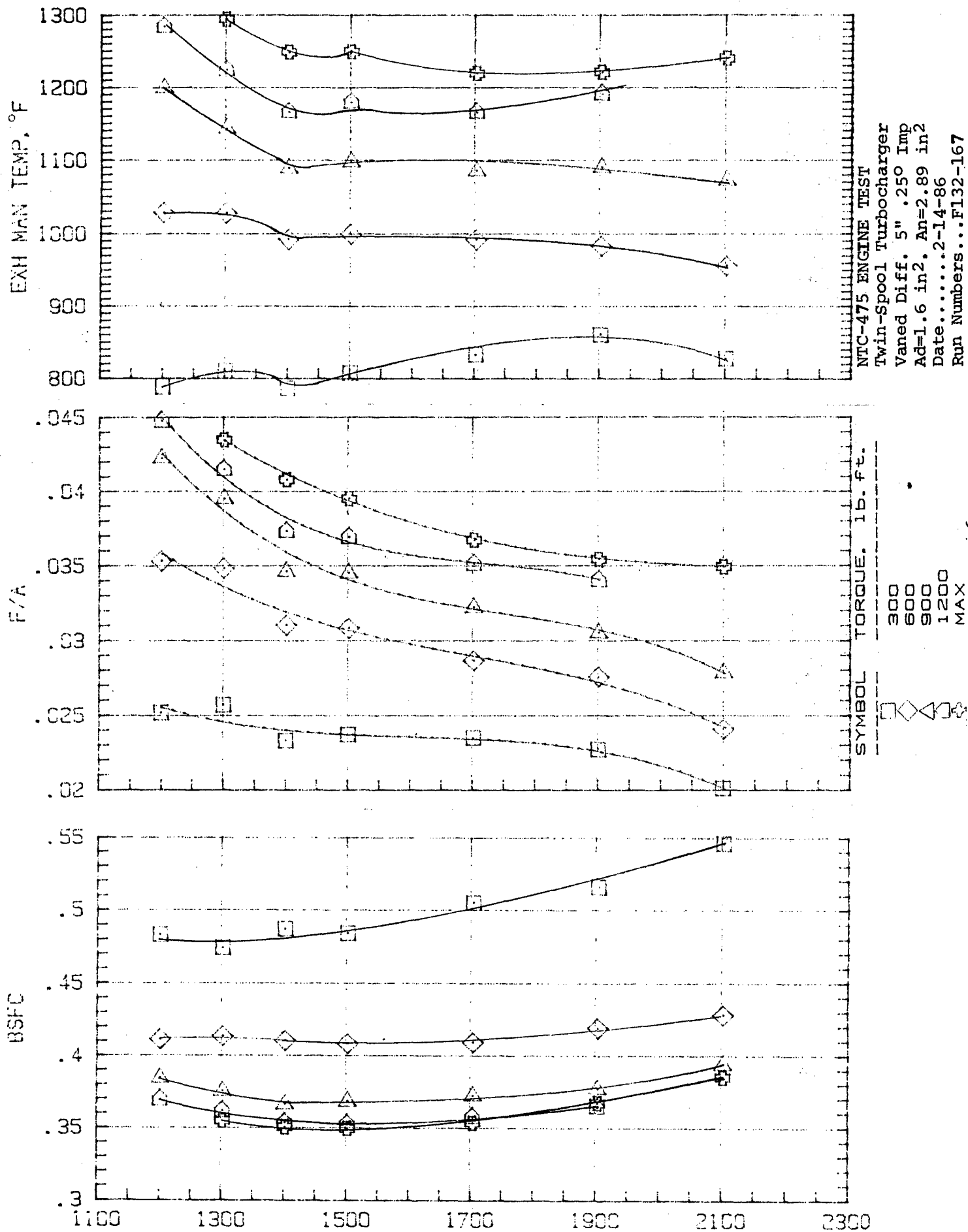
Figure 43. Variation of exhaust manifold gas tempetature, fuel/air ratio, and brake specific fuel consumption as a function of engine speed and torque, twin-spool turbocharger / NTC-475 diesel engine test.
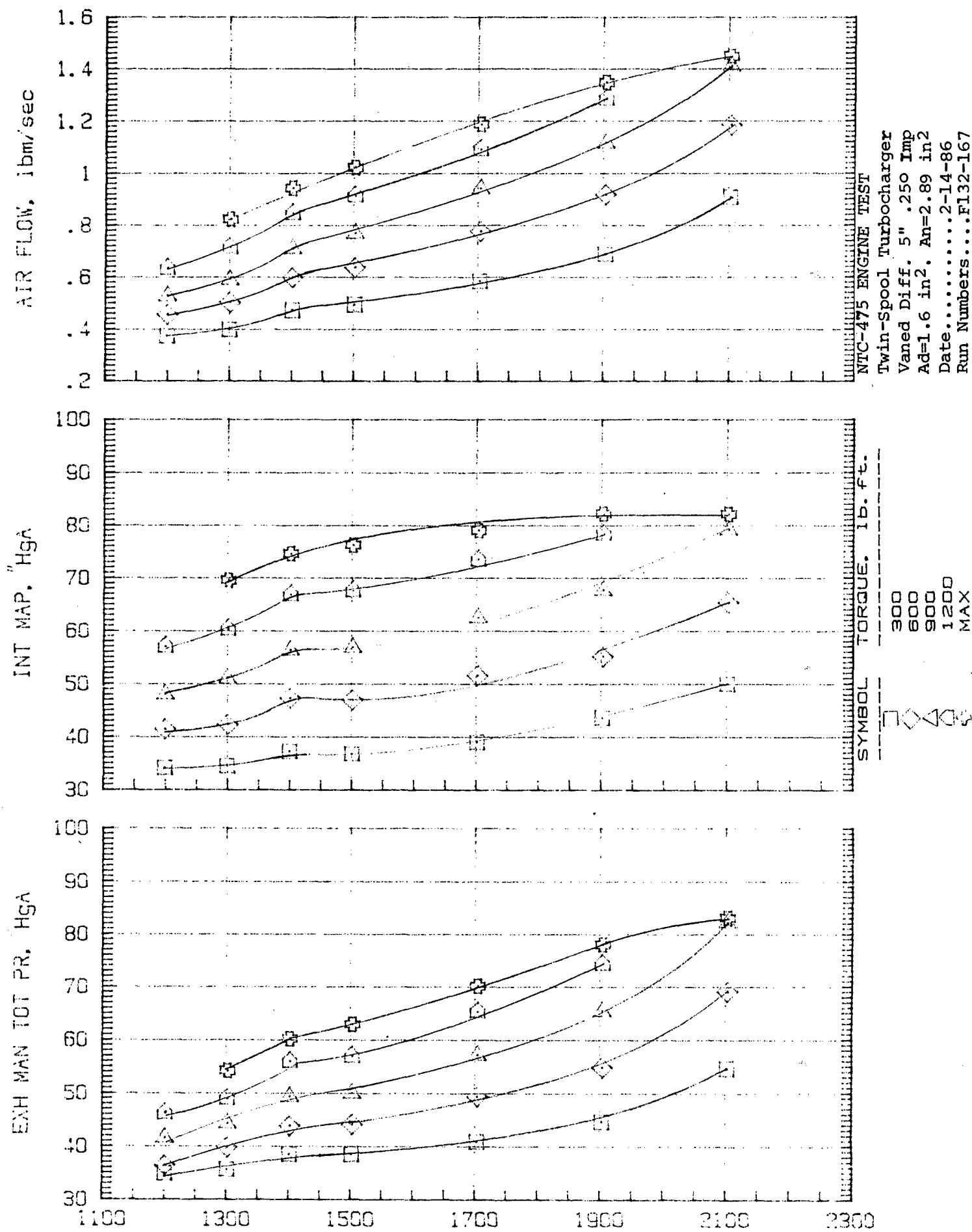
Figure 44. Variation of engine air flow, intake manifold absolute pressure, and exhaust manifold absolute pressure as a function of engine speed and torque, twin-spool turbocharger / NTC-475 diesel engine test.
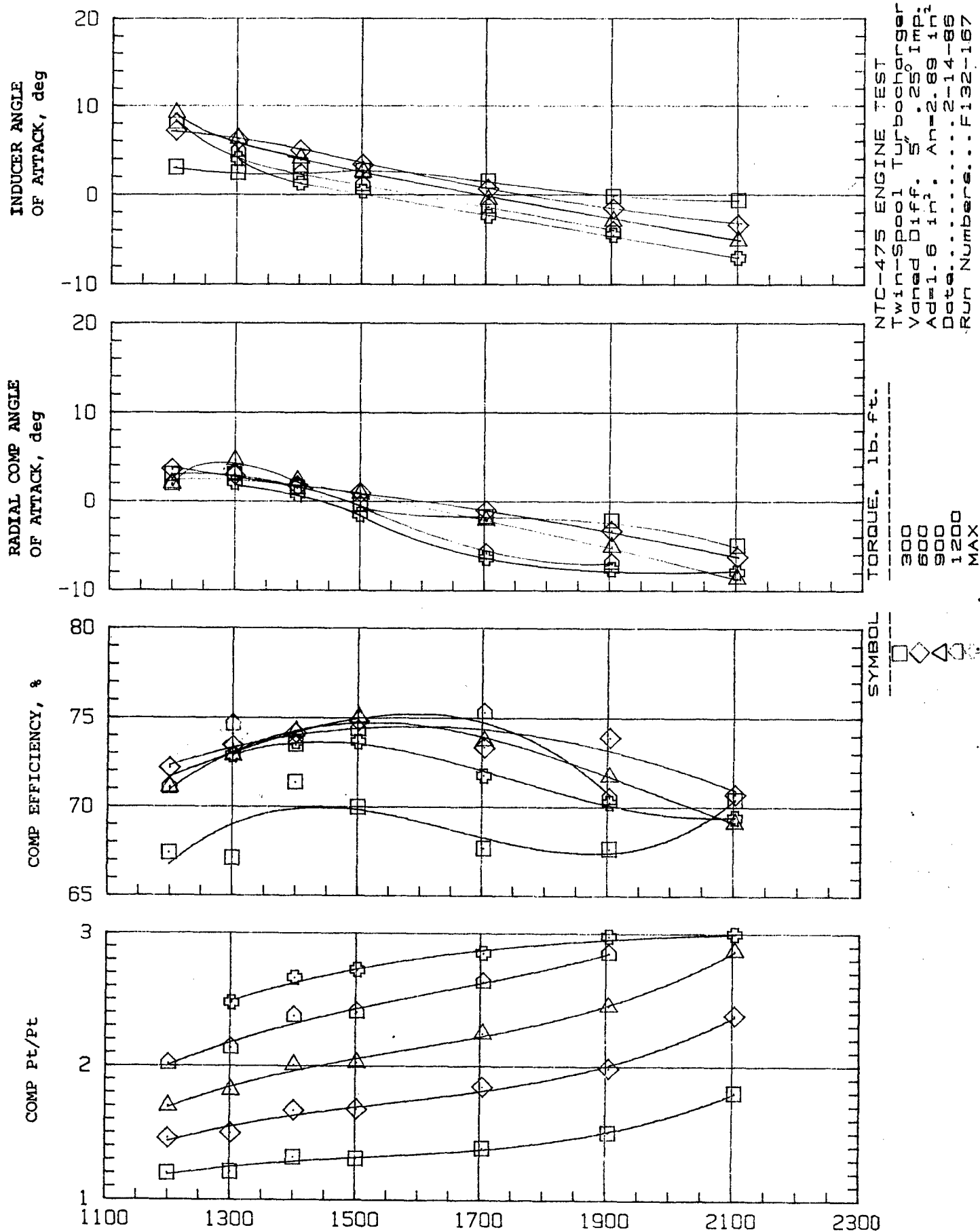
Figure 45. Variation of inducer angle of attack, radial compressor angle of attack, compressor efficiency, and compressor pressure ratio as a function of engine speed and torque, twin-spool turbocharger / NTC-475 diesel engine test.
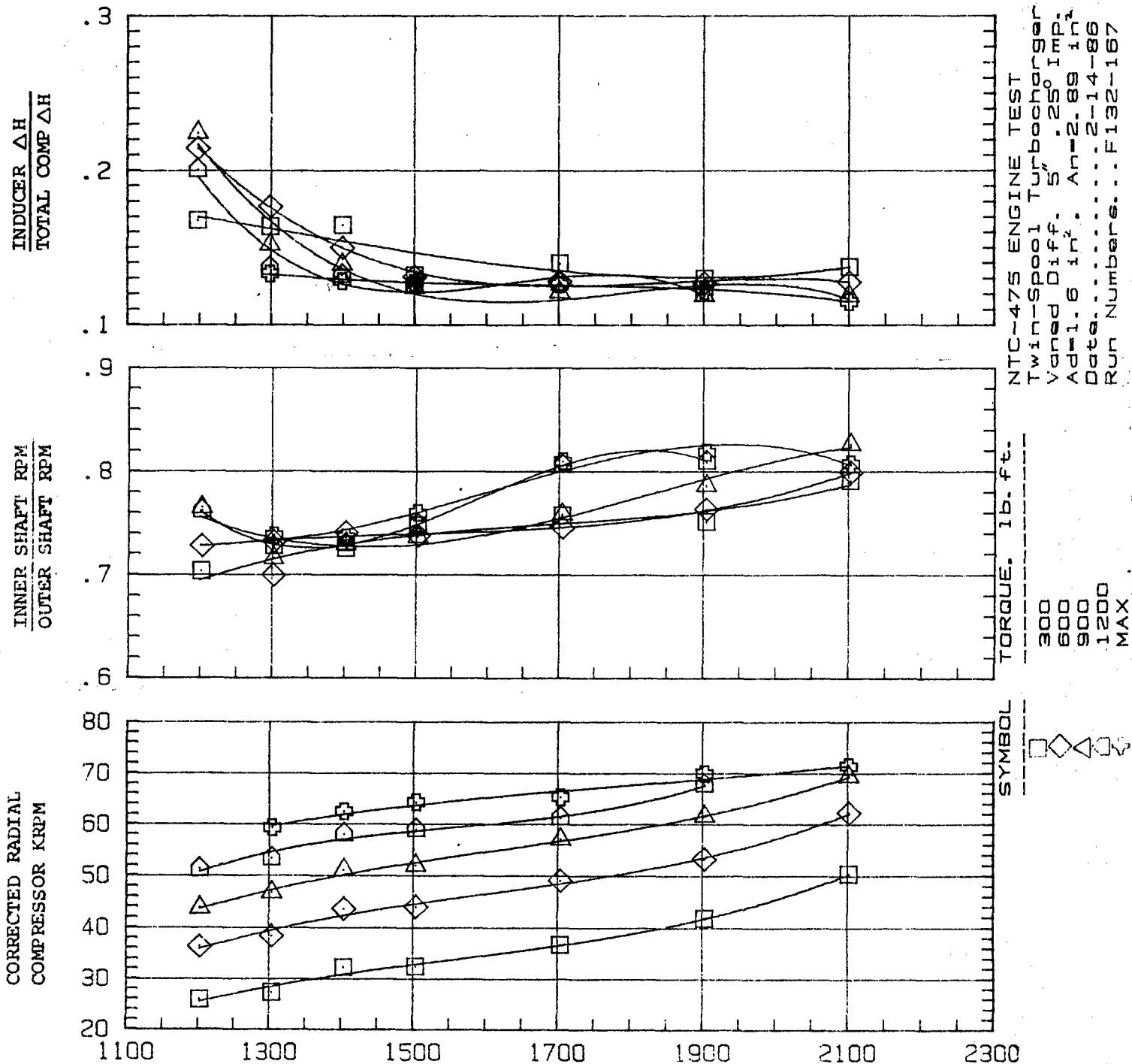
Figure 46. Variation of inducer work ratio, shaft speed ratio, and corrected radial compressor speed as a function of engine speed and torque, twin-spool turbocharger / NTC-475 diesel engine test.
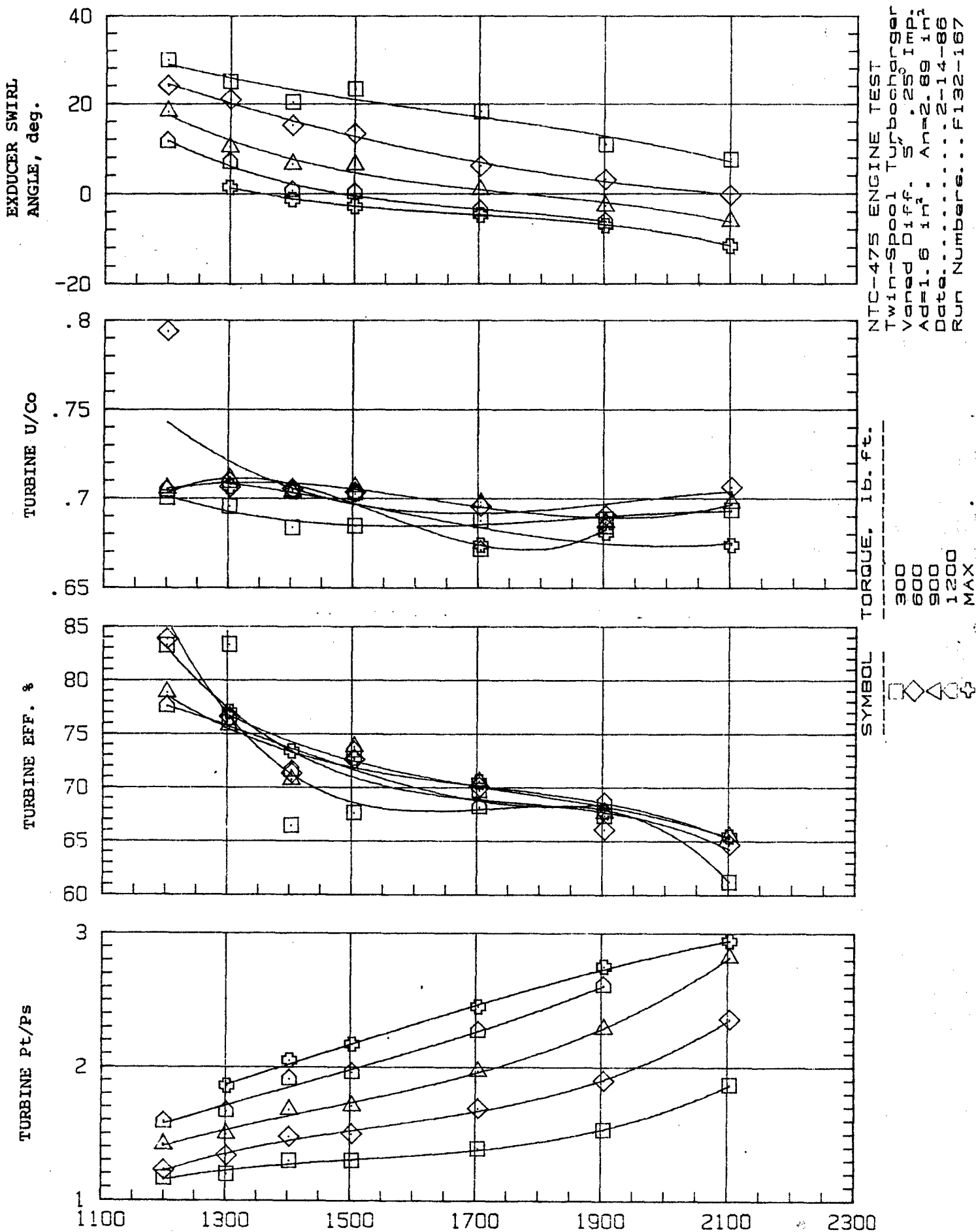
Figure 47. Variation of exducer exit gas swirl angle, turbine U/Co, turbine efficiency, and turbine pressure ratio as a function of engine speed and torque, twin-spool turbocharger / NTC-475 diesel engine test.
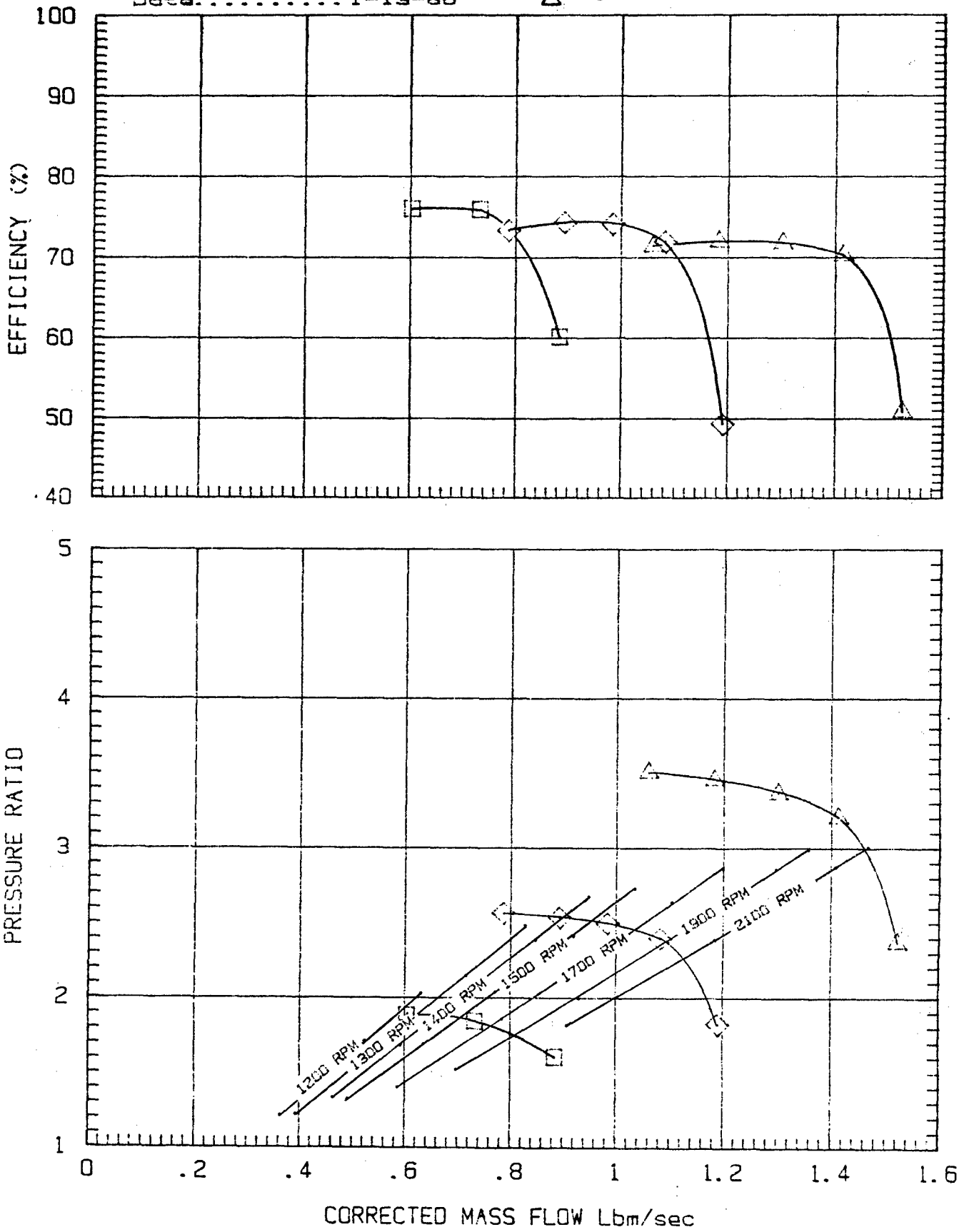
Figure 48. Compressor map of twin-spool turbocharger with experimentally
determined NTC-475 engine operating speed lines superimposed.

8.0 CONCLUDING REMARKS

Based upon the results of the work reported herein, the following conclusions are drawn:

1. The twin-spool turbocharger has been successfully developed to the point where it could replace the original two-stage turbocharger system of the Cummins NTC-475 diesel engine.

2. The efficiency of the twin-spool turbocharger at engine lugging speeds served to maintain high intake manifold pressure, thereby yielding essentially the same BHP, BSFC and torque from the NTC-475 as available with the original two-stage turbocharger system.

3. The ratio of shaft speeds in the final twin-spool turbocharger was observed to be ideal. This ratio was found to vary automatically with respect to flow condition, thereby providing self-compensation for aerodynamic performance over a wide range of airflow.

4. The twin-spool turbocharger configuration developed for the NTC-475 occupies less volume than the two-stage system, thereby minimizing the volume for the engine packaging envelope, often a major concern in military vehicle applications. In addition, induction and exhaust ducting and related insulation requirements are simplified and reduced.

5. The twin-spool turbocharger system, albeit successfully developed during this effort, is thought to have the potential for further optimization and performance enhancement. An improved system could sustain even higher intake manifold pressure during engine lug operation, and, in conjunction with a commensurate increase in fuel flow, would allow even higher engine BHP, torque and improved BSFC to be obtained.

6. Further improvement of the twin-spool turbocharger mechanical

    design would involve continued development of the original concen-

    tric shaft design, with the outer shaft supporting the inner shaft.

    It is felt that the successful implementation of this design would

    result in a simpler, more practical and economical turbocharger

    assembly.

REFERENCES

1. Berenyl, Steven G., "Advanced Diesel Technology", TARADCOM Final
   Technical Report No. 12305 for U.S. Army Tank-Automotive
   Command, Warren, Michigan, August 1977.

2. Harp, James L. and Yano, Robert A., "A Broad Range Turbocharger
   Using Compressor Bleed Techniques", Final Report SR-32 for
   U.S. Army Tank-Automotive Command, Warren, Michigan, January
   1981.

3. Hill, Philip G. and Peterson, Carl R., "Mechanics and Thermodynamics
   of Propulsion", Addison-Wesley Publishing Co., Reading,
   Massachusetts, p. 267 (1965).

APPENDIX A

- ENGINE BASELINE DATA WITH TABULATED RESULTS, AND

- ENGINE/TWIN-SPOOL TURBOCHARGER DATA WITH TABULATED RESULTS

| RUN NO. | ENG. RPM | T-18 RPM | HC 3 RPM | VNT. IN T. | TEMPERATURES °F | | | | | | | | |
					T 18 COMP IN	T 18 COMP OUT	HC 3 COMP OUT	INT. MAN.	HC 3 TURB. IN	HC 3 TURB. IN	HC 3 TURB OUT	T 18 TURB IN	T 18 TURB OUT
F1	1305	14700	27800	85	86	100	132	178	807	823	718	730	672
F2	1304	21100	39000	85	89	118	182	180	1032	1034	936	926	852
F3	1302	26800	47000	90	93	139	232	181	1148	1137	1006	1229	944
F29	1300	32000	53200	79	86	151	270	181	1204	1184	1050	1067	980
F28	1300	37200	58800	82	86	172	315	186	1266	1247	1090	1106	989
F4	1399	16400	28700	93	94	112	147	178	817	804	714	730	677
F5	1401	23000	40800	94	95	128	197	180	1020	1015	826	911	832
F6	1399	28900	48400	95	97	150	248	183	1132	1121	988	1007	927
F27	1404	34400	54400	88	88	162	285	183	1184	1162	1021	1040	935
F26	1400	38000	58600	81	87	170	301	184	1193	1193	995	1024	883
F7	1498	17800	30200	95	98	119	158	177	829	805	723	746	699
F8	1501	25300	42300	94	98	139	214	180	1023	1011	893	912	843
F9	1504	31400	49800	97	98	161	265	184	1120	1109	975	972	905
F25	1500	36900	55100	76	84	169	297	184	1164	1140	1005	1019	919
F24	1502	40200	58800	79	84	179	316	185	1184	1175	929	1013	870
F10	1697	21300	33900	96	98	126	175	177	855	822	733	753	696
F11	1700	29500	45300	95	100	153	239	182	1022	1003	882	898	822
F12	1703	35900	51800	95	100	179	292	186	1112	1095	953	969	871
F23	1698	41700	56600	80	88	194	328	187	1157	1132	992	1001	889
F22	1701	44400	59100	91	93	214	360	191	1200	1172	1026	1035	910
F13	1904	25000	37900	88	90	129	190	179	871	841	740	761	701
F14	1899	33800	48000	88	92	162	259	184	1019	994	865	882	798
F15	1906	40400	53200	89	94	193	315	189	1108	1083	939	952	845
F21	1904	49300	58100	95	92	221	364	192	1180	1146	1001	1010	881
F20	1901	47800	59300	84	90	227	374	194	1198	1164	1011	1022	880
F16	2106	28300	40900	91	94	142	214	180	882	867	753	774	708
F17	2102	37700	50200	91	95	181	287	185	1031	1018	869	887	788
F18	2098	44800	55600	92	95	214	344	192	1123	1102	743	962	831
F19	2101	50100	58500	85	84	236	386	197	1201	1167	1005	1017	860

TC 475 BASELINE TEST DATA

TEMPERATURES °F						PRESSURES PSIA											
INT. MAN	HC3 TURB. IN	HC3 TURB. IN	HC3 TURB. OUT	T18 TURB. IN	T18 TURB. OUT	T18 FTIF ST	T18 COMP OUT T	HC3 PTIP ST	HC3 COMP OUT T	INT. MAN	HC3 TURB. IN T	HC3 TURB. OUT S	T18 TURB. IN T	T18 TURB. OUT S	BAR. HGA	FUEL FLOW LF/HR	TORQ IN. HG.
178	807	823	718	730	672	14.6	14.8	15.8	17.0	16.7	17.2	15.0	15.3	14.4	29.23	34.7	19.65
180	1022	1024	926	926	852	15.0	15.7	18.2	21.0	20.7	19.3	15.5	16.1	14.4		59.0	35.0
181	1148	1137	1006	1229	944	15.7	17.2	21.1	25.5	25.2	21.5	16.2	17.1	14.5	↓	82.0	50.8
181	1204	1184	1050	1067	980	16.3	18.9	24.5	30.7	30.3	24.2	17.0	18.2	14.5	29.15	104	65.9
186	1266	1247	1090	1106	989	17.1	20.6	28.1	36.5	36.0	27.4	18.1	19.8	14.6	↓	130	81.7
178	817	804	714	730	677	14.7	15.0	16.0	17.4	17.1	17.7	15.2	15.5	14.4	29.23	35.8	19.65
180	1020	1015	826	911	832	15.2	16.1	18.7	21.8	21.5	20.0	15.8	16.4	14.4		62.5	35.2
183	1132	1121	988	1007	927	15.8	17.55	21.6	26.5	26.1	22.5	16.6	17.5	14.5	↓	87.0	50.5
183	1184	1162	1021	1040	935	16.7	19.6	25.3	32.0	31.6	25.8	17.6	19.1	14.6	2921	112	65.9
184	1193	1193	995	1024	883	17.1	20.7	27.8	36.4	35.9	28.2	18.4	20.2	14.6	↓	137	79.6
177	829	805	723	740	699	14.8	15.2	16.1	17.9	17.5	18.2	15.3	15.8	14.5	29.23	38.3	19.65
180	1023	1011	893	912	843	15.4	16.6	19.3	22.8	22.4	21.0	16.15	16.9	14.5		67.5	35.2
184	1120	1109	975	992	905	16.1	18.4	22.4	27.9	27.5	24.0	17.1	18.3	14.5	↓	93.5	50.6
184	1164	1140	1005	1019	919	17	20.5	26.3	33.9	33.3	27.65	18.37	19.95	14.6	29.21	119.5	65.9
185	1184	1175	989	1013	870	17.5	21.7	28.8	38.0	37.4	30.3	19.2	21.2	14.6	↓	141	72.2
177	855	822	733	753	696	15.0	15.7	16.8	19.2	18.8	19.7	15.8	16.4	14.4	29.23	46.5	19.65
182	1022	1003	882	898	822	15.85	17.7	20.5	24.9	24.4	23.4	17.0	18.0	14.5		78.0	35.2
186	1112	1095	953	969	871	16.75	19.85	24.0	30.5	29.9	27.3	18.2	19.8	14.6	↓	106.5	50.6
187	1157	1132	992	1001	889	17.7	22.3	28.1	36.8	36.1	31.8	20.0	22.0	14.7	29.21	137.0	65.9
191	1200	1172	1026	1035	910	18.3	23.9	30.2	40.0	39.3	34.3	21.0	23.2	14.8	↓	154.0	74.2
179	871	841	740	761	701	15.3	16.4	18.0	21.0	20.4	21.7	16.4	17.2	14.5	29.23	55.5	19.7
184	1019	994	865	882	798	16.4	19.1	22.1	27.6	27.0	26.7	18.0	19.5	14.6		90.0	35.2
189	1108	1083	939	952	845	17.4	21.6	25.8	33.7	32.8	31.5	19.75	21.8	14.8	↓	123.0	50.6
192	1180	1146	1001	1010	881	18.4	24.5	29.8	39.9	38.9	36.8	21.8	24.4	14.8	29.21	156.0	65.9
194	1198	1164	1011	1022	880	18.6	25.2	31.0	41.8	40.9	38.3	22.4	25.2	14.8	↓	166.0	70.4
180	882	867	753	774	708	15.6	17.1	19.7	22.5	21.8	23.8	17.0	18.1	14.6	29.23	62.5	19.6
185	1031	1018	869	887	788	16.9	20.3	23.1	29.8	29.0	29.9	19.1	21.0	14.7		102.5	35.1
192	1128	1102	943	962	831	19.0	23.5	27.1	36.45	35.5	35.8	21.4	24.0	14.9	↓	140.0	50.1
197	1201	1167	1005	1017	860	19.0	26.6	31.4	43.5	42.25	42.5	24.0	27.4	15.0	29.21	178.0	65.1

TEST DATA

PRESSURES PSIA

B MEPTIP LTIST	HC3 PTIP ST OUT	HC3 COMP OUT T	INT. MAN	HC3 TURE IN T	HC3 TURE OUT S	T18 TURB IN T	T18 TURB UT S	BAR. HGA	FUEL FLOW LF/HR	TORQ IN. HG	EXH MAN PRES IN H2	INT. MAN PRES IN.HG	PTIC IN. H20	ΔP VNT. IN. H20
8	15.8	17.0	16.7	17.2	15.0	15.3	14.4	29.23	34.7	19.65	36.4	34.7	10.9	.96
7	18.2	21.0	20.7	19.3	15.5	16.1	14.4		59.0	35.0	41.2	42.9	11.7	1.49
2	21.1	25.5	25.2	21.5	16.2	17.1	14.5	↓	82.0	50.8	46.4	52.6	10.0	2.24
9	24.5	30.7	30.3	24.2	17.0	18.2	14.5	29.15	104	65.9	52.4	62.4	7	3.27
6	28.1	36.5	36.0	27.4	18.1	19.8	14.6	↓	130	81.7	60.5	74.2	10	4.60
0	16.0	17.45	17.1	17.7	8.2	15.5	14.4	29.23	35.8	19.65	37.3	35.2	10.9	1.19
.1	18.7	21.8	21.5	20.0	15.8	16.4	14.4		62.5	35.2	43.3	44.5	11.5	1.89
.55	21.6	26.5	26.1	22.5	16.6	17.5	14.5	↓	87.0	50.5	49.5	53.9	11.3	2.75
.6	25.3	32.0	31.6	25.8	17.6	19.1	14.6	29.21	112	65.9	56.7	65.2	11	4.05
.7	27.8	36.4	35.9	28.2	18.4	20.2	14.6	↓	137	79.6	63.1	74.5	11	5.25
2	16.1	17.9	17.5	18.2	15.3	15.8	14.5	29.23	38.3	19.65	38.6	36.?	11.0	1.41
.6	19.3	22.8	22.4	21.0	16.15	16.9	14.5		67.5	35.2	45.4	45.?	11.3	2.36
.4	22.4	27.9	27.5	24.0	17.1	18.3	14.5	↓	93.5	53.6	53.0	56.?	11.3	3.52
.5	26.3	33.9	33.3	27.65	18.37	19.95	14.6	29.21	119.5	65.9	61.2	68.2	11.0	5.10
.7	28.8	38.0	37.4	30.3	19.2	21.2	14.6	↓	141	72.2	62.5	77.9	10.0	6.65
7	16.8	19.2	18.8	19.7	15.8	16.4	14.4	29.23	45.5	19.65	42.3	51.5	11.1	2.05
7	20.5	24.9	24.4	23.4	17.0	18.0	14.5		78.0	35.2	48.7	50.4	11.2	3.52
.85	24.0	30.5	29.9	27.3	18.3	19.8	14.6	↓	106.5	50.6	60.8	61.5	11.5	5.25
.3	28.1	36.8	36.1	31.8	20.0	22.0	14.7	29.21	132.0	65.9	71.4	74.5	11.0	7.51
.9	30.2	40.0	39.3	34.3	21.0	23.2	14.8	↓	154.0	74.2	76.8	80.8	11.0	8.95
4	18.0	21.0	20.4	21.7	16.4	17.2	14.5	29.23	55.5	19.7	47.0	42.7	11.0	2.94
1	22.1	27.6	27.0	26.7	18.0	19.5	14.6		90.0	35.2	59.0	55.7	10.7	5.15
.6	25.8	33.7	32.8	31.5	19.75	21.8	14.8	↓	123.0	50.6	70.2	67.8	10.9	7.66
.5	29.8	39.9	38.9	36.8	21.8	24.4	14.8	29.21	156.0	65.9	82.0	79.9	13.5	10.70
.2	31.0	41.8	40.9	38.3	22.4	25.2	14.8	↓	166.0	70.4	85.8	83.8	14.5	11.67
7	18.7	22.5	21.8	23.8	17.0	18.1	14.6	29.23	62.5	19.65	52.0	45.1	11.1	3.99
.3	23.1	29.8	29.0	29.9	19.1	21.0	14.7		102.5	35.1	66.5	59.7	11.3	7.07
.5	27.1	36.45	35.5	35.8	21.4	24.0	14.9	↓	140.0	50.6	80.8	73.2	11.3	10.5
.6	31.4	43.5	42.25	42.5	24.0	27.4	15.0	29.21	178.0	65.6	95.3	87.1	17.7	14.25

TABLE NO. II NTC 475 BASELINE

Run Number	Engine RPM	Engine Torque	Horse Power	Fuel Flow	BS FC	Venturi Air Flow	F/A	Exhaust Flow lb/sec	Intake Man. Pr. psia	Intake Man. Pr. Hg A	Intake Man. Temp °F	Theoretical Air Flow lb/sec	Vol. Eff.	BMEP
						ENGINE RESULTS								
F1	1300	300	74.3	34.7	.467	.393	.025	.403	16.7	34.7	178	.383	1.026	52
F2	1300	600	149	59.0	.396	.489	.034	.506	20.7	42.9	180	.473	1.034	105
F3	1300	900	223	82.0	.368	.596	.038	.619	25.25	52.0	181	.574	1.038	158
F29	1300	1200	297	104.0	.350	.726	.040	.755	30.3	62.4	181	.689	1.054	211
F28	1300	1512	374	130.0	.348	.857	.042	.893	36.0	74.2	186	.812	1.055	266
F4	1400	300	80	35.8	.448	.434	.023	.444	17.1	35.2	178	.420	1.032	52.
F5	1400	600	160	62.5	.391	.546	.032	.563	21.5	44.5	180	.528	1.033	105.
F6	1400	900	240	87.0	.363	.657	.037	.681	26.1	53.9	183	.638	1.030	158
F27	1400	1200	320	112.0	.350	.801	.039	.832	31.6	65.2	183	.772	1.038	211.
F26	1400	1470	392	137	.349	.916	.042	.954	35.9	74.5	184	.878	1.043	259
F7	1500	300	85.7	38.3	.447	.471	.023	.482	17.5	36.3	177	.464	1.016	52.
F8	1500	600	171	67.5	.395	.610	.031	.629	22.4	46.1	180	.588	1.037	105
F9	1500	900	257	93.5	.364	.741	.035	.767	27.45	56.5	184	.716	1.034	158.
F25	1500	1200	343	119.5	.348	.907	.037	.940	33.3	68.2	184	.867	1.046	211.
F24	1500	1443	412	141	.342	1.031	.038	1.07	37.4	77A	185	.980	1.052	254
F10	1700	300	97	45.5	.469	.567	.022	.579	18.75	38.7	177	.561	1.010	52.9
F11	1700	600	194	78.0	.402	.743	.029	.765	24.4	50.4	182	.725	1.024	105.1
F12	1700	900	291	106.5	.366	.905	.033	.935	29.9	61.5	186	.881	1.027	158.
F23	1700	1200	389	137.0	.352	1.093	.035	1.131	36.1	74.5	187	1.064	1.027	211.6
F22	1700	1364	442	154.0	.348	1.179	.036	1.222	39.3	80.8	191	1.149	1.026	240.(
F13	1900	300	109	55.5	.509	.684	.023	.700	20.4	42.3	179	.682	1.003	52.9
F14	1900	600	217	90.0	.415	.902	.028	.927	27.0	55.7	184	.894	1.009	105.8
F15	1900	900	326	123.0	.377	1.095	.031	1.129	32.8	67.8	189	1.078	1.016	158.7
F21	1900	1200	434	156.0	.359	1.293	.034	1.336	38A	79.9	192	1.269	1.019	211.6
F20	1900	1288	466	166.0	.356	1.350	.034	1.396	40.6	83.8	194	1.328	1.017	227.
F16	2100	300	120	62.5	.521	.793	.022	.810	21.8	45.1	180	.804	.987	52.9
F17	2100	600	240	102.5	.427	1.051	.027	1.079	28.45	59.7	185	1.057	.994	105.8
F18	2100	900	360	140.0	.389	1.274	.031	1.313	35.5	73.2	192	1.282	.994	158.7
F19	2100	1194	478	178.0	.372	1.510	.033	1.559	42.25	87.1	197	1.514	.997	210.6

①

F/A	EXHAUST FLOW lb/sec	INTAKE MAN. PR, psia	INTAKE MAN. PR, H₂O A	INTAKE MAN TEMP, °F	THEORETICAL AIR FLOW lb/sec	VOL. EFF.	BMEP, psi	T18A85 TURBINE ΔHcomp Btu/sec	P₁/P₈	U/Co	SWIRL ANGLE	η_T/C	A turb, in²	ΔHcomp Btu/sec	P₁/P₈
.025	.403	16.7	34.7	178	.383	1.026	52.91	1.34	1.06	.647	2.9°	.686	6.91	3.05	1.17
.034	.506	20.7	42.9	180	.473	1.034	105.8	3.45	1.12	.637	1.9°	.660	5.95	7.61	1.28
.038	.619	25.25	52.0	181	.574	1.038	158.7	6.66	1.18	.644	0.1°	.660	5.60	13.47	1.37
.040	.755	30.3	62.4	181	.689	1.054	211.6	11.46	1.26	.649	-3.2°	.664	5.45	20.98	1.47
.042	.893	36.0	74.2	186	.812	1.055	266.7	17.90	1.36	.647	-4.3°	644	5.19	29.77	1.58
.023	.444	17.1	35.2	178	.420	1.032	52.9	1.90	1.08	.656	3.5°	.728	6.59	3.69	1.19
.032	.563	21.5	44.5	180	.528	1.033	105.8	4.38	1.14	.647	1.5°	.655	5.87	9.15	1.31
.037	.681	26.1	53.9	183	.638	1.030	158.7	8.46	1.21	.656	-.4°	.681	5.55	15.65	1.41
.039	.832	31.6	65.2	183	.772	1.038	211.6	14.40	1.31	.649	-2.2°	656	5.21	23.94	1.52
.042	.954	35.9	74.5	184	.878	1.043	259.3	18.48	1.38	.658	-2°	.618	5.14	29.17	1.61
.023	.482	17.5	36.3	177	.464	1.016	52.9	2.41	1.09	.657	2.6°	.724	6.36	4.47	1.21
.031	.629	22.4	46.1	180	.588	1.037	105.8	6.07	1.17	.657	0.2°	.691	5.77	11.11	1.34
.035	.767	27.45	56.5	184	.716	1.034	158.7	11.35	1.26	.646	-1.9°	.666	5.30	18.74	1.46
.037	.940	33.3	68.2	184	.867	1.046	211.6	18.74	1.37	.652	-5°	.663	5.21	28.23	1.57
.038	1.07	37.4	77A	185	.980	1.052	254.5	23.8	1.45	.654	-5.4°	.626	5.16	34.33	1.67
.022	.579	18.75	38.7	177	.561	1.010	52.9	3.86	1.14	.637	2°	.634	5.68	6.76	1.28
.029	.765	24.4	50.4	182	.725	1.024	105.8	9.57	1.24	.650	-1.7°	.646	5.40	15.52	1.39
.033	.935	29.9	61.5	186	.881	1.027	158.7	17.37	1.36	.653	-4.1°	.655	5.19	24.85	1.56
.035	1.131	36.1	74.5	187	1.064	1.027	211.6	28.17	1.50	.657	-7.2°	.657	5.08	35.61	1.67
.036	1.222	39.3	80.8	191	1.149	1.026	240.6	34.68	1.57	.656	-8.6°	.660	5.05	41.84	1.72
.023	.700	20.4	42.3	179	.682	1.003	52.9	6.48	1.19	.652	0°	.670	5.59	10.13	1.37
.028	.927	27.0	55.7	184	.894	1.009	105.8	15.35	1.34	.651	-3.8°	.653	5.19	21.27	1.55
.031	1.129	32.8	67.8	189	1.078	1.016	158.7	26.35	1.47	.660	-6.5°	.661	5.11	32.47	1.67
.034	1.336	38.9	79.9	192	1.269	1.019	211.6	40.55	1.65	.699	-5.9°	.649	5.02	44.45	1.77
.034	1.396	40.9	83.8	194	1.328	1.017	227.2	44.95	1.70	.656	-11°	.644	5.00	48.23	1.80
.022	.810	21.8	45.1	180	.804	.987	52.9	9.25	1.24	.656	-1.6°	.653	5.44	13.88	1.45
.027	1.029	28.95	59.7	185	1.057	.994	105.8	21.97	1.43	.655	-5.6°	.654	5.12	27.08	1.64
.031	1.313	35.5	73.2	192	1.282	.994	158.7	36.84	1.61	.661	-8.3°	.650	5.01	40.25	1.76
.033	1.559	42.25	87.1	197	1.514	.997	210.6	55.78	1.83	.650	-12.8°	.640	4.95	55.24	1.86

ΔHcmp Btu/sec	Pt/Ps	U/Co	SWIRL ANGLE	η t/c	Ann Eff. %		ΔHcmp Btu/sec	Pt/Ps	U/Co	SWIRL ANGLE	η t/c	Ann Eff. %
		T/8185 TURBINE							HC3-5 TURBINE			
1.34	1.06	.647	2.9°	.686	6.91		3.05	1.17	.582	5.1°	.571	3.39
3.45	1.12	.637	1.9°	.660	5.95		7.61	1.28	.619	6.3°	.630	3.21
6.66	1.18	.644	0.1°	.660	5.60		13.47	1.37	.638	3.4°	.667	3.22
11.46	1.26	.649	-3.2°	.664	5.45		20.98	1.47	.644	-.4°	.677	3.24
17.90	1.36	.647	-4.3°	644	5.19		29.77	1.58	.645	-2.4°	.666	3.20
1.90	1.08	.656	3.5°	.728	6.59		3.69	1.19	.589	2.9°	.582	3.47
4.38	1.14	.647	1.5°	.655	5.87		9.15	1.31	.623	4.3°	.629	3.25
8.46	1.21	.656	-.4°	.681	5.55		15.65	1.41	.631	1.3°	.650	3.19
14.40	1.31	.649	-2.2°	656	5.21		23.94	1.52	.635	-1.8°	.651	3.18
18.48	1.38	.658	-2°	618	5.14		29.17	1.61	.642	-1.7°	.610	3.19
2.41	1.09	.657	2.6°	.724	6.36		4.47	1.21	.579	0.6°	.566	3.39
6.07	1.17	.657	0.2°	.691	5.77		11.11	1.34	.617	0.1°	.625	3.31
11.35	1.26	.646	-1.9°	.666	5.30		18.74	1.46	.621	-2.2°	.632	3.22
18.74	1.37	.652	-5°	.663	5.21		28.23	1.57	.626	-5.4°	.645	3.24
23.8	1.45	.654	-5.4°	.626	5.16		34.33	1.67	.626	-5.8°	.604	3.22
3.96	1.14	.637	2°	.634	5.68		6.76	1.28	.572	-2.4°	.553	3.31
9.57	1.24	.650	-1.7°	.646	5.40		15.52	1.39	.680	1.5°	.641	3.48
17.37	1.36	.653	-4.1°	.655	5.19		24.85	1.56	.601	-6.9°	-595	3.22
28.7	1.50	.657	-7.2°	.657	5.08		35.61	1.67	.607	-9.2°	.601	3.21
34.68	1.57	.656	-8.6°	.660	5.05		41.84	1.72	.612	-9.6°	.609	3.22
6.48	1.19	.652	0°	.670	5.59		10.13	1.37	.569	-5.3°	.542	3.27
15.35	1.34	.651	-3.8°	.653	5.19		21.27	1.55	.581	-8.2°	.559	3.20
26.35	1.47	.660	-6.5°	.661	5.11		32.47	1.67	.586	-10.6°	.567	3.20
40.55	1.65	.699	-5.9°	.649	5.02		44.45	1.77	.590	-12.5°	.577	3.21
44.95	1.70	.656	-11°	.644	5.00		48.23	1.80	.592	-12.6°	.571	3.21
9.25	1.24	.656	-1.6°	.653	5.44		13.88	1.45	.560	-8°	.533	3.20
21.97	1.43	.655	-5.6°	.654	5.12		27.08	1.64	.570	-11°	.532	3.19
36.84	1.61	.661	-8.3°	.650	5.01		40.25	1.76	.574	-13°	.544	3.18
55.78	1.83	.650	-12.8°	.640	4.95		55.21	1.86	.577	-14.3°	.552	3.18

NTC 475 BASELINE TEST RESULTS

RUN NUMBER	ENGINE RPM	ENGINE TORQUE		T18A85 COMPRESSOR						HC3-5 COMPRESSOR				
				CORRECTED RPM	CORRECTED AIR FLOW	PRESSURE RATIO	EFFICIENCY	ACTUAL RPM		CORRECTED RPM	CORRECTED AIR FLOW	PRESSURE RATIO	EFFICIENCY	ACTUAL RPM
F1	1305	300		14,627	.393	1.06	.647	14,700		36,732	.375	1.15	.714	27,700
F2		600		21,023	.491	1.13	.650	21,100		37,873	.447	1.34	.775	37,000
F3		900		26,609	.599	1.23	.712	26,700		44,771	.57	1.46	.75	47,000
F29		1200		31,971	.720	1.34	.732	32,000		50,245	.567	1.62	.755	53,200
F28	↓	1512		37,166	.857	1.48	.739	37,200		54,603	.625	1.77	.776	58,800
F4	1400	300		16,369	.437	1.07	.639	16,400		38,014	.413	1.16	.714	28,700
F5		600		22,792	.551	1.15	.690	22,900		39,280	.491	1.35	.763	40,800
F6		900		28,587	.664	1.26	.706	28,900		45,749	.553	1.51	.770	48,400
F27		1200		34,366	.803	1.40	.748	34,400		50,922	.609	1.63	.752	54,400
F26	↓	1470		37,930	.918	1.42	.779	38,000		54,504	.664	1.76	.833	58,600
F7	1500	300		17,591	.477	1.09	.647	17,800		39,302	.446	1.18	.703	30,200
F8		600		25,004	.617	1.19	.627	25,300		40,343	.537	1.37	.750	42,200
F9		900		31,013	.750	1.32	.722	31,400		45,653	.600	1.52	.746	49,800
F25		1200		36,934	.907	1.47	.737	36,900		51,284	.663	1.65	.751	55,100
F24	↓	1400		40,237	.988	1.55	.758	40,200		54,303	.718	1.75	.801	58,200
F10	1700	300		21,050	.574	1.12	.675	21,300		32,693	.523	1.22	.700	33,900
F11		600		29,102	.753	1.27	.736	29,500		42,714	.621	1.41	.722	45,300
F12		900		35,416	.918	1.42	.745	35,900		47,839	.689	1.54	.731	51,800
F22		1200		41,586	1.096	1.60	.734	41,700		51,668	.749	1.65	.743	56,600
F23	↓	1364		44,079	1.188	1.71	.752	44,400		53,144	.765	1.67	.724	59,100
F13	1900	300		24,886	.625	1.17	.652	25,200		36,457	.604	1.28	.699	37,900
F14		600		33,589	.907	1.37	.730	33,700		44,931	.704	1.44	.704	48,200
F15		900		40,070	1.103	1.55	.736	42,400		49,150	.774	1.56	.718	52,200
F21		1200		48,986	1.310	1.77	.747	46,300		51,976	.823	1.63	.705	58,100
F20	↓	1288		47,582	1.369	1.82	.744	47,800		53,817	.839	1.66	.719	59,300
F16	2100	300		28,069	.749	1.23	.683	28,300		38,916	.680	1.32	.678	40,900
F17		600		37,359	1.051	1.46	.723	37,700		46,288	.783	1.47	.694	50,200
F18		900		43,799	1.225	1.62	.742	44,300		49,997	.841	1.55	.622	54,600
F19	↓	1024		50,146	1.525	1.74	.729	50,300		52,751	.885	1.63	.633	58,500

| PRESSURES PSIA | | | | | | | | | H.A | | | EXH MAN | INT MAN | | ΔP | TURB OUT |
IN D	1/8 UP RAD	1/8 DOWN RAD	PT IP ST	PT IP ST	COMP OUT T	INT MAN ST	TURB IN T	TURB IN T	TURB IN ST	BAR HGA	FUEL FLOW LB/HR	TORQ IN HG	PRES IN HG T	PRES IN HG ST	PTIC IN H2O	VNT IN H2O	ΔP IN H2O
1	14.3	14.3	15.7	/	16.9	16.7	17.2	17.2	34.2	29.30	36.0	20.0	35.0	34.1	12.5	0.94	-.5
9	14.4	14.5	17.7	/	21.0	20.7	19.25	19.3	38.9	''	62.0	35.5	39.2	42.0	12.0	1.51	-1.7
9	14.6	14.75	20.1	/	25.4	25.0	21.5	21.5	43.4	''	83.0	50.2	43.8	50.8	12.5	2.13	-2.5
9	14.8	15.0	22.4	/	29.8	29.5	23.8	23.8	47.9	''	106.0	65.2	48.5	60.2	12.5	3.10	-4.
8	15.1	15.3	25.0	/	34.5	34.1	26.4	26.4	53.2	''	128.0	79.2	53.8	69.5	12.5	4.13	-5.7
2	14.3	14.3	16.5	/	18.4	18.1	18.6	18.6	37.5	29.30	39.0	19.7	32.9	36.9	12.5	1.31	-.5
7	14.5	14.6	19.25	/	23.3	23.0	21.3	21.2	43.2	''	66.0	35.5	43.3	47.1	13.0	2.15	-.3
5	14.75	14.8	21.5	/	28.0	27.6	24.0	24.0	48.6	''	88.0	52.6	48.9	56.2	12.5	3.09	-2
7	14.9	15.0	24.2	/	33.2	32.75	27.35	27.25	55.1	''	113.0	65.9	55.6	66.8	12.0	4.39	-2
6	15.0	15.1	26.1	/	37.2	36.6	29.4	29.4	59.0	''	138.0	79.9	59.9	74.6	12.5	5.47	-1.7
9	14.3	14.3	16.4	/	18.2	17.9	18.6	18.6	37.2	29.30	41.5	19.7	37.9	36.5	12.5	1.47	-2.
5	14.5	14.6	19.2	/	23.4	23.0	21.4	21.4	43.1	''	70.0	35.2	43.6	46.8	12.1	2.48	-3.
8	14.7	14.8	21.6	/	28.4	27.9	24.3	24.4	49.2	''	95.0	50.8	49.6	56.8	12.0	3.63	-3.
5	14.9	14.9	24.3	/	33.7	33.1	27.8	27.8	55.9	''	121.	65.9	56.6	67.6	12.0	5.14	-5.
5	15.0	15.1	26.3	/	38.1	37.4	30.8	30.8	62.0	''	145.	78.6	52.7	76.3	12.5	6.51	-6.
5	14.4	14.3	17.1	/	19.4	19.0	19.9	19.8	40.0	29.30	49.	19.7	40.4	38.8	12.0	2.09	-3.5
7	14.5	14.6	20.3	/	25.8	25.3	24.1	24.0	48.2	''	80.	35.4	49.0	51.5	12.5	3.74	-5.
4	14.7	14.75	23.0	/	31.4	30.7	28.0	27.9	55.9	''	109.	50.8	56.9	62.6	12.5	5.53	-6.8
2	14.8	14.8	25.6	/	36.9	36.1	32.	32.	64.3	''	138.	65.6	65.2	73.6	12.0	7.57	-7.5
3	14.7	14.7	26.8	/	39.9	39.0	34.4	35.0	69.0	''	157.	74.5	70.1	79.2	12.0	8.82	-10.
6	14.3	14.3	18.0	/	21.1	20.5	21.8	21.7	43.6	29.25	56.	19.7	44.3	43.6	11.5	2.98	-4.5
7	14.5	14.5	21.3	/	27.7	27.0	26.8	26.8	54.0	''	91.	35.2	54.6	55.2	12.0	5.30	-7.
15	14.5	14.5	24.4	/	34.3	32.4	32.2	32.0	64.1	''	123.	50.6	65.4	67.9	12.0	7.93	-9.
3	14.6	14.41	26.6	/	39.8	38.75	36.7	36.5	73.6	''	158.	65.9	74.5	78.7	12.0	10.54	-10.
1	14.5	14.2	27.3	/	41.7	40.6	38.5	38.3	76.9	''	172.	70.7	78.2	82.5	12.0	11.48	-11.
5	14.5	14.5	20.4	/	25.3	24.6	26.8	26.7	54.5	29.29	65.5	19.7	54.5	50.1	12.1	4.76	-1.0
8	14.5	14.4	24.1	/	33.4	32.5	34.1	33.9	68.8	''	103.	35.2	69.2	65.6	12.1	8.46	0
2	14.1	14.1	26.8	/	40.2	39.0	40.6	40.4	82.0	''	142.	50.6	82.5	79.5	12.1	12.05	0
6	14.0	13.8	27.4	/	41.9	40.5	41.1	40.8	82.6	''	183.	65.2	83.4	82.5	12.5	13.40	-12.

	TEMPERATURES °F							PRESSURES PSIA									
ND UT OT	COMP OUT	INT MAN	TURB IN	TURB IN	TURB RMS 1	TURB RMS 2	TURB RMS 3	1/8 UP IND	1/8 DOWN IND	1/8 UP RAD	1/8 DOWN RAD	PTIP ST	PTIP ST	COMP OUT T	INT MAN ST	TURB IN T	TURB IN T
94	135	178	821	798	672	723	698	13.9	13.9	14.3	14.3	15.7	/	16.9	16.7	17.2	17.
01	176	179	1041	1017	859	900	849	13.8	13.9	14.4	14.5	17.7	/	21.0	20.7	19.25	19.
08	226	182	1158	1133	990	1005	972	13.7	13.9	14.6	14.75	20.1	/	25.4	25.0	21.5	21.
111	263	184	1244	1210	1033	1045	997	13.6	13.9	14.8	15.0	22.4	/	29.8	29.5	23.8	23
117	308	186	1312	1282	1116	1102	1072	13.4	13.8	15.1	15.3	25.0	/	34.5	34.1	26.4	26.
82	133	173	821	771	643	673	638	13.8	14.0	14.3	14.3	16.5	/	18.4	18.1	18.6	18
95	192	180	1012	975	839	852	822	13.6	13.6	14.5	14.6	19.25	/	23.3	23.0	21.3	21
03	240	183	1110	1072	884	921	901	13.6	13.85	14.75	14.8	21.5	/	28.0	27.6	24.0	24
11	290	185	1186	1151	937	958	927	13.3	13.7	14.9	15.0	24.2	/	33.2	32.75	27.35	27.
115	322	189	1267	1237	994	1021	991	13.1	13.6	15.0	15.1	26.1	/	37.2	36.6	29.4	29
92	145	176	825	789	658	685	643	13.8	13.9	14.3	14.3	16.4	/	18.2	17.9	18.6	18
101	201	180	1015	986	843	857	816	13.7	13.85	14.5	14.6	19.2	/	23.4	23.0	21.4	21
106	248	183	1115	1085	923	927	894	13.6	13.8	14.7	14.8	21.6	/	28.4	27.9	24.3	2
114	297	186	1198	1166	1001	982	957	13.2	13.6	14.9	14.9	24.3	/	33.7	33.1	27.8	2
121	336	191	1265	1240	920	1023	995	13.0	13.35	15.0	15.1	26.3	/	38.1	37.4	30.8	3
98	166	178	852	814	694	719	682	13.8	13.8	14.4	14.3	17.1	/	19.4	19.0	19.9	19
105	229	181	1010	977	838	838	804	13.4	13.7	14.5	14.6	20.3	/	25.8	25.3	24.1	2
111	280	185	1104	1072	898	895	966	13.1	13.4	14.7	14.75	23.0	/	31.4	30.7	28.0	2
118	320	190	1187	1150	964	945	913	12.8	13.0	14.8	14.8	25.6	/	36.9	36.1	32.	3
122	354	193	1236	1210	965	968	911	12.5	12.8	14.7	14.7	26.8	/	39.9	39.0	34.4	3
103	191	179	881	842	718	735	721	13.5	13.6	14.3	14.3	18.0	/	21.1	20.5	21.8	2
107	246	183	999	971	805	802	755	13.1	13.7	14.5	14.5	21.3	/	27.7	27.0	26.8	2
112	307	189	1107	1079	860	866	821	12.6	12.85	14.5	14.5	24.4	/	34.3	32.4	32.2	3
118	354	195	1209	1180	936	933	870	12.2	12.3	14.6	14.41	26.6	/	39.8	38.75	36.7	3
118	366	197	1236	1214	950	940	860	12.0	12.1	14.5	14.2	27.3	/	41.7	40.6	38.5	3
92	212	182	831	826	623	659	659	13.2	13.5	14.5	14.5	20.4	/	25.3	24.6	26.8	3
102	287	189	971	945	693	737	741	12.5	12.8	14.5	14.4	24.1	/	33.4	32.5	34.1	3
108	347	197	1089	1063	767	809	815	12.0	12.0	14.1	14.1	26.8	/	40.2	39.0	40.6	4
121	377	198	1248	1242	965	947	877	11.7	11.6	14.0	13.8	27.4	/	41.9	40.5	41.1	4

RUN NO.	IND RPM	RAD RPM	TEMPERATURES °F										
			VNT IN	COMP IN	SHRD ST	IND OUT TOT	COMP OUT	INT MAN	TURB IN	TURB IN	TURB RMS 1	TURB RMS 2	TURB RMS 3
F140	19200	27440	83	86	94	94	135	178	821	798	672	723	698
F141	28200	38520	81	85	97	101	176	179	1041	1017	859	900	849
F142	33700	47040	89	87	103	108	226	182	1158	1133	990	1005	972
F143	39000	53660	78	87	103	111	263	184	1244	1210	1033	1045	997
F144	44000	59630	77	88	107	117	308	186	1312	1282	1116	1102	1072
F135	23200	31960	70	72	81	82	133	173	821	771	643	673	638
F136	32200	43460	77	78	91	95	192	180	1012	975	809	852	822
F137	37300	51120	81	81	97	103	240	183	1110	1072	584	921	901
F138	42500	58180	79	84	103	111	290	185	1186	1151	937	968	937
F139	46100	62640	78	85	104	115	322	189	1267	1237	994	1021	991
F145	24300	32500	81	84	91	92	145	176	825	789	658	685	643
F146	32600	44180	83	86	97	101	201	180	1015	996	843	857	816
F147	38500	52240	79	86	100	106	248	183	1115	1085	923	927	894
F148	44400	57310	79	88	104	114	297	186	1198	1166	1001	982	957
F149	49200	64,740	81	90	107	121	336	191	1265	1240	980	1023	995
F150	27900	36830	82	87	95	98	166	178	852	814	694	719	682
F151	36800	49320	81	87	99	105	229	181	1010	977	838	838	804
F152	43600	57440	81	88	102	111	280	185	1104	1072	898	895	866
F153	49700	61690	87	89	105	118	320	190	1187	1150	964	945	913
F154	53200	65,680	80	89	106	122	354	193	1236	1210	965	968	911
F160	31700	42130	87	90	99	103	191	179	881	842	718	735	721
F161	40900	53500	82	87	98	107	246	183	999	971	805	802	755
F162	48700	61890	83	86	100	112	307	189	1107	1079	860	866	821
F163/164	55100	68000	81	86	102	118	354	195	1209	1180	936	933	870
F165/166	57300	70000	75	84	101	118	366	197	1236	1214	950	940	860
F132	39,600	50,000	68	73	83	92	212	182	831	826	623	659	659
F133	49,500	61,850	70	75	88	102	287	189	971	945	693	737	741
F134	57,100	69,040	66	76	91	108	347	197	1089	1063	767	809	815
F167	57,800	71,670	76	88	101	121	377	198	1248	1242	965	947	877

Left-margin RPM band labels: 1300, 1400, 1500, 1700, 1900, 2100

③

RUN NUMBER	ENGINE RPM	ENGINE TORQUE	HORSE-POWER	FUEL FLOW, lb/hr	BSFC	VENTURI AIRFLOW, lb/sec	F/A	EXHAUST FLOW, lb/sec	INTAKE MAN. PR. psia	INTAKE MAN. PR. "HgA	INTAKE MAN. TEMP, °F	THEORETICAL AIR FLOW, lb/sec	VOLUMETRIC EFFICIENCY	
F140	1302	306.	75.9	36.0	0.474	0.390	0.0256	0.400	16.7	34.1	178	0.380	1.025	
F141	1302	605.	150.0	62.0	0.413	0.495	0.0348	0.512	20.7	42.0	179	0.469	1.055	
F142	1301	892.	221.0	83.0	0.375	0.583	0.0395	0.626	25.0	50.9	182	0.564	1.034	
F143	1302	1186.	293.7	106.0	0.361	0.709	0.0415	0.738	29.5	60.2	184	0.664	1.067	
F144	1298	1463.	361.7	128.	0.354	0.818	0.0435	0.834	34.1	69.5	186	0.764	1.071	
F135	1402	300.	80.1	39.	0.487	0.466	0.0232	0.477	18.1	36.9	173	0.447	1.042	
F136	1398	605.	161.1	66.	0.410	0.592	0.0310	0.610	23.0	47.1	180	0.562	1.054	
F137	1401	900.	240.2	88.	0.366	0.706	.0346	0.730	27.6	56.2	183	0.670	1.053	
F138	1402	1200.	320.5	113.	0.353	0.842	0.0373	0.873	32.75	66.5	185	0.794	1.060	
F139	1403	1476.	394.4	138.	0.350	0.939	0.0408	0.977	36.6	74.6	189	0.882	1.064	
F145	1500	300.	85.7	41.5	0.484	0.488	.0236	0.500	17.9	36.5	176	0.471	1.036	
F146	1501	600.	171.5	70.	0.408	0.632	.0308	0.651	23.0	46.8	180	0.601	1.052	
F147	1499	903.	257.8	95.	0.368	0.766	0.0345	0.792	27.9	56.8	183	0.725	1.057	
F148	1503	1200.	343.5	121.	0.352	0.910	0.0369	0.944	33.1	67.6	186	0.860	1.059	
F149	1502	1451.	415.1	145.	.349	1.020	0.0395	1.060	37.4	76.3	191	0.963	1.060	
F150	1699	300.	97.1	49.	~~0.505~~0.505	0.581	.0234	0.595	19.0	38.8	178	0.565	1.029	
F151	1702	604.	195.8	80.	0.409	0.776	.0286	0.798	25.2	51.5	181	0.749	1.037	
F152	1704	903.	293.1	109.	0.372	0.941	.0322	0.971	30.7	62.6	185	0.905	1.040	
F153	1702	1194.	387.1	138.	0.357	1.092	.0351	1.130	36.1	73.6	190	1.054	1.036	
F154	1704	1369.	444.3	157.	0.353	1.188	.0367	1.232	39.0	79.2	193	1.133	1.049	
F160	1901	302.	108.6	56.	0.516	0.689	.0226	0.705	22.0	43.6	179	0.695	0.982	
F161	1902	620.	217.4	91.	0.419	0.920	.0275	0.945	27.0	55.2	182	0.893	1.030	
F162	1904	900.	326.4	123.	0.377	1.120	.0305	1.154	33.4	67.9	189	1.091	1.026	
F163/164	1900	1200.	434.3	158.	0.364	1.289	0.034	1.333	38.75	78.7	195	1.251	1.030	
F165/166	1904	1294.	469.3	172.	0.367	1.351	.0364	1.399	40.6	82.5	197	1.310	1.031	
F132	2099	300	119.9	65.5	.546	.912	.020	.931	24.6	50.1	182	.896	1.018	
F133	2105	600	240.6	103.	.428	1.191	.0240	1.220	32.5	65.6	189	1.17	1.043	
F134	2103	900	360.5	142.	.394	1.418	.0278	1.458	39.0	79.5	197	1.392	1.047	
F167	2105	1186.	475.5	183.	0.385	1.456	.0349	1.507	40.5	82.5	198	1.444	1.002	

(1)

	EXHAUST FLOW, lb/sec	INTAKE MAN. PR. PSIA	INTAKE MAN. PR. IN,HgA	INTAKE MAN. TEMP, °F	THEORETICAL AIR FLOW, lb/sec	VOLUMETRIC EFFICIENCY	BMEP, PSI	IND RPM / RAD RPM	COMPRESSOR EFFICIENCY	PRESSURE RATIO	CORRECTED SPEED, RPM	CORRECTED MASS FLOW, lb/sec	ΔHcomp, BTU/sec		PRESSURE RATIO	U/Cu	THEORETICAL SWIRL ANGLE
256	0.400	16.7	34.1	178	0.380	1.025	54.0	.700	.624	1.21	27400	.391	4.64		1.20	.695	25.
348	0.512	20.7	42.0	179	0.469	1.055	106.7	.732	.734	1.50	38520	.494	10.94		1.34	.706	21.
395	0.606	25.0	50.9	182	0.564	1.034	157.4	.716	.728	1.82	46950	.584	19.68		1.50	.711	10.4
115	0.738	29.5	60.2	184	0.664	1.067	209.3	.727	.746	2.14	53560	.711	30.33		1.67	.709	7.0
435	0.834	34.1	69.5	186	0.764	1.071	258.1	.738	.728	2.48	59470	.821	43.74		1.86	.706	1.4
232	0.477	18.1	36.9	173	0.447	1.042	52.9	.726	.713	1.32	32350	.460	6.90		1.30	.693	20.4
510	0.610	23.0	47.1	180	0.562	1.054	106.7	.741	.741	1.67	43740	.580	16.4		1.48	.705	15.2
146	0.730	27.6	56.2	183	0.670	1.053	158.8	.730	.742	2.01	51310	.704	27.28		1.68	.703	6.6
573	0.873	32.75	66.5	185	0.794	1.060	211.7	.730	.734	2.38	58230	.840	42.13		1.91	.704	.7
108	0.977	36.6	74.6	189	0.882	1.064	260.4	.736	.736	2.67	62640	.940	54.08		2.05	.703	-1.3
36	0.500	17.9	36.5	176	0.471	1.036	52.9	.748	.699	1.31	32530	.499	7.23		1.30	.694	23.4
08	0.651	23.0	46.8	180	0.601	1.052	105.9	.738	.748	1.68	44140	.632	17.66		1.50	.703	13.4
145	0.792	27.9	56.8	183	0.725	1.057	159.3	.737	.750	2.03	52100	.766	30.16		1.71	.706	6.47
69	0.944	33.1	67.6	186	0.860	1.059	211.7	.749	.743	2.41	59150	.912	46.21		1.96	.702	.3
195	1.060	37.4	76.3	191	0.963	1.060	256.0	.76	.736	2.73	64445	1.026	60.97		2.17	.702	-2.8
34	0.595	19.0	38.8	178	0.565	1.029	52.9	.758	.676	1.39	36760	.582	11.15		1.39	.687	18.3
86	0.798	25.3	51.5	181	0.749	1.037	106.6	.746	.733	1.85	49230	.778	26.78		1.69	.695	6.2
2	0.971	30.7	62.6	185	0.905	1.040	159.3	.759	.737	2.25	57280	.945	43.92		1.97	.697	.9
51	1.130	36.1	73.6	190	1.054	1.036	210.7	.806	.753	2.64	61470	1.096	61.32		2.27	.670	-3.6
7	1.232	39.2	79.2	193	1.133	1.049	241.5	.81	.717	2.86	65440	1.192	76.54		2.45	.673	-4.65
16	0.705	22.5	43.6	179	0.695	0.982	52.9	.752	.676	1.51	41940	.692	16.91		1.53	.688	11.1
25	0.945	27.0	55.2	182	0.893	1.030	105.9	.764	.739	1.99	53400	.923	35.56		1.90	.690	3.3
05	1.154	33.4	67.9	189	1.091	1.026	158.8	.787	.717	2.46	61830	1.123	60.18		2.29	.686	-2.6
4	1.333	38.75	78.7	195	1.251	1.030	211.7	.810	.705	2.86	67940	1.292	83.89		2.61	.683	-6.1
4	1.399	40.6	82.5	197	1.310	1.031	228.3	.819	.702	2.99	70060	1.352	92.63		2.75	.680	-6.9
0	.931	24.6	50.1	182	.896	1.018	52.9	.792	.704	1.81	50560	.902	29.89		1.87	.693	7.82
40	1.220	32.3	65.6	189	1.17	1.043	105.9	.800	.707	2.39	62425	1.180	60.35		2.36	.706	-.16
78	1.458	39.0	79.5	197	1.392	1.047	158.8	.827	.691	2.88	69620	1.406	91.96		2.82	.697	-5.93
9	1.507	40.5	82.5	198	1.444	1.002	209.3	.808	.694	3.01	71470	1.463	102.2		2.94	.673	-11.4

$$\overline{A_{nozz\,eff}} = 2.92 \pm .1 \, in^2$$

TURBOCHARGER RESULTS ———→

COMPRESSOR ————————→   TURBINE ————————→

RAD RPM	COMPRESSOR EFFICIENCY	PRESSURE RATIO	CORRECTED SPEED, RPM	CORRECTED MASS FLOW, lb/sec	ΔHcomp, BTU/sec		PRESSURE RATIO	U/Cu	THEORETICAL SWIRL ANGLE	PROBE SWIRL ANGLE	AVG. TURB. EFFICIENCY ηt/s	TURBINE EFFICIENCY ΔHe/ΔHa	Pturb to/Pbar	Anozz eff, in²	Imap-Emap ΔP "H₂A"		
0	.624	1.21	27400	.391	4.64		1.20	.695	25.	n.a.	1.90	.935	1.19	3.18	-.90		
2	.734	1.50	38520	.494	10.94		1.34	.706	21.	30.	1.50	.767	1.34	3.05	2.80		
6	.728	1.82	46950	.584	19.68		1.50	.711	10.4	20.	1.02	.759	1.49	2.92	7.00		
7	.746	2.14	53565	.711	30.33		1.67	.709	7.0	18.9	1.02	.765	1.66	3.04	11.70		
8	.728	2.48	59470	.821	43.74		1.86	.706	1.4	6.9	.821	.772	1.94	3.06	15.70		
6	.713	1.32	32350	.460	6.90		1.30	.693	20.4	20.	1.65	.665	1.29	2.85	-1.00		
1	.741	1.67	43740	.580	16.4		1.48	.705	15.2	20.5	1.21	.714	1.48	2.86	3.80		
5	.742	2.01	51310	.704	27.28		1.68	.703	6.6	19.1	1.01	.708	1.67	2.84	7.30		
0	.734	2.38	58230	.840	42.13		1.91	.704	.7	16.7	.895	.717	1.90	2.88	11.20		
6	.736	2.67	62640	.940	54.08		2.05	.703	-1.3	20.3	.910	.735	2.04	2.99	14.70		
8	.699	1.31	32530	.498	7.23		1.30	.694	23.4	17.5	1.72	.677	1.29	3.01	-1.40		
8	.748	1.68	44140	.632	17.66		1.50	.703	13.4	15.0	1.14	.727	1.49	3.02	3.20		
7	.750	2.03	52100	.766	30.16		1.71	.706	6.47	16.1	.953	.739	1.69	3.02	7.20		
9	.743	2.41	59150	.912	46.21		1.96	.702	.3	14.0	.809	.735	1.93	3.05	11.00		
	.736	2.73	64445	1.026	60.97		2.17	.702	-2.8	n.a.	.780	.728	2.14	3.06	13.60		
8	.676	1.39	36760	.582	11.15		1.39	.687	18.3	16.7	1.26	.698	1.38	3.06	-1.60		
6	.733	1.85	49230	.778	26.78		1.69	.695	6.2	10.8	.916	.701	1.67	3.00	2.50		
9	.737	2.25	57280	.945	43.92		1.97	.697	.9	2.6	.831	.706	1.94	3.02	5.70		
6	.753	2.64	61470	1.096	61.32		2.27	.670	-3.6	n.a.	.763	.682	2.23	3.03	8.40		
	.717	2.86	65440	1.192	76.54		2.45	.673	-4.65	7.6	.825	.706	2.39	3.08	9.10		
2	.676	1.51	41940	.692	16.91		1.53	.688	11.1	9.0	.986	.674	1.51	3.01	-.70		
4	.739	1.99	53420	.923	35.56		1.90	.690	3.3	8.3	.904	.661	1.87	3.01	.60		
7	.717	2.46	61830	1.123	60.18		2.29	.686	-2.6	6.0	.836	.677	2.24	3.01	2.50		
0	.705	2.86	67940	1.292	83.99		2.61	.683	-6.1	6.0	.803	.687	2.55	3.07	4.20		
9	.702	2.99	70060	1.352	92.63		2.75	.680	-6.9	n.a.	.828	.678	2.67	3.08	4.30		
2	.704	1.81	50560	.902	29.89		1.87	.693	7.80	18.0	.933	.612	1.86	2.72	-4.4		
0	.707	2.39	62423	1.180	60.35		2.36	.706	-.16	10.8	.830	.647	2.36	2.80	-3.6		
7	.691	2.88	69620	1.406	91.96		2.82	.697	-5.93	10.7	.786	.655	2.82	2.85	-3.0		
8	.694	3.01	71470	1.463	102.2		2.94	.673	-11.4	n.a.	.793	.655	2.85	3.11	-.90		

| RUN NO. | IND RPM | RAD RPM | TEMPERATURES °F | | | | | | | | | | | 1/8 UP IND | 1/ DO IN |
			VNT IN	COMP IN	SHRD ST	IND OUT TOT	COMP OUT	INT MAN	TURB IN	TURB IN	TURB RMS 1	TURB RMS 2	TURB RMS 3		
F155	18200	25850	75	77	84	84	119	172	796	779	668	685	646	13.8	13
F156	26400	36520	82	79	93	97	163	177	1039	1020	925	915	848	13.8	14
F157	33700	44050	82	87	107	115	212	181	1214	1190	1102	1070	1006	13.8	13
F158	39300	51590	84	88	122	122	258	184	1301	1273	1142	1127	1058	13.6	13

1

| ...ERATURES °F | | | | | | PRESSURES PSIA | | | | | | | | | | H.A |
MP/T	INT MAN	TURB IN	TURB IN	TURB RMS 1	TURB RMS 2	TURB RMS 3	1/8 UP IND	1/8 DOWN IND	1/8 UP RAD	1/8 DOWN RAD	PT IP ST	PT IP ST	COMP OUT T	INT MAN ST	TURB IN T	TURB IN T	TURB IN ST
	172	796	779	668	685	646	13.8	13.9	14.2	14.2	15.6	—	16.7	16.4	16.8	16.8	34.1
	177	1039	1020	925	915	848	13.8	14.0	14.2	14.5	17.4	—	20.3	20.1	17.5	17.6	37.4
	181	1214	1190	1102	1070	1006	13.8	13.9	14.4	14.6	19.3	—	23.7	23.4	20.1	20.2	42.7
	184	1301	1273	1142	1127	1058	13.6	13.9	14.7	14.9	21.4	—	28.2	28.0	22.4	22.5	44.8

B WN D	1/8 UP RAD	1/8 DOWN RAD	PT IP ST	PT IP ST	COMP OUT T	INT MAN ST	TURB IN T	TURB IN T	TURB IN ST (H.A.)	BAR HGA	FUEL FLOW LB/HR	TORQ IN HG	EXH MAN PRES INHG T	INT MAN PRES IN HG ST	PTIC IN H2O	ΔP VNT IN H2O	TURB OUT ΔP IN H2O
9	14.2	14.2	15.6	—	16.7	16.4	16.8	16.8	34.1	29.25	33.	19.6	34.2	33.7	12.0	.815	-1.0
2	14.2	14.5	17.4	—	20.3	20.1	17.5	17.6	37.4	"	57.	35.5	35.7	41.1	12.	1.24	-2
9	14.4	14.6	19.3	—	23.7	23.4	20.1	20.2	42.7	"	79.	50.9	41.0	47.8	12.0	1.67	-4.5
9	14.7	14.9	21.4	—	28.2	28.0	22.4	22.5	44.9	"	101.	65.5	45.7	56.8	11.5	2.44	-6.5

PRESSURES PSIA

RUN NUMBER	ENGINE RPM	ENGINE TORQUE	HORSE-POWER	FUEL FLOW, lb/hr	BSFC	VENTURI AIRFLOW, lb/sec	F/A	EXHAUST FLOW, lb/sec	INTAKE MAN.PR. psia	INTAKE MAN.PR. H₂A	INTAKE MAN.TEMP, °F	THEORETICAL AIR FLOW, lb/sec	VOLUMETRIC EFFICIENCY	BMEP, psi	IND RPM / PAD RPM
F155	1203	298.	69.3	33.	0.483	0.365	0.0251	0.374	16.4	33.7	172	0.349	1.044	52.6	.704
F156	1203	605.	138.6	57.	0.411	0.448	0.0353	0.464	20.1	41.1	177	0.424	1.057	106.7	.728
F157	1195	905.	206.0	79.	0.384	0.519	.0423	0.541	23.4	47.8	181	0.487	1.066	159.7	.765
F158	1205	1192.	223.6	101.	0.369	0.626	.0448	0.654	28.0	56.8	184	0.583	1.074	210.3	.762

1200

1400

1500

1700

1900

2100

1

| | | | | | | | | TURBOCHARGER RESULTS | | | | | | | TURBINE | | |
| | | | | | | | | COMPRESSOR | | | | | | | | | |
FLOW, lb/sec	INTAKE MAN. PR. psia	INTAKE MAN. PR. "HgA	INTAKE MAN. TEMP. °F	THEORETICAL AIR FLOW, lb/sec	VOLUMETRIC EFFICIENCY	BMEP, psi	IND RPM / RAD RPM	COMPRESSOR EFFICIENCY	PRESSURE RATIO	CORRECTED SPEED, RPM	CORRECTED MASS FLOW, lb/sec	ΔH_{comp}, Btu/sec		PRESSURE RATIO	U/C$_0$	THEORETICAL SWIRL ANGLE	PROBE SWIRL ANGLE
574	16.4	33.7	172	0.349	1.044	52.6	.704	.673	1.20	26040	.363	3.73		1.17	.700	29.4	11.3
64	20.1	41.1	177	0.424	1.057	106.7	.728	.721	1.46	36450	.447	9.15		1.23	.794	36.8	11.0
41	234	47.8	181	0.487	1.066	159.7	.765	.719	1.70	43970	.521	15.77		1.42	.705	18.3	9.4
54	28.0	56.8	184	0.583	1.074	210.3	.762	.710	2.02	51450	.627	25.85		1.59	.704	11.6	10.4

RAD RPM	COMPRESSOR						TURBINE										
	COMPRESSOR EFFICIENCY	PRESSURE RATIO	CORRECTED SPEED, RPM	CORRECTED MASS FLOW, lb/sec	$\Delta H_{comp.}$, btu/sec		PRESSURE RATIO	u/c_o	THEORETICAL SWIRL ANGLE	PROBE SWIRL ANGLE	AVG. TURB. EFFICIENCY $\eta_{T/S}$	TURBINE EFFICIENCY $\Delta H_c/\Delta H_s$			IMAP-EMAP. $\Delta P.$ "H_2A		
4	.673	1.20	26040	.363	3.73		1.17	.700	29.9	11.3	2.4	.834			-.50		
28	.721	1.46	36450	.447	9.15		1.23	.794	36.8	11.0	1.8	1.21			5.40		
.5	.710	1.70	43970	.521	15.77		1.42	.725	18.3	9.4	1.06	.790			6.80		
52	.710	2.02	51450	.627	25.85		1.59	.704	11.6	10.4	.953	.777			11.10		

A-8

DISTRIBUTION LIST

	Copies
U.S. Army Tank-Automotive Command ATTN: DRSTA-RGRD Warren, MI 48090	20
U.S. Army Tank-Automotive Command ATTN: DRSTA-TSL Warren, MI 48090	14
Commander Defense Technical Information Center Bldg. 5, Cameron Station ATTN: DDAC Alexandria, VA 22314	12
Dr. Charles Church DAMA-ZE, Pentagon Washington, D. C. 20330	2
Manager Defense Logistics Studies Information Exchange ATTN: AMXMC-D Fort Lee, VA 23801-6044	2
Commander U.S. Army Tank-Automotive Command ATTN: AMSTA-DDL (Technical Library) Warren, MI 48397-5000	2
Commander U.S. Army Tank-Automotive Command ATTN: AMSTA-CF (Mr. Charles Salter) Warren, MI 48397-5000	1
U.S. Army Tank-Automotive Command ATTN: DRSTA-IRR Warren, MI 48090	1
U.S. Army Tank-Automotive Command ATTN: DRSTA-TSE Warren, MI 48090	1